東　京　大　學

地震研究所彙報

第26號　第1~4册

昭和23年1～12月

目　次

論文及報告　　頁

1. 層のある媒質を傳はる表面波の研究 (1) (英文) ……佐藤泰夫 1
2. 聯立方程式 $(\nabla^2-aD)u_i=b\frac{\partial\theta}{\partial x_i}$ を充す變位ポテンシヤル (英文) ……谷本勉之助 5
3. 電氣傳導度が不均一な球殼中の電流分布 (英文) ……力武常次 11
4. 地球磁場の地方的異常について (英文) ……力武常次 17
5. 油壺に於ける地殼變動の觀測　第一報 (英文) ……萩原尊禮・力武常次・山田重平 23
6. 津浪の局部的現象 (其一) (英文) ……那須信治 27
7. 地質學的岩石學的に見た昭和21年の櫻島の活動　その二, 新熔岩の岩石記載 (英文) ……森本良平 37
8. 鹿兒島縣肝屬郡垂水町唉花平產鐵橄欖石の產出狀態 (英文) …森本良平 41
9. 四國足摺岬の花崗岩類 (I) (英文) ……森平良平 45
10. 瀨戸川層群中に發達する Fracture System (英文) ……村井勇 49
11. 地震計の振動倍率算定のためのノモグラム (英文) ……池上良平 55
12. M_2 地震波の實在性について (英文) ……金井清 57
13. 各種地盤上の地震動 (I) 高知市に於ける觀測 (英文) ……水上武・佐久間修三 61
14. 各種地盤上の地震動 (II) 御坊町及び切目村に於ける觀測 (英文) ……佐久間修三 67
15. 東京における月毎の有感地震の頻度に關する統計的研究 (英文) ……岸上冬彥 73
16. 1949年海南市の月毎の地震回數について (英文) ……岸上冬彥 81
17. 地震動最大振幅の異常分布について (英文) ……池上良平 83
18. 震度と震央距離との關係 (英文) ……佐藤泰夫 91
19. 捩り振子を應用した低域濾波器による地震波の研究 (第一報) (英文) ……秋間哲夫 95
20. 和歌山縣御坊町附近における地震動と地盤の性質 (エスペラント) ……宮村攝三 101

所　報

本彙報ハ年4回（但シ第1號ヨリ第6號マデハ不定期ニ，第7號ハ3冊トシテ發行セリ），彙報別冊ハ不定期ニ發行ス.

本彙報掲載ノ論文及ビ報告ノ内容ニ關シテハ著者ノミニ責任アルモノトス.

本彙報ニ關スル照會ハ東京大學地震研究所長ヘ宛テラレタシ.

The Bulletin is published quarterly. (Vols. I–VI were published at irregular intervals and Vol. VII consisted of three parts.)
Supplementary Volume is published at irregular interval.

The authors of the papers alone are responsible for the statements and opinions contained in their respective papers.

All communications relating to this Bulletin should be addressed to the Director of the Earthquake Research Institute, Tokyo University.

ERRATA

Page	*Line*			*Read*	
4	17	:	differantiable	*Read*	differentiable
5	12	:	aquntity	,,	quantity
8	foot-note	:	$-{}^2\Gamma+3\frac{\partial^2}{\partial x^3}$	,,	$-\Gamma^2+3\frac{\partial^2}{\partial x^2}$
10	12	:	$2(1-\sigma)\square$	,,	$2(1-\sigma)\square_1'$
11	1	:	Studing	,,	Studying

1. *Mathematical Study of the Propagation of Waves upon Stratified Medium.* (1)

By Yasuo SATÔ,

Earthquake Research Institute.

(Read Dec. 16, 1947.—Received March 30, 1949.)

INTRODUCTION.

Since the celebrated work of H. Lamb[1], the generation and propagation of waves upon the surface of elastic body is studied by a number of eminent authors[2]. They are, however, so skillful—consequently intricate—that no one could apply their results to a more complicated problem such as the propagation of waves upon stratified medium. Hence, it seems to the author that it is not useless to state a simple way, if not an exact way, of calculation applicable to practical cases.

PART I. PRELIMINARY ANALYSIS.

§ 1. Asymptotic expansion of a definite integral $\int_a^b F(\xi) \begin{matrix}\cos\\ \sin\end{matrix} \xi x d\xi$.

A form of definite integral shown above often appears in the problem of elastic waves. Here we shall show a general and convenient way of getting the asymptotic expansion of such an integral. We know already that this integral tends tc zero when x becomes large without limit. (Riemann-Lebesgue's lemma[3]). Use notations

$$I(x) = I_c(x) + iIs(x) = \int_a^b F(\xi) \exp(i\xi x) d\xi, \qquad \Phi(\xi) = F(\xi) \cos \xi x$$

When x is sufficiently large, $\cos \xi x$ generally varies far more rapidly than the function $F(\xi)$, therefore $\Phi(\xi)$ may be regarded as a cos-curve whose amplitude is represented by $F(\xi)$, and the integral $I_c(x)$ is the algebraic sum of the area between the curve $\Phi(\xi)$ and ξ-axis. On the other hand, since two neighbouring area elements are nearly equal and have different signs, they cansel with each other, and the values of integral is determined only by the two limits of integral and points where $F'(\xi)$ becomes infinity. The following calculations are lead by the above idea.

---

(1) H. LAMB, *Phil. Trans* **A** 203, 1 (1904) 1.
(2) H. NAKANO, *Jap. Journ. Astro. Geophys.* **2** (1925) 1.
K. SEZAWA and G. NISIMURA, *Bull. Earthq. Res. Inst.* **6** (1929) 1, 7 (1929) 41.
T. SAKAI, *Geophys. Mag.* **14** (1936) 582.
(3) WHITTAKER and WATSON, *Modern Analysis* p. 172.

§ 2. When $F(\xi)$ is differentiable at the closed domain $[a, b]$.

We assume as $0 \leq a < b$, and $z = \xi x$. Then, by partial integration

$$I_c(x) = \int_{ax}^{bx} F\left(\frac{z}{x}\right)\frac{1}{x}dz = \frac{1}{x}\left[F\left(\frac{z}{x}\right)\sin z\right]_{ax}^{bx} - \frac{1}{x}\int_{ax}^{bx} F'\left(\frac{z}{x}\right)\sin z\frac{1}{x}dz$$

$$= x^{-1}[F(b)\sin bx - F(a)\sin ax] + x^{-2}[F'(b)\cos bx - F'(a)\cos ax]$$

$$+ x^{-3}[F''(b) \;,, \; + F''(a) \;,, \;] + x^{-4}[F'''(b) \;,, \; - F'''(a) \;,, \;] + \cdots \tag{2·1}$$

Similarly

$$I_s(x) = x^{-1}[-F(b)\cos bx + F(a)\cos ax] + x^{-2}[F'(b)\sin bx - F'(a)\sin ax]$$

$$+ x^{-3}[F''(b) \;,, \; - F''(a) \;,, \;] + x^{-4}[-F'''(b) \;,, \; + F'''(a) \;,, \;] + \cdots \tag{1·2}$$

§ 3 When $F(\xi)$ contains $\sqrt{\xi^2 - a^2}$.

We assume that $F(\xi)$ can be expanded at $\xi = a$ as a power series of $(\xi - a)^{\frac{1}{2}}$ that begins by the term $(\xi - a)^{-\frac{1}{2}}$. We use the following notations.

$$\begin{cases} F(\xi) = F_{-1}(a)\dfrac{1}{2}(\xi - a)^{\frac{1}{2}} + F^0(\xi) \\ \qquad F^0(\xi) \equiv F_0(a) + F_1(a)(\xi - a)^{\frac{1}{2}} + F_2(a)(\xi - a) + \cdots\cdots\cdots \\ F^{0\prime}(\xi) = F_1(a)\cdot\dfrac{1}{2}(\xi - a)^{-\frac{1}{2}} + F^1(\xi) \\ \qquad F^1(\xi) = F_2(a) + F_3(a) - \dfrac{3}{2}(\xi - a)^{\frac{1}{2}} + F_4(a)\cdot 2(\xi - a) + \cdots \text{ etc.} \end{cases} \tag{3·1}$$

$$F^k(a) = k!\, F_k(a)$$

Denote $C + iS = \int_{ax}^{bx}(z - ax)^{-\frac{1}{2}}\exp(iz)dz$,

then we have, using Fresnel's integrals; $C\{\quad\}$ and $S\{\quad\}$[4]

$$C + iS = \sqrt{(2\pi)}\cdot\exp(iax)C\{(b-a)x\} + i\sqrt{(2\pi)}\exp(iax)S\{(b-a)x\}$$

$$= \sqrt{\pi}\cdot \quad \exp i(ax + \pi/4) + x^{-\frac{1}{2}}(b-a)^{-\frac{1}{2}}\exp i(bx - \pi/2) + \cdots \tag{3·2}$$

From (3·1)

$$I_c(x) = x^{-\frac{1}{2}}F_{-1}(a)\int_{ax}^{bx}(z - ax)^{-\frac{1}{2}}\cos z\,dz + x^{-1}\int_{ax}^{bx}F^0\left(\frac{z}{x}\right)\cos z\,dz \quad \cdots \tag{3·3}$$

Since the first term is calculated in (3·2), applying partial integration

(4) TERAZAWA, *Sûgakugairon* p. 189.

to the second term,

2nd term

$$= x^{-1}\left[F^0\left(\frac{z}{2}\right)\sin z\right]_{ax}^{bx} - x^{-1}\left[F_1(a)\cdot\frac{1}{2}\left(\frac{z}{x}-a\right)^{-\frac{1}{2}} + F'\left(\frac{z}{x}\right)\right]\sin z\cdot\frac{1}{x}dz$$

$$= x^{-1}[F^0(b)\sin bx - F^0(a)\sin ax] - x^{-\frac{3}{2}}F_1(a)\cdot\frac{1}{2}S - x^{-2}\int_{ax}^{bx}F^1\left(\frac{z}{x}\right)\sin z\,dz \tag{3·4}$$

Introducing (3·2) and (3·4) into (3·3), we have

$$I_c(x) = x^{-\frac{1}{2}}F_{-1}(a)\sqrt{\pi}\cdot\cos(ax+\pi/4) + x^{-1}[F(b)\sin bx - F_0(a)\sin ax]$$
$$-x^{-\frac{3}{2}}F_1(a)\frac{1}{2}\sqrt{\pi}\cdot\sin(\quad ,, \quad) + x^{-2}[\cdots\cdots\cdots\cdots\cdots\cdots] + \cdots \tag{3·5}$$

Similarly

$$I_s(x) = x^{-\frac{1}{2}}F_{-1}(a)\sqrt{\pi}\cdot\sin(ax+\pi/4) - x^{-1}[F(b)\cos bx - F_0(a)\cos ax]$$
$$+x^{-\frac{1}{2}}F_1(a)\frac{1}{2}\sqrt{\pi}\cdot\cos(\quad ,, \quad) + x^{-2}[\cdots\cdots\cdots\cdots\cdots\cdots] + \cdots \tag{3·6}$$

When $F(\xi)$ contains $\sqrt{\xi^2-b^2}$, we may have similar results also. Using proper consideration with respect to the argument of $\sqrt{\xi^2-b^2}$, we obtain the following results

$$I_c(x) = -ix^{-\frac{1}{2}}F_{-1}(b)\sqrt{\pi}\cdot\sin(bx+\pi/4) + x^{-1}[F_0(b)\sin bx - F(a)\sin ax]$$
$$-ix^{-\frac{3}{2}}F_1(b)\frac{1}{2}\sqrt{\pi}\cdot\cos(\quad ,, \quad) + x^{-2}[\cdots\cdots\cdots\cdots\cdots\cdots] + \cdots \tag{3·7}$$

$$I_s(x) = ix^{-\frac{1}{2}}F_{-1}(b)\sqrt{\pi}\cdot\cos(\quad ,, \quad) - x^{-1}[F_0(b)\cos bx - F(a)\cos ax]$$
$$-ix^{-\frac{3}{2}}F_1(b)\frac{1}{2}\sqrt{\pi}\cdot\sin(\quad ,, \quad) + x^{-2}[\cdots\cdots\cdots\cdots\cdots\cdots] + \cdots \tag{3·8}$$

Where $$F(\xi) = F_{-1}(b)(\xi-b)^{-\frac{1}{2}} + F_0(b) + F_1(b)(\xi-b)^{\frac{1}{2}} + \cdots$$
$$\equiv \exp(-i\pi/2)F_{-1}(b)(b-\xi)^{-\frac{1}{2}} + F^0(\xi) \qquad \cdots\cdots\cdots\cdots (3·9)$$

§4 When $F(\xi)$ contains $\sqrt{\xi^2-c^2}$, where $a<c<b$.

Using the results of the above article, we can easily obtain the formulae which are corresponding to this case. Dividing the integral $\int_a^b$ to two

parts $\int_a^c$ and $\int_c^b$, and applying (3·5), (3·6), (3·7) and (3·8), we have at once,

$$\begin{cases} I_c(x) = x^{-\frac{1}{2}}F_{-1}(c)\sqrt{\pi}\cdot\exp\{-i(cx+\pi/4)\}+x^{-1}[F(b)\sin bx-F(a)\sin ax] \\ \qquad -x^{-\frac{3}{2}}F_1(c)\dfrac{1}{2}\sqrt{\pi}\cdot\exp\{-i(cx-\pi/4)\}+x^{-2}[\cdots\cdots\cdots] \\ I_s(x) = x^{-\frac{1}{2}}F_{-1}(c)\sqrt{\pi}\cdot\exp\{-i(cx-\pi/4)\}+x^{-1}[F(b)\cos bx-F(a)\cos ax] \\ \qquad +x^{-\frac{3}{2}}F_1(c)\dfrac{1}{2}\sqrt{\pi}\cdot\exp\{-i(cx+\pi/4)\}+x^{-2}[\cdots\cdots\cdots] \end{cases} \tag{4·1}$$

From the above expressions we notice at a glance, that the asymptotic expansions are determined by the coefficients at the two limits of integration and the points where the derivative becomes infinity. This is what we expected at the beginning of this paper. Here, we will add that the coefficients at a and b are involved as the same forms with §2.

§5. Further development of formulae.

For the convenience of practical use, we shall here set forth another formula. Generally, if $F(\xi)$ is expressed as

$$F(\xi) = A_{-1}(\xi)(\xi^2-c^2)^{-\frac{1}{2}}+A_0(\xi)+A_1(\xi)(\xi^2-c^2)^{\frac{1}{2}}+\cdots\cdot \tag{5·1}$$

where $A_{-1}(\xi)$, $A_0(\xi)$, $\cdots\cdot$ are functions that are identically zero, or not zero and differantiable at $\xi = c$.

In this case, $F(\xi)$ may be developed in the following scheme; the proof is self-evident.

$$\begin{aligned} F(\xi) = {} & A_{-1}(c)\cdot(2c)^{-\frac{1}{2}}(\xi-c)^{-\frac{1}{2}}+A_0(c) \\ & +\{-A_{-1}(c)/(4c)(+A_{-1}'(c)+A_1(c)\cdot 2c\}(2c)^{-\frac{1}{2}}(\xi-c)^{\frac{1}{2}}+\cdots\cdot \end{aligned} \tag{5·2}$$

Combining (4·1) with the above expression, we arrive at formulae which are convenient for practical use.

We may test the validity of new formulae by applying them to integrals whose asymptotic expansion is already known; e. g. Bessel function $J_0(x) = \dfrac{2}{\pi}\displaystyle\int_1^\infty \frac{\sin \xi x}{\sqrt{\xi^2-1}}d\xi$,[5] or the problem of generation of elastic waves treated by H. Lamb. $u_0 = \dfrac{Q}{\pi\mu}\displaystyle\int_0^\infty \frac{\xi(2\xi^2-k^2-\alpha\beta)}{(2\xi^2-k^2)^2-4\xi^2\alpha\beta}\sin \xi x\, d\xi$,[6] etc. $(\alpha = \sqrt{\xi^2-k^2},\ \beta = \sqrt{\xi^2-k^2})$.

(5) WATSON, *Bessel Functions* p. 194.
(6) Ibid. (1), Expression (52).

2. *Potentials of the Simultaneous Equations* $(\Gamma^2 - aD)u_i = b\frac{\partial\theta}{\partial x_i}$.*

By Bennosuke TANIMOTO,

Shibaura Institute of Technology, Tokyo.

(Read Oct. 19, 1948.—Received June 15, 1949.)

In the fields of mathematical physics, i.e. elasticity, hydrodynamics, electricity, etc., there have frequently appeared simultaneous linear partial differential equations of the forms

$$(\Gamma^2 - aD)u_i = b\frac{\partial\theta}{\partial x_i} \qquad (i = 1, 2, 3), \tag{1}$$

where Γ^2 denotes Laplace's operator in three dimensions, D an operator such as 0, $\partial^2/\partial t^2$, $\partial/\partial t$, $\partial/\partial x + \partial/\partial y + \partial/\partial z$, etc., u_i a component of a vector aquntity, and θ a scalar quantity.

So far as the present stage of my work is concerned, potential equations of (1) have ever been obtained in the forms

$$(\Gamma^2 - aD)(\Gamma^2 - cD')\chi = 0 \tag{2}$$

and

$$(\Gamma^2 - aD)\varphi = 0 \quad \text{provided} \quad \theta = 0, \tag{3}$$

D' being some operator. The vector components, and the tensor components, are given by certain operations performed on χ and φ. It is noted that φ is in general independent of χ. From the mathematical point of view potential functions thus found may be termed 'solutions' of the original simultaneous equations (1).

The procedure of obtaining (2) will be sufficient by taking

$$u = \left\{\kappa\frac{\partial}{\partial x}\Gamma^2 + \kappa'\left(\frac{\partial}{\partial y} + \frac{\partial}{\partial z}\right)\Gamma^2\right\}\chi + \mathcal{D}\chi, \quad \cdots\cdots, \tag{4}$$

$\mathcal{D}$ being an operator determinable according to aD in (1); κ, κ' being constants. The operator Γ^2 here proposed represents

$$\Gamma^2 = \frac{\partial^2}{\partial y\partial z} + \frac{\partial^2}{\partial z\partial x} + \frac{\partial^2}{\partial x\partial y}, \tag{5}$$

---

* Communicated by G. NISHIMURA.

which has frequently been used in the series of my work. The principal part of the right-hand side of (4) has been first obtained in the case of statical elasticity (cf. I), by commencing with the most generalized form of the so-called Maxwell's stress-functions and the Morera's.[1] The φ-part is due, for instance, to the substitution $u=0$, $v \neq 0$, $w \neq 0$; for χ and u will satisfy the same differential equation, so that the correspondence between them is complete; and then we may have

$$u=0, \qquad v=\frac{\partial\varphi}{\partial z}, \qquad w=-\frac{\partial\varphi}{\partial y}; \tag{6}$$

and the cyclical interchanges of u, v, w and x, y, z are also solutions of (1). Again, the sum of these three sets of solutions is a solution of (1), which is the form for φ adopted in this paper.

Several examples of potentials which have been obtained hitherto will be shown in the following:

I. STATICAL ELASTICITY RULED BY HOOKE'S LAW.

In this case fundamental equations when no body forces act can be expressed in the forms

$$\left(\frac{\partial}{\partial x}, \frac{\partial}{\partial y}, \frac{\partial}{\partial z}\right)\Delta+(1-2\sigma)\Gamma^2(u, v, w)=0, \tag{7}$$

Δ being cubical dilatation, and σ Poisson's ratio. Potential equations of (7) have been found to be

$$\Gamma^4\chi=0 \qquad \text{and} \qquad \Gamma^2\varphi=0. \tag{8}$$

In terms of these potentials the displacements are given by

---

1) The potential χ of the statical elasticity was obtained by putting

$$\begin{aligned} Y_z = &\left[a\Gamma^2+b\frac{\partial^2}{\partial x^2}+c\frac{\partial^2}{\partial y\partial z}+d\frac{\partial}{\partial x}\left(\frac{\partial}{\partial y}+\frac{\partial}{\partial z}\right)\right]\chi_1 \\ &+e\left(\frac{\partial^2\chi_2}{\partial y^2}+\frac{\partial^2\chi_3}{\partial z^2}\right)+f\left(\frac{\partial^2\chi_2}{\partial z^2}+\frac{\partial^2\chi_3}{\partial y^2}\right)+g\frac{\partial^2}{\partial x^2}(\chi_2+\chi_3) \\ &+h\frac{\partial^2}{\partial y\partial z}(\chi_2+\chi_3)+i\frac{\partial}{\partial x}\left(\frac{\partial\chi_2}{\partial y}+\frac{\partial\chi_3}{\partial z}\right)+j\frac{\partial}{\partial x}\left(\frac{\partial\chi_2}{\partial z}+\frac{\partial\chi_3}{\partial y}\right), \cdots\cdots, \end{aligned}$$

and further by putting

$$\chi_1=\left[\alpha\Gamma^2+\beta\frac{\partial^2}{\partial x^2}+\gamma\frac{\partial^2}{\partial y\partial z}+\delta\frac{\partial}{\partial x}\left(\frac{\partial}{\partial y}+\frac{\partial}{\partial z}\right)\right]\chi, \cdots\cdots,$$

which is of homogeneous quadratic form, the linear form of the substitution having resulted in failure.

$$u = \left\{-\frac{\partial}{\partial x}\nabla^2 + (1-\sigma)\left(\frac{\partial}{\partial y}+\frac{\partial}{\partial z}\right)\nabla^2\right\}\chi + \left(\frac{\partial}{\partial y}-\frac{\partial}{\partial z}\right)\varphi, \cdots\cdots, \quad (9)$$

v, w being given by cyclical interchange of x, y, z. χ may be divided in two parts, one being harmonic, χ_1, say, and the other biharmonic proper. The former χ_1 is at once seen to be the same as the known displacement-potential, if we write $\nabla^2\chi_1 = \phi$. It can easily be verified that $x\phi$, $y\phi$, $z\phi$ and $r^2\phi$, where $r^2 = (x-x_0)^2+(y-y_0)^2+(z-z_0)^2$, are all biharmonic, provided ϕ is harmonic.

An application of the present potentials has been made to one of Boussinesq's problems of simple type; and its solution is in general compatible with the shearing forces as well as the normal pressure.[2)]

II. Dynamical Elasticity ruled by Hooke's Law.

In this case fundamental equations can take the forms

$$\frac{\partial \Delta}{\partial x} + (1-2\sigma)\nabla^2 u = (1-2\sigma)\frac{\rho}{\mu}\frac{\partial^2 u}{\partial t^2}, \cdots\cdots \quad (10)$$

Potential equations of these have been found to be

$$\Box_1\Box_2\chi = 0 \quad \text{and} \quad \Box_2\varphi = 0, \quad (11)$$

where
$$\Box_1 = \nabla^2 - \frac{\rho}{\lambda+2\mu}\frac{\partial^2}{\partial t^2}, \quad \Box_2 = \nabla^2 - \frac{\rho}{\mu}\frac{\partial^2}{\partial t^2}. \quad (12)$$

In terms of these potentials the displacements are given by

$$u = \left\{-\frac{\partial}{\partial x}\nabla^2 + (1-\sigma)\left(\frac{\partial}{\partial y}+\frac{\partial}{\partial z}\right)\Box_1\right\}\chi + \left(\frac{\partial}{\partial y}-\frac{\partial}{\partial z}\right)\varphi, \cdots\cdots \quad (13)$$

Two kinds of functions χ_1 and χ_2 which satisfy the equations $\Box_1\chi_1 = 0$ and $\Box_2\chi_2 = 0$ respectively are both included in χ; and it will easily be seen that χ_1 corresponds to the irrotational wave, and that χ_2 and φ correspond to the two kinds of equivoluminal waves.

III. Dynamical Visco-Elasticity ruled by Voigt's Law.

In this case fundamental equations take the forms

2) The known Boussinesq's potential method is not compatible with the shearing forces, since it gives the expressions $Y_z = z\frac{\partial^2 V}{\partial y \partial z}$ and $Z_x = z\frac{\partial^2 V}{\partial z \partial x}$ (cf. Love's Elasticity, p. 193), both of which reduce to zero at the plane surface of a semi-infinite solid, where $z = 0$.

$$(\lambda+\mu)\frac{\partial\Delta}{\partial x}+\mu\nabla^2 u+(\lambda'+\mu')\frac{\partial^2\Delta}{\partial x\partial t}+\mu'\nabla^2\frac{\partial u}{\partial t}=\rho\frac{\partial^2 u}{\partial t^2},\ \cdots\cdots \tag{14}$$

Potential equations of these have been found to be

$$\Box_1'\Box_2'\chi=0 \quad \text{and} \quad \Box_2'\varphi=0, \tag{15}$$

where
$$\Box_1'=\Box_1+\frac{\lambda'+2\mu'}{\lambda+2\mu}\frac{\partial}{\partial t}\nabla^2, \qquad \Box_2'=\Box_2+\frac{\mu'}{\mu}\frac{\partial}{\partial t}\nabla^2. \tag{16}$$

In terms of these potentials the displacements are given by

$$u=\left\{-\frac{\partial}{\partial x}\left(1+\frac{\lambda'+\mu'}{\lambda+\mu}\frac{\partial}{\partial t}\right)\nabla^2+(1-\sigma)\left(\frac{\partial}{\partial y}+\frac{\partial}{\partial z}\right)\Box_1'\right\}\chi+\left(\frac{\partial}{\partial y}-\frac{\partial}{\partial z}\right)\varphi,\ \cdots \tag{17}$$

IV. OSEEN'S EQUATIONS FOR VISCOUS FLUID.

Fundamental equations of motion take the forms

$$U\frac{\partial}{\partial x}(u,v,w)=-\frac{1}{\rho}\left(\frac{\partial}{\partial x},\frac{\partial}{\partial y},\frac{\partial}{\partial z}\right)p+\nu\nabla^2(u,v,w). \tag{18}$$

(Cf. Lamb's Hydrodynamics, p. 610.) Potential equations of these have been found to be

$$\nabla^2\left(\nabla^2-2k\frac{\partial}{\partial x}\right)\chi=0 \quad \text{and} \quad \left(\nabla^2-2k\frac{\partial}{\partial x}\right)\varphi=0. \tag{19}$$

In terms of these potentials the velocities and pressure are given by

$$\left.\begin{aligned} u&=\left(\frac{\partial^2}{\partial x^2}-\nabla^2\right)\chi+\left(\frac{\partial}{\partial y}-\frac{\partial}{\partial z}\right)\varphi, & v&=\frac{\partial^2\chi}{\partial x\partial y}+\left(\frac{\partial}{\partial z}-\frac{\partial}{\partial x}\right)\varphi,\\ w&=\frac{\partial^2\chi}{\partial x\partial z}+\left(\frac{\partial}{\partial x}-\frac{\partial}{\partial y}\right)\varphi, & p&=\mu\frac{\partial}{\partial x}\left(\nabla^2-2k\frac{\partial}{\partial x}\right)\chi. \end{aligned}\right\} \tag{20}$$

If the uniform flow U is directed to the diagonal line whose direction cosines are all $1/\sqrt{3}$, the fundamental equations of motion will take the forms

$$\frac{U}{\sqrt{3}}\left(\frac{\partial}{\partial x'}+\frac{\partial}{\partial y'}+\frac{\partial}{\partial z'}\right)u'=-\frac{1}{\rho}\frac{\partial p}{\partial x'}+\nu\nabla'^2u',\ \cdots\cdots, \tag{21}$$

which reduce to the general formulation (1).[3]

3) The derivation of (19) and (20) has been done by beginning with (21). It will be found that the transformation between (21) and (18) is effected by the following scheme:

	x'	y'	z'
x	α	α	α
y	$-\alpha$	β	γ
z	$-\alpha$	γ	β

$$\alpha=\frac{1}{\sqrt{3}},\quad \beta=\frac{1}{2}\left(1+\frac{1}{\sqrt{3}}\right),\quad \gamma=-\frac{1}{2}\left(1-\frac{1}{\sqrt{3}}\right);$$

and in this case the operator ∇^2 transforms to

$$\nabla'^2=\frac{\partial^2}{\partial y'\partial z'}+\frac{\partial^2}{\partial z'\partial x'}+\frac{\partial^2}{\partial x'\partial y'}=\frac{1}{2}\left(-{}^2\nabla+3\frac{\partial^2}{\partial x^2}\right).$$

V. Unsteady Oseen's Equations.

When the uniform flow, U, in x-direction varies with time t, fundamental equations will be written

$$\frac{\partial}{\partial t}(U+u, v, w)+U\frac{\partial}{\partial x}(u, v, w) = -\frac{1}{\rho}\left(\frac{\partial}{\partial x}, \frac{\partial}{\partial y}, \frac{\partial}{\partial z}\right)p + \nu\nabla^2(u, v, w). \quad (22)$$

Potential equations of these have been found to be

$$\nabla^2\left(\nabla^2 - 2k\frac{\partial}{\partial x}-\frac{1}{\nu}\frac{\partial}{\partial t}\right)\chi = 0 \quad \text{and} \quad \left(\nabla^2 - 2k\frac{\partial}{\partial x}-\frac{1}{\nu}\frac{\partial}{\partial t}\right)\varphi = 0. \quad (23)$$

In terms of these potentials the velocities and pressure are given by

$$\left.\begin{aligned} u &= \left(\frac{\partial^2}{\partial x^2}-\nabla^2\right)\chi - U + \left(\frac{\partial}{\partial y}-\frac{\partial}{\partial z}\right)\varphi, \quad v = \frac{\partial^2\chi}{\partial x\partial y}+\left(\frac{\partial}{\partial z}-\frac{\partial}{\partial x}\right)\varphi, \\ w &= \frac{\partial^2\chi}{\partial x\partial z}+\left(\frac{\partial}{\partial x}-\frac{\partial}{\partial y}\right)\varphi, \qquad p = \mu\frac{\partial}{\partial x}\left(\nabla^2 - 2k\frac{\partial}{\partial x}-\frac{1}{\nu}\frac{\partial}{\partial t}\right)\chi. \end{aligned}\right\} \quad (24)$$

If attention is confined to the two potentials of the second degree in χ, (24) can be written

$$\left.\begin{aligned} u &= -\frac{\partial\Phi}{\partial x}+\frac{1}{2k}\frac{\partial\Psi}{\partial x}-\Psi-\frac{1}{U}\frac{\partial}{\partial t}\int\Psi dx - U, \quad v = -\frac{\partial\Phi}{\partial y}+\frac{1}{2k}\frac{\partial\Psi}{\partial y}, \\ w &= -\frac{\partial\Phi}{\partial z}+\frac{1}{2k}\frac{\partial\Psi}{\partial z}, \qquad p = \rho U\frac{\partial\Phi}{\partial x}+\rho\frac{\partial\Phi}{\partial t}, \end{aligned}\right\} \quad (25)$$

where $\nabla^2\Phi = 0$ and $\left(\nabla^2 - 2k\frac{\partial}{\partial x}-\frac{1}{\nu}\frac{\partial}{\partial t}\right)\Psi = 0.$ (26)

By means of this system of equations, I have found an approximation to the resistance experienced by a sphere moving unsteadily through a viscous fluid, the result of which is $6\pi\mu aU/(1-3\nu U'/U^3)$, U' being the given acceleration of the sphere.

Appendix. In the case of symmetrical strain of a solid of revolution, stress-equations are in general written

$$\frac{\partial\widehat{rr}}{\partial r}+\frac{\partial\widehat{rz}}{\partial z}+\frac{\widehat{rr}-\widehat{\theta\theta}}{r}-\frac{\partial U}{\partial r} = 0, \quad \frac{\partial\widehat{rz}}{\partial r}+\frac{\partial\widehat{zz}}{\partial z}+\frac{\widehat{rz}}{r}-\frac{\partial W}{\partial z} = 0, \quad (27)$$

U, W being some functions of r, z and t. If Hooke's law is referred to, we can obtain, after some amount of calculation,[4]

4) Cf. Love's Elasticity, pp. 274-276; and further introduce the integral $\iint Urdrdz$.

$$\left.\begin{aligned} &(1-\sigma)\Gamma^4\chi = -(1-2\sigma)\Gamma^2\int Udz - \frac{\partial U}{\partial z} + \frac{\partial W}{\partial z}, \\ &u = -\frac{1}{2\mu}\frac{\partial^2\chi}{\partial r\partial z}, \quad w = \frac{1}{2\mu}\left\{2(1-\sigma)\Gamma^2 - \frac{\partial^2}{\partial z^2}\right\}\chi + \frac{1-2\sigma}{\mu}\int Udz, \end{aligned}\right\} \tag{28}$$

where and in what follows Γ^2 denotes $\frac{\partial^2}{\partial r^2} + \frac{1}{r}\frac{\partial}{\partial r} + \frac{\partial^2}{\partial z^2}$.

In cases of a uniform gravitation (ρg) in the positive z-direction and of a centrifugal force of constant angular velocity (ω) rotating about the z-axis, it is sufficient to take $U = W$, and $U = -\rho gz$ and $U = -\frac{1}{2}\rho\omega^2 r^2$ respectively. In the case of elastic vibration, we can take $\frac{\partial U}{\partial r} = \rho\frac{\partial^2 u}{\partial t^2}$ and $\frac{\partial W}{\partial z} = \rho\frac{\partial^2 w}{\partial t^2}$; and then we obtain

$$\Box_1\Box_2\chi = 0, \quad u = -\frac{1}{2\mu}\frac{\partial^2\chi}{\partial r\partial z}, \quad w = \frac{1}{2\mu}\left\{2(1-\sigma)\Box_1 - \frac{\partial^2}{\partial z^2}\right\}\chi. \tag{29}$$

Further if Voigt's law is referred to, we can obtain

$$\left.\begin{aligned} &\Box_1'\Box_2'\chi = 0, \\ &u = -\frac{1}{2\mu}\left(1+\frac{\lambda'+\mu'}{\lambda+\mu}\frac{\partial}{\partial t}\right)\frac{\partial^2\chi}{\partial r\partial z}, \quad w = \frac{1}{2\mu}\left\{2(1-\sigma)\Box - \left(1+\frac{\lambda'+\mu'}{\lambda+\mu}\frac{\partial}{\partial t}\right)\frac{\partial^2}{\partial z^2}\right\}\chi. \end{aligned}\right\} \tag{30}$$

In the case of thermo-elastic equations ruled by Duhamel's law, similar calculation will afford

$$\left.\begin{aligned} &\Gamma^4\chi = -\frac{Ec}{1-\sigma}\Gamma^2\int Tdz, \\ &u = -\frac{1}{2\mu}\frac{\partial^2\chi}{\partial r\partial z}, \quad w = \frac{1}{2\mu}\left\{2(1-\sigma)\Gamma^2 - \frac{\partial^2}{\partial z^2}\right\}\chi + 2(1+\sigma)c\int Tdz, \end{aligned}\right\} \tag{31}$$

T being a distribution of temperature, E Young's modulus, and c the linear coefficient of thermal expansion of the solid.

Acknowledgment. I should like to express my sincere thanks to many who have kindly helped me. Of these the following names should strongly be remembered:

Dr. Y. TANAKA, Hon. Prof. of Tokyo Univ., who is my respected teacher; Dr. G. NISHIMURA, Prof. of Tokyo Univ., and Researcher of Earthq. Res. Inst., Tokyo Univ.; Dr. T. SAKAI, Prof. of Tokyo Univ.; Mr. E. SASAKI, President & Managing Director of his Book Company, Hongo, Tokyo; Dr. S. MATSUNAWA, President of Shibaura Inst. of Techn., Tokyo; Dr. H. M. WESTERGAARD, Prof. of Harvard Univ., Mass., U. S. A.; Dr. H. C. KELLY, Acting Chief of Sci. & Techn. Div., SCAP, GHQ, Tokyo; Dr. E. T. IGLEHART, formerly Vice-President of Aoyama Gakuin Univ., Tokyo.

3. *A Method of Studing the Distribution of Electric Currents in a Spherical Shell Having Non-Uniform Conductivity.*

By Tsuneji RIKITAKE,

Earthquake Research Institute.

(Read Oct. 19, 1948.—Received Apr. 10, 1949.)

1. Among the studies on the earth's magnetic field, we have a number of problems in which distributions of electric currents in a thin spherical shell are discussed. However, few investigations have been made hitherto in regard to shell having heterogeneous conductivity on account of mathematical difficulty. In this paper, the writer proposed a method of studying the distribution of electric currents in a thin spherical shell when the conductivity is given with sum of spherical surface harmonics.

2. In stationary state, Ohm's law is given by

$$E_\theta - \frac{\partial S}{a\partial\theta} = L\frac{\partial J}{a\sin\partial\phi}, \quad E_\phi - \frac{\partial S}{a\sin\theta\partial\phi} = -L\frac{\partial J}{a\partial\theta} \tag{1}$$

where E_θ, E_ϕ, S, J, and a denote respectively southward and eastward components of electromotive force, electrostatic potential, current-function and the radius of the shell. L is defined by $1/\int\sigma dD$, that is the reciprocal of the total conductivity.

Eliminating S from (1), we get

$$\left.\begin{aligned} \Phi(\theta,\phi) &= a\sin\theta\left\{\frac{\partial E_\theta}{\partial\phi} - \frac{\partial}{\partial\theta}(\sin\theta E_\phi)\right\}, \\ \text{where} \\ \Phi(\theta,\phi) &= \frac{\partial L}{\partial\phi}\frac{\partial J}{\partial\phi} + \sin^2\theta\frac{\partial L}{\partial\theta}\frac{\partial J}{\partial\theta} \\ &\quad + L\sin^2\theta\left\{\frac{\partial}{\sin\theta\partial\theta}\left(\sin\theta\frac{\partial J}{\partial\theta}\right) + \frac{1}{\sin^2\theta}\frac{\partial^2 J}{\partial\phi^2}\right\}. \end{aligned}\right\} \tag{2}$$

If we assume that J and L are expressed by

Table

	c_0^0	c_1^0	c_1^1	c_2^0	c_2^1	c_2^2	c_3^0	c_3^1
ξ_0^0	$+0.3333a_0^0$ $-0.13333a_2^0$	$+0.06667a_1^0$ $-0.2857a_3^0$	$-0.2000a_1^1$ $-0.2333a_3^1$	$-0.4095a_2^0$ $-0.1333a_0^0$	$-0.3714a_2^1$	$-0.2571a_2^2$	$-0.7272a_3^0$ $-0.2857a_1^0$	$-0.2333a_1^1$ $-0.6767a_3^1$
ξ_1^0	$-2.0667a_1^0$ $-0.1714a_3^0$	$-0.06667a_0^0$ $-2.4382a_2^0$	$-1.7715a_2^1$	$+0.0151a_1^0$ $-2.3316a_3^0$	$-0.3859a_1^1$ $-2.1321a_3^1$	$-1.5246a_3^2$	$-0.1714a_0^0$ $-0.7890a_2^0$	$-0.6771a_2^1$
ξ_1^1	$-1.8000a_1^1$ $-0.1400a_3^1$	$-1.5753a_2^1$	$+0.2000a_0^0$ $+0.7258a_2^0$ $-1.2371a_2^2$	$-0.0742a_1^1$ $-1.1172a_3^1$	$-0.1897a_1^0$ $+0.6727a_3^0$ $-1.0646a_3^2$	$+0.1485a_1^1$ $+0.1932a_3^1$ $-1.2256a_3^3$	$-0.2177a_2^1$	$-0.1400a_0^0$ $+0.1422a_2^0$ $-0.1704a_2^2$
ξ_2^0	$+0.6667a_0^0$ $-6.0096a_2^0$	$-2.4127a_1^0$ $-3.8290a_3^0$	$+0.4286a_1^1$ $-3.6823a_3^1$	$-0.0096a_0^0$ $-1.7450a_2^0$	$-1.8459a_2^1$	$+0.5716a_2^2$	$+0.4560a_1^0$ $-2.7422a_3^0$	$-0.1833a_1^1$ $-2.3163a_3^1$
ξ_2^1	$-5.9714a_2^1$	$-0.6322a_1^1$ $-4.5356a_3^1$	$-0.6322a_1^0$ $+2.5406a_3^0$ $-3.1798a_3^2$	$-0.2232a_2^1$	$+0.0286a_0^0$ $-0.2232a_2^0$ $-1.1710a_2^2$	$-1.1710a_2^1$	$+0.0666a_1^1$ $-0.4947a_3^1$	$-0.4946a_1^0$ $-0.4947a_3^0$ $-0.9739a_3^2$
ξ_2^2	$-5.8571a_2^2$	$-2.3281a_3^2$	$-1.5673a_1^1$ $+0.9282a_3^1$ $-3.3471a_3^3$	$+1.0290a_2^2$	$-0.4979a_2^1$	$+0.1429a_0^0$ $+1.0290a_2^0$	$+0.7958a_3^2$	$-0.0818a_1^1$ $-0.6382a_3^1$ $+0.3556a_3^3$
ξ_3^0	$+0.4000a_1^0$ $-12.0000a_3^0$	$+0.4000a_0^0$ $-4.9200a_2^0$	$+2.1015a_2^1$	$-2.5200a_1^0$ $-3.0596a_3^0$	$+0.7159a_1^1$ $-2.2779a_3^1$	$+2.6877a_3^2$	$-0.0030a_0^0$ $-1.4598a_2^0$	$-1.7121a_2^1$
ξ_3^1	$+0.3267a_1^1$ $-11.9905a_3^1$	$-4.5638a_2^1$	$+0.3267a_0^0$ $-3.3636a_2^0$ $+0.7070a_2^2$	$-1.4044a_1^1$ $-2.0966a_3^1$	$-2.3000a_1^0$ $-0.0149a_3^0$ $-2.6611a_3^2$	$+0.1414a_1^1$ $-2.3961a_3^1$ $+0.9895a_3^3$	$+0.5506a_2^1$	$+0.0095a_0^0$ $-0.8966a_2^0$ $-1.0107a_2^2$
ξ_3^2	$-11.9525a_3^2$	$-3.4286a_2^2$	$-3.3093a_2^1$	$+0.3863a_3^2$	$-1.5205a_1^1$ $-1.4093a_3^1$ $-2.4728a_3^3$	$-1.6398a_1^0$ $+3.1990a_3^0$	$+1.4098a_2^2$	$-0.3137a_2^1$
ξ_3^3	$-11.8889a_3^3$	0	$-3.6513a_2^2$	$+3.1738a_3^3$	$-1.8261a_3^2$	$-2.0082a_1^1$ $+1.5009a_3^1$	0	$+0.4572a_2^2$
			d_1^1		d_2^1	d_2^2		d_3^1

II.

c_3^2	c_3^3	d_1^1	d_2^1	d_2^2	d_3^1	d_3^2	d_3^3	
$-0.5242a_3^2$	$-0.2700a_3^3$	$-0.2000b_1^1$ $-0.2333b_3^1$	$-0.3714b_2^1$	$-0.2571b_2^2$	$-0.2333b_1^1$ $-0.6767b_3^1$	$-0.5242b_3^2$	$-0.2700b_3^3$	
$-0.3744a_3^2$	0	$-1.7715b_2^1$	$-0.3859b_1^1$ $-2.1321b_3^1$	$-1.5246b_3^2$	$-0.6771b_2^1$	$-0.3774b_2^2$	0	
$+0.0856a_2^1$	$+0.1826a_2^2$	$-1.2371b_2^2$	$-1.0646b_3^2$	$+0.1485b_1^1$ $+0.1932b_3^1$ $-1.2256b_3^2$	$-0.1704b_2^2$	$+0.0856b_2^1$	$+0.1826b_2^2$	η_1^1
$-1.1124a_3^2$	$+0.6425a_3^3$	$+0.4286b_1^1$ $-3.6823b_3^1$	$-1.8459b_2^1$	$+0.5716b_2^2$	$-0.1833b_1^1$ $-2.3163b_3^1$	$-1.1124b_3^2$	$+0.6425b_3^3$	
$+0.0152a_1^1$ $-0.9739a_3^1$ $-1.1044a_3^3$	$-1.1044a_3^2$	$-3.1798b_3^2$	$-1.1710b_2^2$	$-1.1710b_2^1$	$-0.9739b_3^2$	$+0.0152b_1^1$ $-0.9739b_3^1$ $-1.1044b_3^3$	$-1.1044b_3^2$	η_2^1
$+0.8669a_1^0$ $+0.7958a_3^0$	$+0.5651a_1^1$ $+0.3556a_3^1$	$+1.5673b_1^1$ $-0.9282b_3^1$ $-3.3471b_3^3$	$+0.4979b_2^1$	0	$+0.0818b_1^1$ $+0.6382b_3^1$ $+0.3556b_3^3$	0	$+0.5651b_1^1$ $+0.3556b_3^1$	η_2^2
$+0.8985a_2^2$	0	$+2.1015b_2^1$	$+0.7159b_1^1$ $-2.2779b_3^1$	$+2.6877b_3^2$	$-1.7121b_2^1$	$+0.8985b_2^2$	0	
$-1.5655a_2^1$	$+0.09487a_2^2$	$+0.7070b_2^2$	$-2.6611b_3^2$	$+0.1414b_1^1$ $-2.3961b_3^1$ $+0.9895b_3^3$	$-1.0107b_2^2$	$-1.5655b_2^1$	$+0.09487b_2^2$	η_3^1
$+0.0475a_0^0$ $+0.3863a_2^0$	$-1.0586a_2^1$	$+3.3093b_2^1$	$+1.5205b_1^1$ $+1.4093b_3^1$ $-2.4728b_3^3$	0	$+0.3137b_2^1$	0	$-1.0586b_2^1$	η_3^2
$-0.4098a_2^1$	$+0.1111a_0^0$ $+1.5556a_2^0$	$+3.6513b_2^2$	$+1.8261b_3^2$	$+2.0082b_1^1$ $-1.5009b_3^1$	$-0.4572b_2^2$	$+0.4098b_2^1$	0	η_3^3
d_3^2	d_3^3	$-c_1^1$	$-c_2^1$	$-c_2^2$	$-c_3^1$	$-c_3^2$	$-c_3^3$	

$$\left.\begin{aligned} J &= \sum_{n,m} P_n^m(a_n^m \cos m\phi + b_n^m \sin m\phi)\,, \\ L &= \sum_{l,k} P_l^k(c_l^k \cos k\phi + d_l^k \sin k\phi)\,, \end{aligned}\right\} \tag{3}$$

Φ becomes

$$\begin{aligned} \Phi(\theta,\phi) = \sum_{n,m,l,k} \Big[& \frac{1}{(2n+1)(2l+1)} \{(nl+1)\sqrt{(n+1)^2-m^2}\sqrt{(l+1)^2-k^2}P_{n+1}^m P_{l+1}^k \\ & -(nl+1+1)\sqrt{(n+1)^2-m^2}\sqrt{l^2-k^2}P_{n+1}^m P_{l-1}^k \\ & -(n+1l+1)\sqrt{n^2-m^2}\sqrt{(l+1)^2-k^2}P_{n-1}^m P_{l+1}^k \\ & +(n+1\,l+1+1)\sqrt{n^2-m^2}\sqrt{l^2-k^2}P_{n-1}^m P_{l-1}^k\} \\ & -n(n+1)P_n^m P_l^k\Big](a_n^m \cos m\phi + b_n^m \sin m\phi)(c_l^k \cos k\phi + d_l^k \sin k\phi) \\ & + \sum_{n,m,l,k} mkP_n^m P_l^k(b_n^m \cos m\phi - a_n^m \sin m\phi)(d_l^k \cos k\phi - c_l^k \sin k\phi)\,, \end{aligned} \tag{4}$$

with the aid of the recurrence formulae.

As will be studied in the succeeding sections, the righthand-side of (4) can be expanded into a series of the type

$$\Phi(\theta,\phi) = \sum_{\nu,\mu} P_\nu^\mu(\xi_\nu^\mu \cos \mu\phi + \eta_\nu^\mu \sin \mu\phi)\,. \tag{5}$$

3. Now we assume that the product of two series $\sum_{n,m} P_n^m(A_n^m \cos m\phi + B_n^m \sin m\phi)$ and $\sum_{l,k} P_l^k(C_l^k \cos k\phi + D_l^k \sin k\phi)$ is developed into a series of the type

$$\begin{aligned} \sum_{n,m,l,k} P_n^m P_l^k(A_n^m \cos m\phi + B_n^m \sin m\phi)(C_l^k \cos k\phi + D_l^k \sin k\phi) \\ = \sum_{\nu,\mu} P_\nu^\mu(\alpha_\nu^\mu \cos \mu\phi + \beta_\nu^\mu \sin \mu\phi)\,. \end{aligned} \tag{6}$$

Multiplying $P_\nu^\mu \cos \mu\phi \sin\theta d\theta d\phi$ and integrating with respect to ϕ from 0 to 2π and θ from 0 to π, we get

$$\left.\begin{aligned} \alpha_\nu^{k+m} &= \frac{2\nu+1}{4\varepsilon_{k+m}} \sum_{n,l} (A_n^m C_l^k - B_n^m D_l^k) \int_0^\pi P_n^m P_l^k P_\nu^{k+m} \sin\theta\, d\theta\,, \\ \alpha_\nu^{|k-m|} &= \frac{2\nu+1}{4\varepsilon_{|k-m|}} \sum_{n,l} (A_n^m C_l^k + B_n^m D_l^k) \int_0^\pi P_n^m P_l^k P_\nu^{|k-m|} \sin\theta\, d\theta\,, \end{aligned}\right\} \tag{7}$$

where $\varepsilon_\mu = 1$ (for $\mu = 0$), $= 2$ (for $\mu \neq 0$). β_ν^{k+m} and $\beta_\nu^{|k-m|}$ are obtained by exchanging A for B and B for $-A$.

Tabl

	A^0_0	A^0_1	A^1_1	A^0_2	A^1_2	A^2_2	A^0_3	A^1_3	A^2_3	A^3_3	A^0_4	A^1_4	A^2
α^0_0	$+1.0000C^0_0$	$+0.3333C^0_1$	$+0.3333C^1_1$	$+0.2000C^0_2$	$+0.2000C^1_2$	$+0.2000C^2_2$	$+0.1429C^0_3$	$+0.1429C^1_3$	$+0.1429C^2_3$	$+0.1429C^3_3$	$+0.1111C^0_4$	$+0.1111C^1_4$	$+0.11$
α^0_1	$+1.0000C^0_1$	$+1.0000C^0_0$ $+0.4000C^0_2$	$+0.3464C^1_2$	$+0.4000C^0_1$ $+0.2571C^0_3$	$+0.3464C^1_1$ $+0.2425C^1_3$	$+0.1917C^2_3$	$+0.2571C^0_2$ $+0.1905C^0_4$	$+0.2425C^1_2$ $+0.1844C^1_4$	$+0.1917C^2_2$ $+0.1649C^2_4$	$+0.1260C^3_4$	$+0.1905C^0_3$	$+0.1844C^1_3$	$+0.16$
α^1_1	$+1.0000C^1_1$	$+0.3464C^1_2$	$+1.0000C^0_0$ $-0.2000C^0_2$ $+0.3464C^2_2$	$-0.2000C^0_1$ $+0.2099C^1_3$	$+0.3464C^0_1$ $-0.1484C^0_3$ $+0.1917C^2_3$	$+0.3464C^1_1$ $-0.06060C^1_3$ $+0.2347C^2_3$	$-0.1484C^1_2$ $+0.1506C^1_4$	$+0.2099C^2_2$ $-0.06060C^2_3$ $-0.1167C^0_4$ $+0.1304C^2_4$	$+0.1917C^1_2$ $-0.05831C^1_4$ $+0.1543C^3_4$	$+0.2347C^2_2$ $-0.03367C^2_4$ $+0.1782C^3_4$	$-0.1167C^1_3$	$+0.1506C^0_3$ $-0.05831C^2_3$	$+0.13$ -0.033
α_2^0	$+1.0000C^0_2$	$+0.6667C^0_1$ $+0.4285C^0_3$	$-0.3333C^1_1$ $+0.3499C^1_3$	$+1.0000C^0_0$ $+0.2858C^0_2$ $+0.2858C^0_4$	$+0.1429C^1_2$ $+0.2609C^1_4$	$-0.2858C^2_2$ $+0.1844C^2_4$	$+0.4285C^0_1$ $+0.1905C^0_3$	$+0.3499C^1_1$ $+0.1429C^1_3$	0	$-0.2382C^3_3$	$+0.2858C^0_2$ $+0.1443C^0_4$	$+0.2609C^1_2$ $+0.1227C^1_4$	$+0.18$ $+0.057$
α^1_2	$+1.0000C^1_2$	$+0.5774C^1_1$ $+0.4041C^1_3$	$+0.5774C^0_1$ $-0.2474C^0_2$ $+0.3195C^2_3$	$+0.1429C^1_2$ $+0.2609C^1_4$	$+1.0000C^0_0$ $+0.1429C^0_2$ $+0.2474C^2_2$ $-0.1905C^0_4$ $+0.2129C^2_4$	$+0.2474C^1_2$ $-0.07531C^1_4$ $+0.1992C^3_4$	$-0.2474C^1_1$ $+0.06733C^1_3$	$+0.4041C^0_1$ $+0.06733C^0_3$ $+0.1305C^2_3$	$+0.3195C^1_1$ $+0.1305C^1_3$ $+0.1684C^3_3$	$+0.1684C^2_3$	$-0.1905C^1_2$ $+0.03953C^0_4$	$+0.2609C^0_2$ $+0.03953C^0_4$ $-0.07531C^2_2$ $+0.07956C^2_4$	$+0.21$ $+0.079$ $+0.11$
α^2_2	$+1.0000C^2_2$	$+0.3195C^2_3$	$+0.5774C^1_1$ $-0.1010C^1_3$ $+0.3912C^3_3$	$-0.2858C^2_2$ $+0.1844C^2_4$	$+0.2474C^1_2$ $-0.07531C^1_4$ $+0.1992C^3_4$	$+1.0000C^0_0$ $-0.2858C^0_2$ $+0.04763C^0_4$ $+0.2818C^1_4$	$-0.2130C^2_3$	$-0.1010C^1_1$ $+0.1650C^1_3$ $-0.1065C^3_3$	$+0.3195C^0_1$ $-0.2130C^0_3$	$+0.3912C^1_1$ $-0.1065C^1_3$	$+0.04763C^0_2$ $-0.1676C^2_4$	$-0.07531C^1_2$ $+0.1250C^1_4$ $-0.09919C^3_4$	$+0.18$ -0.167 -0.0661
α^0_3	$+1.0000C^0_3$	$+0.6000C^0_2$ $+0.4445C^0_4$	$-0.3464C^1_2$ $+0.3514C^1_4$	$+0.6000C^0_1$ $+0.2667C^0_3$	$-0.3464C^1_1$ $+0.09430C^1_3$	$-0.2982C^2_3$	$+1.0000C^0_0$ $+0.2667C^0_2$ $+0.1818C^0_4$	$+0.09430C^1_2$ $+0.1174C^1_4$	$-0.2982C^2_2$ $-0.05248C^2_4$	$-0.2405C^3_4$	$+0.4445C^0_1$ $+0.1818C^0_3$	$+0.3514C^1_1$ $+0.1174C^1_3$	-0.052
α^1_3	$+1.0000C^1_3$	$+0.5658C^1_2$ $+0.4303C^1_4$	$+0.4398C^0_2$ $-0.1414C^0_2$ $-0.2721C^0_4$ $+0.3043C^2_4$	$+0.4898C^1_1$ $+0.2000C^1_3$	$+0.5658C^0_1$ $+0.09425C^0_3$ $+0.1826C^2_3$	$-0.1414C^1_1$ $+0.2309C^1_3$ $-0.1491C^3_3$	$+0.09425C^1_2$ $+0.1173C^1_4$	$+1.0000C^0_0$ $+0.2000C^0_2$ $+0.2309C^2_2$ $+0.03031C^0_4$ $+0.1355C^2_4$	$+0.1826C^1_2$ $+0.1212C^1_4$ $+0.08018C^3_4$	$-0.1491C^2_2$ $+0.1575C^2_4$ $-0.1389C^3_4$	$-0.2721C^1_1$ $+0.03031C^1_3$	$+0.4303C^0_1$ $+0.1173C^0_3$ $+0.1212C^2_3$	$+0.304$ $+0.135$ $+0.157$
α^2_3	$+1.0000C^2_3$	$+0.4472C^2_2$ $+0.3848C^2_4$	$+0.4472C^1_2$ $-0.1361C^1_4$ $+0.3601C^3_4$	0	$+0.4472C^1_1$ $+0.1826C^1_3$ $+0.2357C^3_3$	$+0.4472C^0_1$ $-0.2982C^0_3$	$-0.2982C^2_2$ $-0.05248C^2_4$	$+0.1826C^1_2$ $+0.1212C^1_4$ $+0.08018C^3_4$	$+1.0000C^0_0$ $-0.2121C^0_4$ $+0.1793C^1_4$	$+0.2357C^1_2$ $-0.1173C^1_4$	$-0.2121C^2_2$	$-0.1361C^1_1$ $+0.1212C^1_3$ $-0.1173C^3_3$	$+0.384$ -0.052
α^3_3	$+1.0000C^3_3$	$+0.2940C^3_4$	$+0.5477C^2_2$ $-0.07857C^2_4$ $+0.4157C^3_4$	$-0.3333C^3_3$	$+0.2357C^2_3$	$+0.5477C^1_1$ $-0.1491C^1_3$	0	$-0.1491C^2_2$ $+0.1575C^2_4$ $-0.1389C^3_4$	$+0.2357C^1_2$ $-0.1173C^1_4$	$+1.0000C^0_0$ $-0.3333C^0_2$ $+0.09091C^0_4$	$+0.09091C^2_3$	$-0.1173C^2_3$	-0.078 $+0.157$
α^0_4	$+1.0000C^0_4$	$+0.5715C^0_3$	$-0.3499C^1_3$	$+0.5144C^0_2$ $+0.2597C^0_4$	$-0.3429C^1_2$ $+0.07115C^1_4$	$+0.08573C^2_2$ $-0.3017C^2_4$	$+0.5715C^0_1$ $+0.2338C^0_3$	$-0.3499C^1_1$ $+0.03897C^1_3$	$-0.2727C^2_3$	$+0.1169C^3_3$	$+1.0000C^0_0$ $+0.2597C^0_2$ $+0.1618C^0_4$	$+0.07115C^1_2$ $+0.08091C^1_4$	-0.301 -0.098
α^1_4	$+1.0000C^1_4$	$+0.5533C^1_3$	$+0.4518C^0_3$ $-0.1749C^2_3$	$+0.4696C^1_2$ $+0.2207C^1_4$	$+0.4696C^0_2$ $-0.1356C^0_2$ $+0.07115C^0_4$ $+0.1432C^2_4$	$-0.1356C^1_2$ $+0.2250C^1_4$ $-0.1785C^3_4$	$+0.4518C^1_1$ $+0.1509C^1_3$	$+0.5533C^0_1$ $+0.1509C^0_3$ $+0.1558C^2_3$	$-0.1749C^1_1$ $+0.1558C^1_3$ $-0.1509C^3_3$	$-0.1509C^2_3$	$+0.07115C^0_2$ $+0.08091C^0_4$	$+1.0000C^0_0$ $+0.2207C^0_2$ $+0.08091C^0_4$ $+0.2250C^2_2$ $+0.1206C^2_4$	$+0.143$ $+0.120$ $+0.0531$
α^2_4	$+1.0000C^2_4$	$+0.4948C^2_3$	$+0.3913C^1_2$ $-0.1010C^1_3$	$+0.3319C^2_2$ $+0.1039C^2_4$	$+0.3833C^1_2$ $+0.1432C^1_4$ $+0.2104C^3_4$	$+0.3319C^0_2$ $-0.3017C^0_4$ $-0.1190C^1_4$	$-0.06748C^2_3$	$+0.3913C^1_1$ $+0.1743C^1_3$ $+0.2025C^2_3$	$+0.4948C^0_1$ $-0.06748C^0_3$	$-0.1010C^1_1$ $+0.2025C^1_3$	$-0.3017C^2_2$ $-0.09891C^2_4$	$+0.1432C^1_2$ $+0.1206C^1_4$ $+0.05319C^3_4$	$+1.000$ $+0.103$ -0.0980 $+0.159$
α^3_4	$+1.0000C^3_4$	$+0.3758C^3_3$	$+0.4629C^2_3$	$-0.09090C^3_4$	$+0.3585C^2_2$ $+0.2104C^2_4$ $+0.2226C^3_4$	$+0.3585C^1_2$ $-0.1785C^1_4$	$-0.3092C^2_3$	$+0.1031C^2_3$	$+0.4629C^1_1$ $+0.1031C^1_3$	$+0.3780C^0_1$ $-0.3092C^0_3$	$-0.1888C^2_4$	$-0.1785C^1_2$ $+0.05319C^1_4$ $-0.1407C^3_4$	$+0.210$ $+0.0531$
α^4_4	$+1.0000C^4_4$	0	$+0.5345C^3_3$	$-0.3636C^4_4$	$+0.2226C^3_4$	$+0.5072C^2_2$ $-0.1190C^2_4$	0	$-0.1785C^3_3$	$+0.2305C^2_3$	$+0.5345C^1_1$ $-0.1785C^1_3$	$+0.1259C^2_4$	$-0.1407C^3_4$	-0.119 $+0.159$
			B^1_1		B^1_2	B^2_2		B^1_3	B^2_3	B^3_3		B^1_4	B^2_4

Table I

A^2_4	A^3_4	A^4_4	B^1_1	B^1_2	B^2_2	B^1_3	B^2_3	B^3_3	B^1_4	B^2_4	B^3_4	B^4_4	
$+0.1111C^2_4$	$+0.1111C^3_4$	$+0.1111C^4_4$	$+0.3333D^1_1$	$+0.2000D^1_2$	$+0.2000D^2_2$	$+0.1429D^1_3$	$+0.1429D^2_3$	$+0.1429D^3_3$	$+0.1111D^1_4$	$+0.1111D^2_4$	$+0.1111D^3_4$	$+.01111D^4_4$	
$0.1649C^2_3$	$+0.1260C^3_3$	0	$+0.3464D^1_2$	$+0.3464D^1_1$ $+0.2425D^1_3$	$+0.1917D^2_3$	$+0.2425D^1_2$ $+0.1844D^1_4$	$+0.1917D^2_2$ $+0.1649D^2_4$	$+0.1260D^3_4$	$+0.1844D^1_3$	$+0.1649D^2_3$	$+0.1260D^3_3$	0	
$0.1304C^2_3$ $0.03367C^3_3$	$+0.1543C^2_3$	$+0.1782C^3_3$	$+0.3464D^2_2$	$+0.1917D^2_3$	$+0.3464D^1_1$ $-0.06060D^1_3$ $+0.2347D^3_3$	$-0.06060D^2_2$ $+0.1304D^2_4$	$+0.1917D^2_2$ $-0.05831D^1_4$ $+0.1543D^3_4$	$+0.2347D^2_2$ $-0.03367D^2_4$ $+0.1782D^1_4$	$-0.05831D^2_3$	$+0.1304D^1_3$ $-0.03367D^3_3$	$+0.1543D^2_3$	$+0.1782D^3_3$	β^1_1
$0.1844C^2_2$ $0.05773C^3_4$	$-0.05050C^3_4$	$-0.2020C^4_4$	$-0.3333D^1_1$ $+0.3499D^1_3$	$+0.1429D^1_2$ $+0.2609D^1_4$	$-0.2858D^2_2$ $+0.1844D^2_4$	$+0.3499D^1_1$ $+0.1429D^1_3$	0	$-0.2382D^3_3$	$+0.2609D^1_2$ $+0.1227D^1_4$	$+0.1844D^2_2$ $+0.05773D^2_4$	$-0.05050D^3_4$	$-0.2020D^4_4$	
$0.2129C^2_2$ $0.07956C^3_4$ $0.1169C^3_4$	$+0.1992C^2_2$ $+0.1169C^2_4$ $+0.1237C^3_4$	$+0.1237C^3_4$	$+0.3195D^2_3$	$+0.2474D^2_2$ $+0.2129D^2_4$	$+0.2474D^1_2$ $-0.07531D^1_4$ $+0.1992D^3_4$	$+0.1305D^2_3$	$+0.3195D^1_1$ $+0.1305D^1_3$ $+0.1684D^3_3$	$+0.1684D^3_3$	$-0.07531D^2_2$ $+0.07956D^3_4$	$+0.2129D^1_2$ $+0.07956D^1_4$ $+0.1169D^3_4$	$+0.1992D^2_2$ $+0.1169D^2_4$ $+0.1237D^1_4$	$+0.1237D^3_4$	β^1_2
$0.1844C^2_2$ $0.1676C^3_4$ $.06613C^3_4$	$+0.1992C^2_2$ $-0.09919C^3_4$	$+0.2818C^2_2$ $-0.06613C^2_4$	$-0.5774D^1_1$ $+0.1010D^1_3$ $+0.3912D^3_3$	$-0.2474D^1_2$ $+0.07531D^1_4$ $+0.1992D^3_4$	$+0.2818D^1_4$	$+0.1010D^1_1$ $-0.1650D^1_3$ $-0.1065D^3_3$	0	$+0.3912D^1_1$ $-0.1065D^1_3$	$+0.07531D^1_2$ $-0.1250D^1_4$ $-0.09919D^3_4$	$-0.06613D^1_4$	$+0.1992D^1_2$ $-0.09919D^1_4$	$+0.2818D^2_2$ $-0.06613D^2_4$	β^2_2
$0.05248C^2_3$	$-0.2405C^3_3$	0	$-0.3464D^1_2$ $+0.3514D^1_4$	$-0.3464D^1_1$ $+0.09430D^1_3$	$-0.2982D^2_3$	$+0.09430D^1_2$ $+0.1174D^1_4$	$-0.2982D^2_2$ $-0.05248D^2_4$	$-0.2405D^3_4$	$+0.3514D^1_1$ $+0.1174D^1_3$	$-0.05248D^2_3$	$-0.2405D^3_3$	0	
$0.3043C^2_1$ $0.1355C^3_1$ $0.1575C^3_3$	$+0.08018C^2_2$	$-0.1389C^3_3$	$-0.1414D^2_2$ $+0.3043D^2_4$	$+0.1826D^2_3$	$-0.1414D^1_1$ $+0.2309D^1_3$ $-0.1491D^3_3$	$+0.2309D^2_2$ $+0.1355D^2_4$	$+0.1826D^2_2$ $+0.1212D^1_4$ $+0.08018D^3_4$	$-0.1491D^2_2$ $+0.1575D^2_4$ $-0.1389D^1_4$	$+0.1212D^2_3$	$+0.3043D^1_1$ $+0.1355D^1_2$ $+0.1575D^3_3$	$+0.08018D^2_3$	$-0.1389D^3_3$	β^3_3
$0.3848C^2_1$ $0.05248C^3_3$	$+0.3601C^2_1$ $+0.08018C^3_3$	$+0.1793C^2_2$	$-0.4472D^1_2$ $+0.1361D^1_4$ $+0.3601D^3_4$	$-0.4472D^1_1$ $-0.1826D^1_3$ $+0.2357D^2_3$	0	$-0.1826D^1_2$ $-0.1212D^1_4$ $+0.08018D^3_4$	$+0.1793D^2_4$	$+0.2357D^1_2$ $-0.1173D^1_4$	$+0.1361D^1_1$ $-0.1212D^1_2$ $-0.1173D^3_3$	0	$+0.3601D^1_1$ $+0.08018D^1_3$	$+0.1793D^2_3$	β^2_3
$0.07857C^2_1$ $0.1575C^3_3$	$+0.2940C^2_1$ $-0.2405C^3_3$	$+0.4157C^2_1$ $-0.1389C^3_3$	$-0.5477D^2_2$ $+0.07857D^2_4$ $+0.4157D^1_4$	$-0.2357D^2_3$	$-0.5477D^1_1$ $+0.1491D^1_3$	$+0.1491D^2_2$ $-0.1575D^2_4$ $-0.1389D^1_4$	$-0.2357D^1_2$ $+0.1173D^1_4$	0	$+0.1173D^2_3$	$+0.07857D^1_1$ $-0.1575D^1_3$	0	$+0.4157D^1_1$ $-0.1389D^1_3$	β^3_3
$0.3017C^2_2$ $0.09891C^2_4$	$-0.1888C^3_4$	$+0.1259C^4_4$	$-0.3499D^1_3$	$-0.3429D^1_2$ $+0.07115D^1_4$	$+0.08573D^2_2$ $-0.3017D^2_4$	$-0.3499D^1_1$ $+0.03897D^1_3$	$-0.2727D^2_3$	$+0.1169D^3_3$	$+0.07115D^1_2$ $+0.08091D^1_4$	$-0.3017D^2_2$ $+0.03891D^2_4$	$-0.1888D^3_4$	$+0.1259D^4_4$	
$0.1432C^2_2$ $0.1206C^3_4$ $.05319C^3_4$	$-0.1785C^2_2$ $+0.05319C^2_4$ $-0.1407C^3_4$	$-0.1407C^3_4$	$-0.1749D^2_3$	$-0.1356D^2_2$ $+0.1432D^2_4$	$-0.1356D^1_2$ $+0.2250D^1_4$ $-0.1785D^3_4$	$+0.1558D^2_3$	$-0.1749D^1_1$ $+0.1558D^1_3$ $-0.1509D^3_3$	$-0.1509D^2_3$	$+0.2250D^2_2$ $+0.1206D^2_4$	$+0.1432D^1_2$ $+0.1206D^1_4$ $+0.05319D^3_4$	$-0.1785D^2_2$ $+0.05319D^2_4$ $-0.1407D^1_4$	$-0.1407D^3_4$	β^3_4
$1.0000C^0_0$ $0.1039C^2_2$ $.09891C^2_4$ $0.1596C^3_4$	$+0.2104C^2_2$ $+0.05319C^3_4$	$-0.1190C^2_2$ $+0.1596C^2_4$	$-0.3913D^1_3$ $-0.1010D^1_3$	$-0.3833D^1_2$ $-0.1432D^1_4$ $+0.2104D^2_4$	$-0.1190D^1_4$	$-0.3913D^1_1$ $-0.1743D^1_3$ $+0.2025D^1_3$	0	$-0.1010D^1_1$ $+0.2025D^1_3$	$-0.1432D^1_2$ $-0.1206D^1_4$ $+0.05319D^3_4$	$+0.1596D^1_4$	$+0.2104D^1_2$ $+0.05319D^1_4$	$-0.1190D^2_2$ $+0.1596D^2_4$	β^2_4
$0.2104C^2_2$ $.05319C^3_4$	$+1.0000C^0_0$ $-0.09090C^2_2$ $-0.1888C^3_4$	$+0.2226C^2_2$ $-0.1407C^3_4$	$-0.4629D^2_3$	$-0.3585D^2_2$ $-0.2104D^2_4$ $+0.2226D^1_4$	$-0.3585D^1_2$ $+0.1785D^1_4$	$-0.1031D^2_3$	$-0.4629D^1_1$ $-0.1031D^1_3$	0	$+0.1785D^2_2$ $-0.05319D^2_4$ $-0.1407D^1_4$	$-0.2104D^1_2$ $-0.05319D^1_4$	0	$+0.2226D^1_2$ $-0.1407D^1_4$	β^3_4
$0.1190C^2_2$ $0.1596C^3_4$	$+0.2226C^2_2$ $-0.1407C^3_4$	$+1.0000C^0_0$ $-0.3636C^2_2$ $+0.1259C^3_4$	$-0.5345D^1_3$	$-0.2226D^2_4$	$-0.5072D^2_2$ $+0.1190D^2_4$	$+0.1785D^1_3$	$-0.2305D^2_3$	$-0.5345D^1_1$ $+0.1785D^1_3$	$+0.1407D^3_4$	$+0.1190D^2_2$ $-0.1596D^3_4$	$-0.2226D^1_3$ $+0.1407D^1_4$	0	β^4_4
B^2_4	B^3_4	B^4_4	$-A^1_1$	$-A^1_2$	$-A^2_2$	$-A^1_3$	$-A^2_3$	$-A^3_3$	$-A^1_4$	$-A^2_4$	$-A^3_4$	$-A^4_4$	

In practice, integrations of products of three spherical harmonics for low degrees are already calculated being used in atomic physics.[1] Using these tables, the writer obtained α's and β's for $n \leqq 4$, $l \leqq 4$ and $\nu \leqq 4$ as shown in Table I. α's are given with linear sum of the corresponding columns multiplied by the indices written at the highest line. β's, which are shown on the most right column, are given with linear sum of the corresponding columns multiplied by the indices written at the lowest line.

4. Using Table I obtained in section 3, ξ's and η's are calculated for $n \leqq 3$, $l \leqq 3$ and $\nu \leqq 3$ being shown in Table II. If the righthand-side of (2), say $a \sin\theta \left\{ \frac{\partial E_\theta}{\partial \phi} - \frac{\partial}{\partial \theta}(\sin\theta\, E_\phi) \right\}$, is given by a series of sphericel harmonics, we get simultaneous equations by equating the corresponding coefficients of both sides. Then, solving these equations, we can obtain J for given L and $\vec{E}$ or L for given J and $\vec{E}$.

5. An approximate method of studying the distributions of electric currents in a thin spherical shell having non-uniform conductivity is described in this paper. Although the results obtained by this method contain errors,[2] especially in the coefficients of higher harmonics, it may be useful to apply the method to some problems of geomagnetism. Actual example will be shown in another paper.

---

1) Condon and Shortley, *Theory of Atomic Spectra*. p. 178.
Shortley, *Phys. Rev.* **54** (1938), 739.
A. Amemiya, *Nippon Sugaku-Butsurigaku-Kaishi*. **17** (1943), 77.
The values in these tables are based on exactly normalized functions. The writer recalculated these values because we use Ad. Schmidt's functions.

2) In order to check the method, we shall study a simple case $L = c_0^0$, $E_\theta = 0$, and $E_\phi = E_0 \sin\theta$. The rigorous solution is easily obtained as follows;

$$a_1^0 = 0.4000\, aE_0/c_0^0, \quad a_3^0 = -0.06667\, aE_0/c_0^0.$$

On the other hand, using Table II we have

$$a_1^0 = 0.3916\, aE_0/c_0^0, \quad a_3^0 = -0.05362\, aE_0/c_0^0.$$

Comparing these values, we find some discrepancies. These discrepancies are due to the fact that we neglect higher harmonics of which degrees are larger than 3.

4. *A Study on Regional Anomaly in the Earth's Magnetic Field.*

By Tsuneji RIKITAKE,

Earthquake Research Institute.

(Read Oct. 19, 1948.—Received Apr. 10, 1949.)

1. Although we do not know whether the main "dipole field" of geomagnetism is due to general nature of a massive rotating body[1] or some mechanism of excitation in the earth,[2] the regional anomaly, which seems peculiar to the earth, is naturally considered to be a secondary effect by a number of investigators. Among these investigations, the possibility of the regional anomaly as the magnetization of the upper part of the earth was quantitatively discussed by T. Nagata[3] showing that the anomaly contained the part that could not be explained by such magnetizatian and moreover the magnetic susceptibility of the subterranean mass must be far beyond the magnitude of the rocks' experimentally obtained.

According to the writer's study[4] on the electrical state of the earth's interior, there is a very sharp discontinuity in the electric conductivity at the depth of 400 *km*. It increases at this level from 10^{-15} *emu* to 10^{-12} *emu*. If we allow the existence of electromotive forces in this region, a comparatively small irregularity in the conductivity-distribution may cause irregular distribution of electric currents which may be thought to correspond to the magnetic anomaly observed at the earth's surface. From this point of view, the writer approximately estimate the non-uniformity in the conductivity assuming that the electromotive force is the same with that which may be responsible for the "dipole field" and the heterogeneity can be condensed in a thin shell.

2. The relation between the current-function and electromotive

1) P. M. S. BLACKETT, *Nature*, **159** (1947) 658.

2) W. M. ELSASSER, *Phys. Rev.*, **55** (1939) 489, **69** (1946) 106, **70** (1946) 202.

3) T. NAGATA, *Bull. Earthq. Res. Inst.*, **20** (1942) 107, **21** (1944) 366.

4) T. RIKITAKE, *Report for International Association of Terrestrial Magnetism and Electricity*, Oslo Assembly, August 1948.

force in a thin spherical shell is given by[5)]

$$\Phi(\theta,\phi) = a\sin\theta\left\{\frac{\partial E_\theta}{\partial\phi} - \frac{\partial}{\partial\theta}(\sin\theta\, E_\phi)\right\}, \tag{1}$$

where

$$\Phi(\theta,\phi) = \frac{\partial L}{\partial\phi}\frac{\partial J}{\partial\phi} + \sin^2\theta\frac{\partial L}{\partial\theta}\frac{\partial J}{\partial\theta} + L\sin^2\theta\left\{\frac{\partial}{\sin\theta\,\partial\theta}\left(\sin\theta\frac{\partial J}{\partial\theta}\right) + \frac{1}{\sin^2\theta}\frac{\partial^2 J}{\partial\phi^2}\right\}. \tag{2}$$

In the expressions E_θ, E_ϕ, J and a denote respectively southward and eastward component of electromotive force, current-function and radius of the shell. L is defined by $1/\int\sigma dD$, that is the reciprocal of the total conductivity.

If we assume that J and L is giyen by

$$J = \sum_{n,m} P_n^m(a_n^m\cos m\phi + b_n^m\sin m\phi), \tag{3}$$

$$L = \sum_{l,k} P_l^k(c_l^k\cos k\phi + d_l^k\sin k\phi), \tag{4}$$

and besides

$$E_\theta = 0, \quad E_\phi = -E_0\sin\theta \tag{5}$$

that may correspond to the electromotive force responsible for the "dipole field," (1) becomes

$$\sum_{\nu,\mu} P_\nu^\mu(\xi_\nu^\mu\cos\mu\phi + \eta_\nu^\mu\sin\mu\phi) = \frac{4}{5}aE_0(P_1^0 - P_3^0). \tag{6}$$

Equating the corresponding coefficients of both sides of (6), we get

$$\xi_1^0 = \frac{4}{5}aE_0, \quad \xi_3^0 = -\frac{4}{5}aE_0 \quad \text{(The other coef. are all zero.)} \tag{7}$$

ξ's and η's are given in Tabelle II of literature (5) as linear combinations of products of $a_n^m c_l^k$ and $b_n^m d_l^k$.

Meanwhile, the magnetic potential of the regional anomaly is given by

$$W = P_1^1(g_1^1\cos\phi + h_1^1\sin\phi) + \sum_{n=2}^{\infty}\sum_{m=0}^{n} P_n^m(g_n^m\cos m\phi + h_n^m\sin m\phi).$$

5) T. RIKITAKE, *Bull. Earthq. Res. Inst.*, **26** (1948) 11.

When we assume that the magnetic field is caused by the electric currents flowing over a spherical surface of radius a, we have the next relations

$$\left.\begin{matrix} a_n^m \\ b_n^m \end{matrix}\right\} = \frac{1}{4\pi}\frac{2n+1}{n}\left(\frac{R}{a}\right)^{n+1}\begin{matrix} g_n^m \\ h_n^m \end{matrix} \tag{8}$$

where R denotes the earth's radius. Under the assumption that the currents flow in a shell the depth of which is 1000 km, a_n^m and b_n^m are calculated on the basis of Dyson and Furners' analysis,[6] the current systems being shown in Fig. 1.

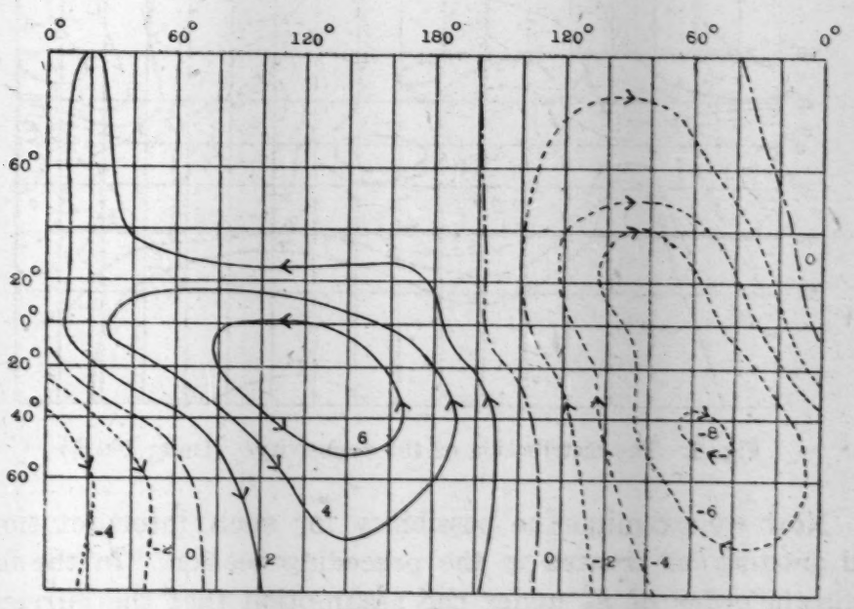

Fig. 1. The current-system for the regional anomaly. 4×10^7 amperes flow between adjacent lines.

Hence, we obtain 16 simultaneous equations from (7) of which solutions become

$$c_0^0=-1,\quad c_1^0=-4,\quad c_1^1=-6,\quad c_2^0=-15,\quad c_2^1=-10,\quad c_2^2=1,$$
$$c_3^0=6,\quad c_3^1=-1,\quad c_3^2=-10,\quad c_3^3=15,\quad d_1^1=-1,\quad d_2^1=-5,$$
$$d_2^2=-1,\quad d_3^1=-2,\quad d_3^2=6,\quad d_3^3=8. \qquad \text{(Unit: } 10aE_0) \tag{9}$$

As shown in the above-mentioned paper,[5] however, the determined coefficients contain some errors, especially the errors in higher degree

6) F. DYSON and H. FURNER, *Geophys. Suppl. M. N. R. A. S.*, **1** (1923), 76.

term may reach about 10%. The distribution of L, except constant part, is obtained by summing up (4) as shown in Fig. 2. Though the determination is not accurate, it is of interest that the largest gradient of L is found near the West Africa where the secular variation is very large. But, we cannot find any close relation between the distribution of L and that of the continents.

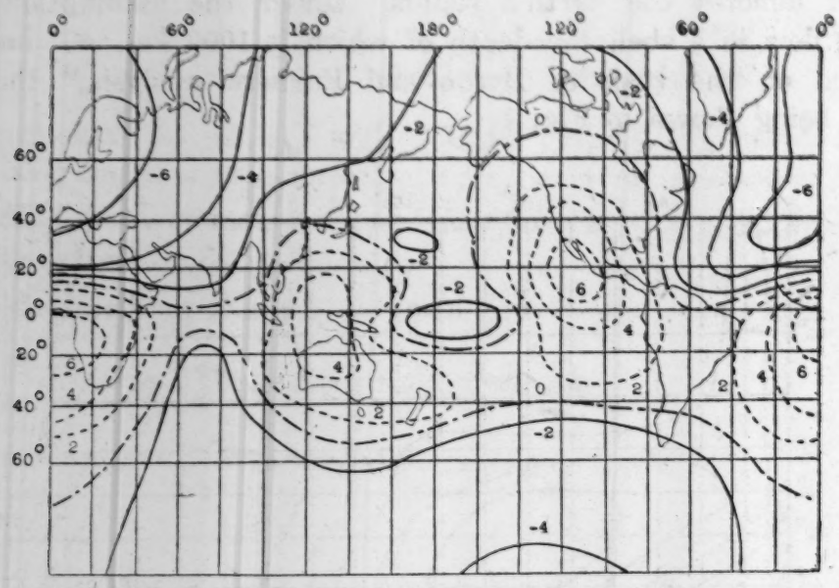

Fig. 2. The distribution of the resistivity. (Unit: $10aE_0$)

3. Now we examine the possibility for such interpretation of the regional anomaly as treated in the preceding section. In the first place, we obtain the order of E_0 under the assumption that the current-density is uniform between the centre of the earth and $r = a$. As is well known, the current density responsible for the "dipole field" is $0.8 \sin\theta$ *amp./cm* when the currents flow just beneath the earth's surface, the current-density expected from the assumption becomes $2.1 \times 10^{-9} \sin\theta$ *amp./cm*^{2}. Giving 10^{-11} *emu* to the conductivity, we have

$$E_0 = 2.1 \times 10^{-7}\ volt/cm = 2.1 \times 10\ emu/cm$$

and consequently

$$aE_0 = 1.1 \times 10^{10}\ emu\,.$$

Hence the largest unevenness in L becomes to the order of 3×10^{12} *emu*. If this unevenness is distributed within 100 *km*, the unevenness reduced to the specific value of the conductivity becomes 3×10^{-20} *emu*.

Taking into consideration that the conductivity amounts to the order of $10^{-12} \sim 10^{-11}$ *emu*, such small difference may be possible.

4. A hypothesis that the regional anomaly in the earth's magnetic field is caused by the electric currents flowing at the depth of 1000 *km* is quantitatively examined. As to the electromotive force, the similar one with that which may cause the main "dipole field" is taken. Though the distribution of the conductivity obtained here has no close relation to the distribution of land and sea, its range is comparatively small so that we easily imagine such heterogeneity. Until we have any other evidence about such non-uniformity in the electrical state at that depth, studies in detail will be postponed.

5. *Observations of the Deformation of the Earth's Surface at Aburatsubo, Miura Peninsula. Part I.*

By Takahiro HAGIWARA, Tsuneji RIKITAKE, and Juhei YAMADA,

Earthquake Research Institute.

(Read April 20, Sept. 21, 1948.—Received April 10, 1949.)

1. The crustal movements of the peninsulas associated with the destructive earthquakes are of great interest in this country. In order to study the secular deformation of a peninsula, the writers began continuous observations of the deformation of the earth's surface at Aburatsubo, near the southern extremity of the Miura Peninsula, the situation being shown in Fig. 1. The instruments were installed in a gallery drilled in the Tertiary sandstone in the site of the Marine Biological Station of Tokyo University. The general view of the topography is shown in Fig. 2. The observations were commenced in March, 1948.

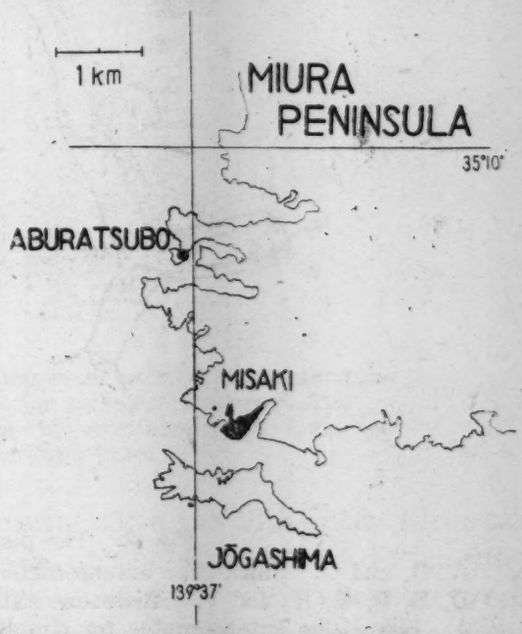

Fig. 1. The map of the southern extremity of Miura Peninsula.

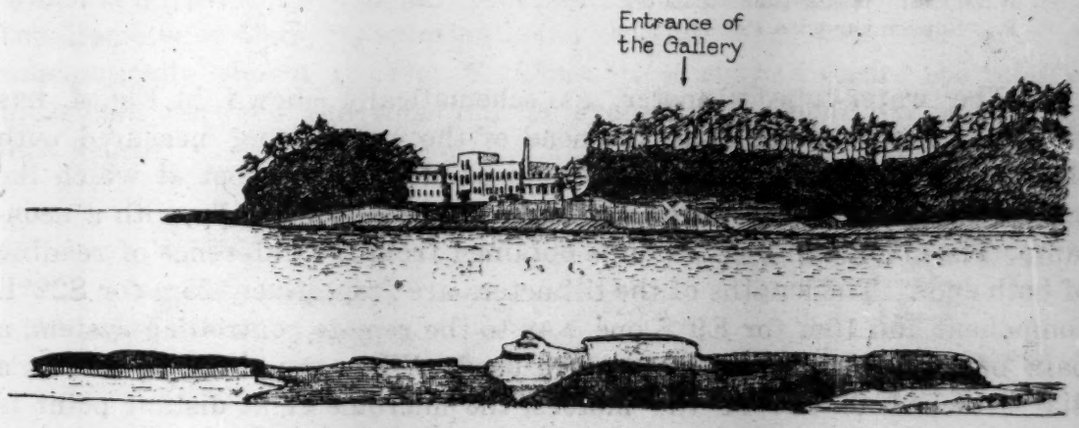

Fig. 2. General view of Aburatsubo sketched from the east-side.

2. A pair of Ishimoto-type all-silica tiltmeters, a pair of water-tube tiltmeters with remote controlling device and the silica-tube extensometers of various types were set up in the gallery as shown in Fig. 3.

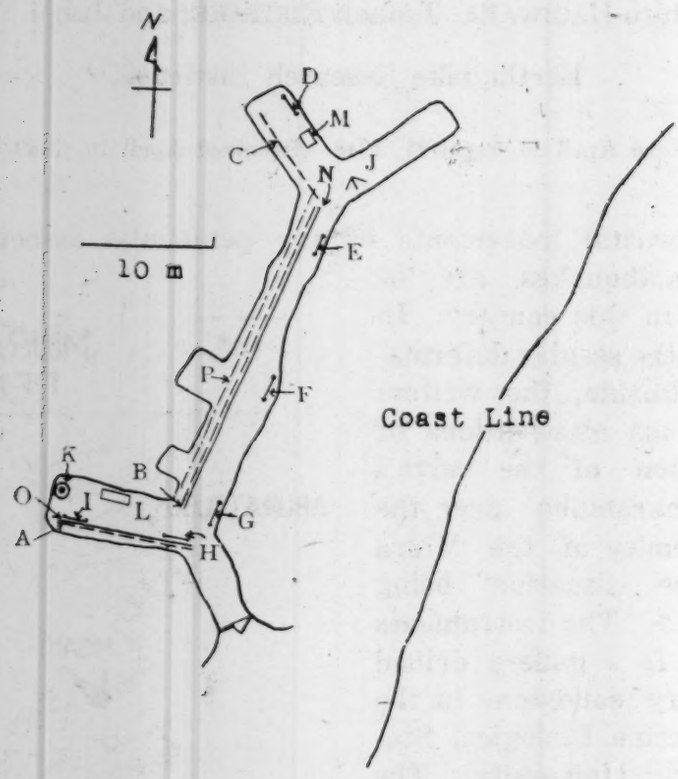

Fig. 3. The plan of the gallery.
A, B, and C: Silica-tube extensometer.
D, E, F, G, H, and I: Silica-tube extensometer, the length of which is 1 m.
J: Silica-tube extensometer for simultaneous recording of three components.
K: Silica-tube extensometer for vertical component.
L and M: Ishimoto-type all-silica tiltmeter.
N and O: Water-tube tiltmeter.
P: Superinvar-wire extensometer.

The water-tube tiltmeter, as schematically shown in Fig. 4, has water-reservoirs at the ends, the head of the water being measured with the micrometers with a sharp platinum-point. The moment at which the micrometer touches the water-surface is detected electrically with a neon-lamp. The change in inclination is obtained from the difference of reading of both ends. The lengths of the tiltmeters are respectively 25m for S22°E component and 10m for E9°S one. As to the remote controlling system, a pair of self-synchronous motors are used. When the observer rotates a dial attached to one of the motors, the micrometer at distant point is rotated synchronously with another motor. According to the results of

the calibration, the errors due to the remote controlling system was found to be negligible.

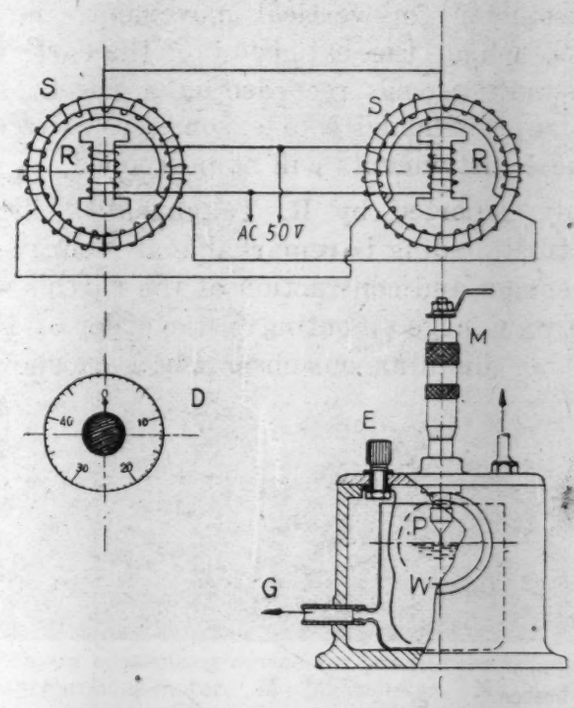

Fig. 4. The schematic view of the main part of the water-tube tiltmeter and the circuit for self-synchronous motors.
S: stater R: rotor D: dial M: micrometer E: electrode
P: platinum W: water G: glass tube.

Two silica-tube extensometers are installed parallel to the tiltmeters, their lengths being the same with those of the tiltmeters. Silica-tubes, 7mm in diameter and 1m in length, are jointed by thin phosphorbronze band and supported on the metal rollers lying on the smooth glass plates. One end of the extensometer is fixed to the concrete-block, the base of which is buried in the ground. Another end is placed on a roller of which the diameter is 6mm, its rotation being magnified with optical lever as schematically shown in Fig. 5. Thus, it is easy to record the relative movement between the tube and the ground with sensitivity of 10^{-7} per unit length.

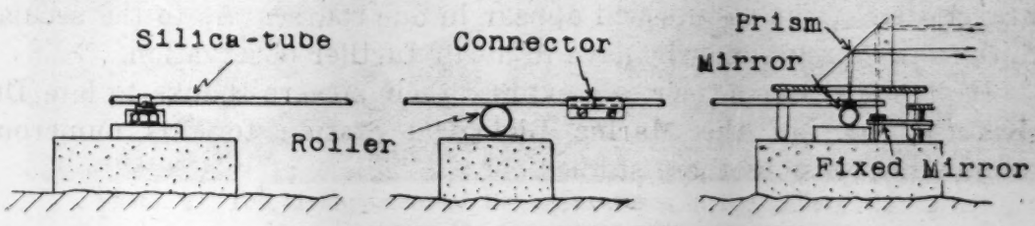

Fig. 5. The schematic view of the main part of the extensometer.

After some months, an extensometer with 8 m's length is added to the direction E65°S. In addition, there were also installed in the gallery a silica-tube extensometer for vertical movement, the short silica-tube extensometers with which the extension of the earth's surface in three directions can be simultaneously recorded on a sheet of paper, and one component of the superinvar-wire extensometer. However, the description in detail of these instruments will be postponed.

3. As already reported by R. Takahashi[1], tilting of the earth's surface caused by tidal loading is remarkable at Aburatsubo. The writers found that the extension and contraction of the earth's surface due to the ocean tide are also very large amouting to the order of 10^{-7}—10^{-6} per unit length. The results of simultaneous observation are shown in Fig. 6. The

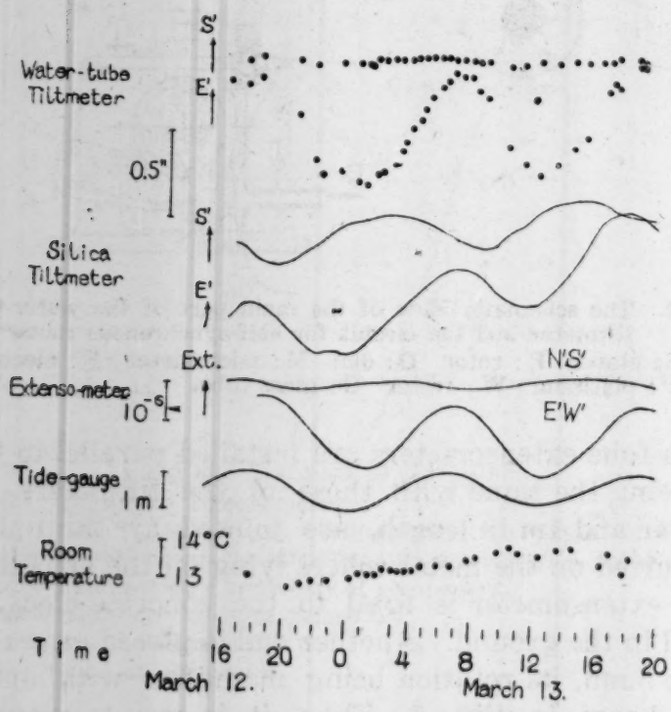

Fig. 6. The results of the simultaneous observations on Mar. 12~13, 1948. N'S' and E'W' denote respectively N22°E and E9°S.

interpretation of the results will appear in due course. As to the secular variation, the discussion will have to await further observation.

In conclusion, the writers express their sincere thanks to late Dr. K. Kikuchi, chief of the Marine Biological Station for his numerous courtesies in course of these studies.

1) R. TAKAHASHI, *Bull. Earthq. Res. Inst.*, **6** (1929), 85.

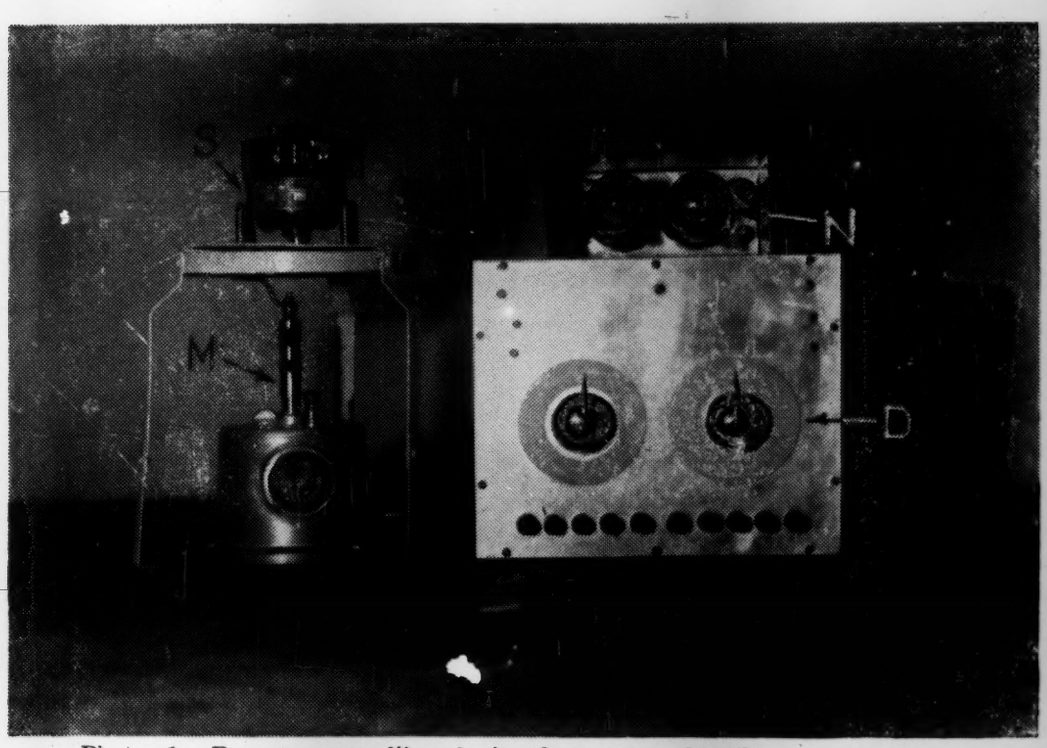

Photo. 1. Remote controlling device for water-tube tiltmeter.
S: Self-synchronous motor. M: Micrometer. N: Neon lamp. D: Dial.

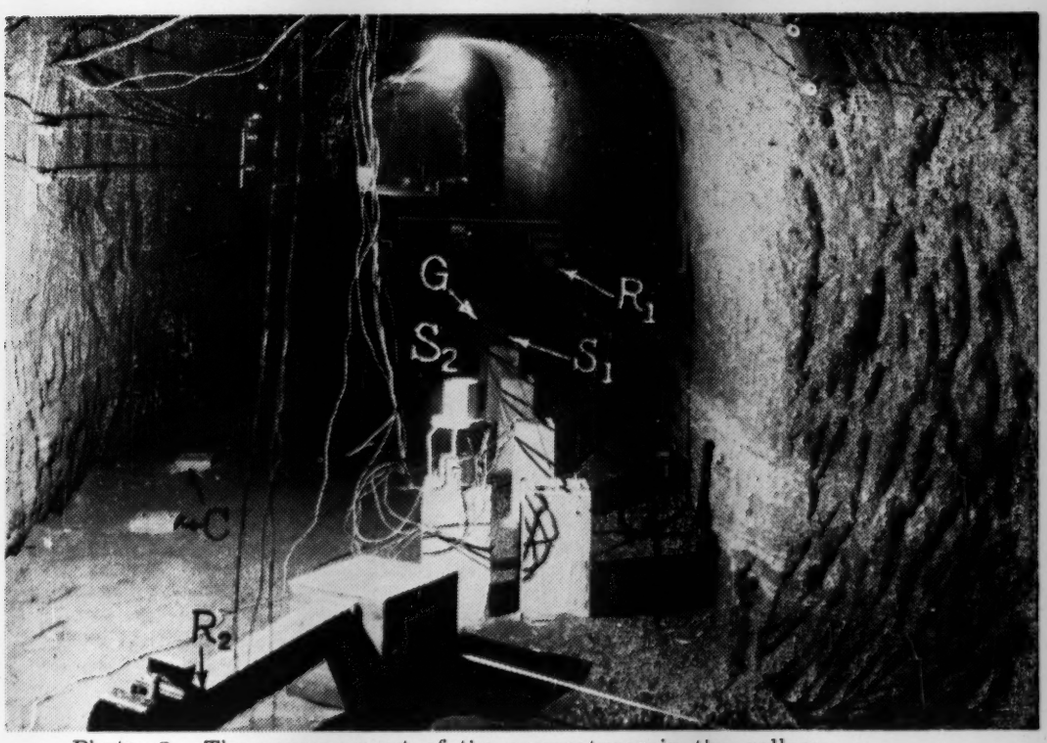

Photo. 2. The arrangement of the apparatuses in the gallery.
R_1: Recorder for superinvar-wire extensometer.
S_1: Silica-tube of the extensometer of N22°E component.
S_2: Self-synchronous motor.
C: Concrete block for 1 m extensometer.
R_2: Recorder for the extensometer of E65°S component.
G: Glass tube filled with water.

6. *Local Phenomena of Tsunami (Part 2).*

By Nobuji NASU,

Earthquake Research Institute.

(Read Feb. 15, 1949.—Received March 31, 1949.)

The estimation of the speed with which the seismic sea waves sweep over the land is necessary for the determination of the extent of their dynamical effects upon structures of various kinds. It will furnish excellent data for the mitigation plan of the damage caused by the tsunami. There are, however, no data which are available for this purpose, because no systematic investigation relating to the intensity of the tsunami was tried in the past destructive tsunamis. During our inspection tour to the districts which suffered a considerable damage in the recent Nankaido tsunami of 1946, good examples were found which enabled us to estimate the speed of the tsunami. Generally speaking, in these estimations only simple cases have to be taken, like in the determination of the seismic intensity from the damage of simple structures. An assumption must be introduced herein, such that the motion of the water is steady; this corresponds to the assumption of the simple harmonic motion which is usually made for the earthquake motion. The principles of the estimation of the velocity treated in this paper are based on the following facts.

First, in a certain area, the change in the height of the tsunami is much influenced by the speed of the flowing water and the geographical feature of this area. This change and the land-feature will be made clear by means of the precise leveling survey, and from the result of it we can estimate the flowing velocity of the tsunami.

Secondly, the force acts on the body submerged in the water varies with the square of the velocity with which the water impinges upon the body. Hence, the estimation of the velocity of the water is possible from the damage caused on the simple structures, if the strengths of these structures are known.

There are, however, various metdods of estimations basing on the facts above mentioned. In the following, the methods which are of practical use will be described.

We shall take up four examples basing on the fact first cited.

(1) *Curved river.* The flowing velocity of the tsunami can be determined from the amount of elevation of the water-surface measured on both sides of the curved river. When the sea water runs up the curved course, the surface of the water becomes higher on the outer river bank than on the inner one by the action of the centrifugal force (Fig. 1.). The difference of height, H, in this case is given by

$$H = \frac{v^2}{g} \log_e \frac{b}{a}, \tag{1}$$

where v denotes the velocity, g the gravity-acceleration, a and b are the radii of curvature of the inner and outer banks respectively. An actual example was the brook which flowed into the sea at the head of Yura Bay, Wakayama Prefecture. Here, the velocity was estimated to be 2.26 m./sec.; the value being calculated for the actually obtained values of $H = 0.19$ m., $a = 50$ m. and $b = 60$ m. Another similar example was at Inami about 500 m. up the river mouth where water-course curved with the radii of $a = 140$ m. and $b = 160$ m. From the elevation of the water-surface which mersured 0.21 m., the velocity worked out as 3.16 m./sec. This value fairly agreed with that determined by another method of estimation which will be cited later in this paper, that is, 3.00 m./sec., the value estimated from the overturning of a concrete wall which stood at a distance of 50 m. from this point.

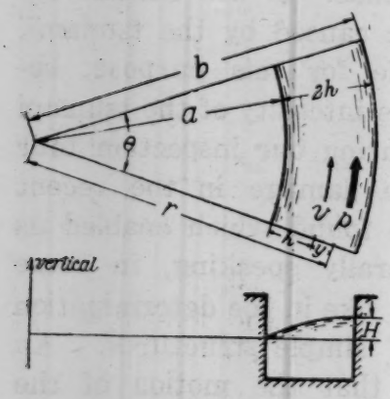

Fig. 1.

In the above example, the velocity is assumed to be uniform throughout the cross-section of the river. It varies, however, considerably across the river. Of course, the velocity is the maximum in the middle of a river and the minimum near the banks, but the point of the maximum velocity is not exactly at the centre of the width of the river, it leans to the inner bank. Putting $b = a + 2h$, $\frac{h}{a} = \alpha$, the velocity at any point where $r = a + h + y$ is given by

$$v = -\frac{1}{2\mu}\frac{\partial p}{\partial \theta}\frac{h}{a}\left\{\left[\frac{(1+2\alpha)^2 \log(1+2\alpha)}{4\alpha+4\alpha^2}\right]\left[1+\alpha+\frac{\alpha y}{h}-\frac{1}{1+\alpha+\frac{\alpha y}{h}}\right]\right.$$
$$\left.-\left(1+\alpha+\frac{\alpha y}{h}\right)\log\left(1+\alpha+\frac{\alpha y}{h}\right)\right\}, \tag{2}$$

and $\bar{v}$, the mean value of v is

$$\bar{v} = -\frac{1}{4\mu}\frac{\partial p}{\partial \theta}\frac{h}{\alpha}\left\{\alpha+\alpha^2-\frac{(1+2\alpha)^2}{4(\alpha+\alpha^2)}[\log(1+2\alpha)]^2\right\}, \qquad (3)$$

or in other forms,

$$v = -\frac{1}{2\mu}\frac{\partial p}{\partial \theta}\left[\frac{(b^2\log b-a^2\log a)}{b^2-a^2}r-\frac{a^2b^2}{b^2-a^2}\left(\log\frac{b}{a}\right)\frac{1}{r}-r\log r\right], \qquad (4)$$

and

$$\bar{v} = -\frac{1}{2\mu}\cdot\frac{1}{b-a}\frac{\partial p}{\partial \theta}\left[\frac{(b^2-a^2)}{4}-\frac{a^2b^2}{b^2-a^2}\log\left(\frac{b}{a}\right)^2\right], \qquad (5)$$

where μ denotes the viscosity, $\frac{\partial p}{\partial \theta}$ the pressure-gradient along the river course and is constant in this case. In Fig. 2, the distribution of the ratio $v:\bar{v}$ in a cross-section is shown for given values of α[1)]

It will be seen that if the curvature of the river is small, that is, α is large, the effect of the curvature is noticeable, but otherwise it is not. Further, the maximum velocity which is expected becomes one and half times as large the estimated mean value.

(2) *Straight water-course with corrugated bottom.* In a street where the flow of the water is limited only in one direction by the houses and walls standing on both sides of the street, a noticeable change in the height of the water can be seen along the street, if the surface of the ground is corrugated. Assuming that such a street is a straight canal having a rectangular cross-section and a sinuous bottom in the from $y = a\sin mx$, Where x is the lengthwise direction of the canal, m a constant and a is also a constant which is small compared with the mean depth of the water in the canal, h.

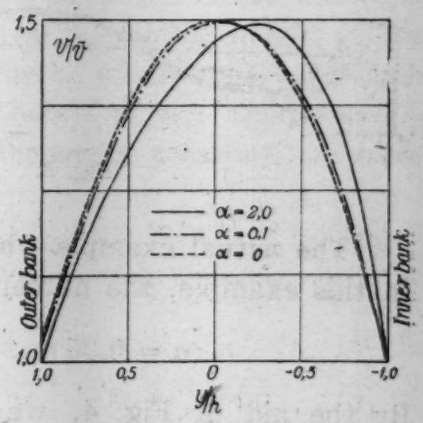

Fig. 2.

The elevation of the free surface of water has the form $y' = b\sin mx$. Then, for a given value of x, the ratio $y':y$, that is, $b:a$ is

$$\frac{b}{a} = \frac{1}{\cosh mh-\frac{g}{mv^2}\sinh mh}, \qquad (6)$$

1) Modern Developments in Fluid Dynamics, Oxford Eng. Sc. Ser. 1, 1938.

where v denotes the general velocity of the water in the canal, g the acceleration due to gravity.[2] The velocity of the water can be determined if $b:a$ is known. The crests and troughs of the free surface and the bottom correspond or are opposite as

$$v^2 \gtrless \frac{g}{m} \tanh mh \tag{7}$$

or

$$v^2 \gtrless c^2 \tag{8}$$

where c is the velocity of propagation of the wave of the length $2\pi/m$ in water of depth h. As an extreme case, if $v = c$, the ratio b/a becomes infinite, this means that the free surface cannot be represented by a simple sine-curve, the assumption from which this calculation started breaks down in this case.

Fig. 3.

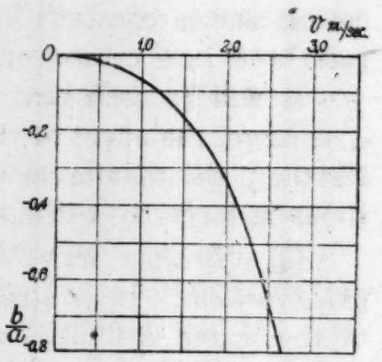

Fig. 4.

The actual example which was found at Kainan is shown in Fig. 3. In this example, the numerical values actually determined are,

$$a = 0.35\,\text{m.},\quad b = 0.12\,\text{m.},\quad b/a = 0.343.$$

By the aid of Fig. 4, we can determine the velocity as 2.0 m./sec. It must be remembered that the estimation is impossible, if $v = 3.95$ m./sec., because in this case the ratio b/a becomes infinite. However, the value estimated here is only one-half of this extreme value, thus there is no objection in this estimation.

(3) *Tsunami dissipation zone.* For convenience, a brief explanation of the tsunami dissipation zone[3] will be given here. The idea is that

---

2) The expression is derivable from a complex potential,

$$w = -Uz + \frac{aU}{\sinh mh}\cos m(z-ih) - \frac{bU}{\sinh mh}\cos mz\,, \qquad z = x+iy\,.$$

3) A. IMAMURA: *Theoretical and Applied Seismology*, p. 134, 1937.

the energy of the tsunami will be dissipated if the water spreads over a wide area which is devoted to this zone after passing through a narrow water course. As the result, the important part of the city or town can escape the full force of tsunami. Hence, in cities which have in their immediate vicinity the water-courses, such as valleys or inhabited lowland, flat ground, these areas should be utilized for this purpose. The lowland which acts as such a safety measure is called the "tsunami dissipation zone."

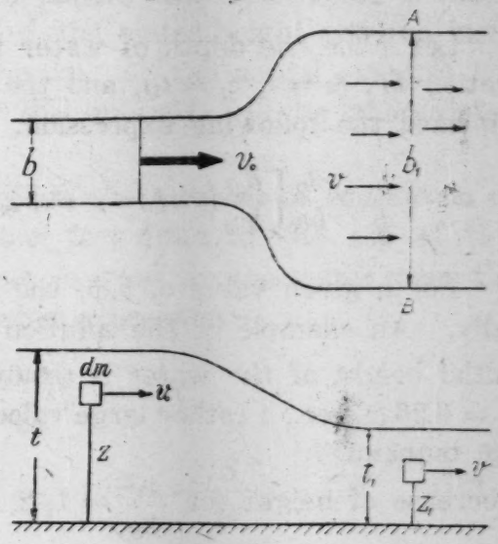

Fig. 5.

Taking up an ideal case as is schematically shown in Fig. 5, the decrease of the water-height in the dissipation zone will be calculated in the following.

Let the cross-section of the narrow course of water be b, the velocity of the elementary volume of water, dm, be v_0 and the height of dm above the ground be z. After spreading over a wider area, of which the width is b_1, dm has a velocity of v and a height of z_1. Then, the difference of height is $z-z_1$. Neglecting the change in pressure, we have

$$\frac{1}{2}dm(v^2-v_0^2) = g\,dm(z-z_1)\,. \tag{9}$$

Put,
$$dm = \frac{\rho}{g}b\,dz\,v_0\,dt = \frac{\rho}{g}b_1\,dz_1\,v\,dt\,, \tag{10}$$

where ρ denotes the density of the water.

It follows,
$$b\,v_0\,dz = b_1\,v\,dz_1\,,$$

and
$$v = \frac{1}{a}\frac{dz}{dz_1}\,, \quad \left(a = \frac{b_1}{v_0 b}\right). \tag{11}$$

Therefore, expression (9) may be written as

$$\frac{dz}{dz_1} = a\sqrt{v_0^2+2g(z-z_0)} = aZ\,. \tag{12}$$

After integration we have

$$a(agz_1+v_0-z) = \log\frac{aZ-1}{av_0-1}. \tag{13}$$

Let t be the depth of water in cross-section b, t_1 be that in cross-section b_1, $(z=t,\ z_1=t_1)$, and the decrease of height $h=t-t_1$. For h we have the following expression.

$$\frac{b_1}{b}+\frac{b_1}{bv_0}\left[\frac{b_1g}{bv_0}(t-h)-\sqrt{v^2+2gh}\right] = \log\frac{b_1\sqrt{v_0^2+2gh}-bv_0}{v_0(b_1-b)}. \tag{14}$$

For a given value of b_1/b, the above equation may be solved graphically. An example of the solution is shown in Fig. 6. In this case, the initial height of the water is assumed to be 5 m., and $\frac{v_0^2}{2g}=2$, that is, $v_0=6.26$ m./sec., a rather large velocity of the tsunami.

Decrease of height for $\frac{v_0^2}{2g}=1, 2, 3$ and

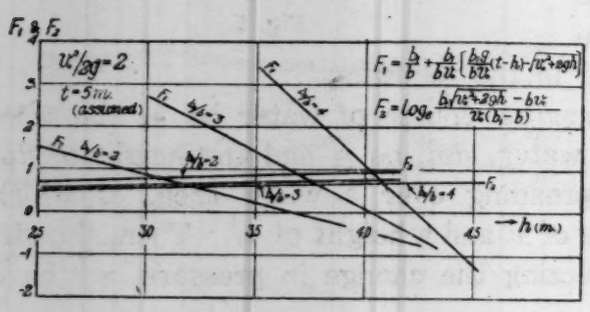

Fig. 6.

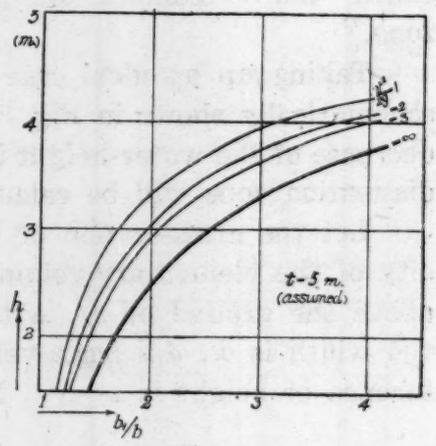

Fig. 7.

∞ is shown in Fig. 7, in which h is plotted against b_1/b, As is clear in this figure, when the area of the dissipation zone is wider, the decrease of the height of tsunami becomes greater, but there are limits in the amount of this decrease as shown by a curve in thick line which corresponds to the extreme case $v=\infty$. In this case, h is given by

$$h = \frac{b_1-b}{b_1}t. \tag{15}$$

Further, it can be seen that the dissipation zone is more effective for a smaller velocity of the tsunami for a given value of b_0/b.

Unfortunately, there could be found no good example in the recent tsunami of 1946, except the lowland which was situated near the village of Hiro, Wakayama Prefecture, where it acted as a dissipation zone to some extent. The height of the water inrushing there was so low that no serious damage was caused. The decrease of the water-height could be seen, but its exact value was uncertain.

(4) *Inclination of the ground and the decrease of the height of tsunami.* As already mentioned in Part 1 of this paper,[4] the velocity of tsunami can be determined from the decrease of the water-height and the inclination of the ground by Chézy's formula. As the actual example has been already given, the description of this method will be abbreviated here.

Now in the following, we shall explain the methods of estimation of the speed which are based on the second fact cited at the top of this paper. As already mentioned, the force exerted by the water upon the submerged body is given by the following expression.

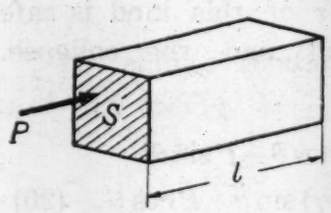

Fig. 8.

$$P = \rho k S \frac{v^2}{2g},$$

$$= Kv^2, \qquad \left(K = \rho k \frac{S}{2g}\right), \tag{16}$$

where P is the pressure, ρ the specific gravity of the water, S the cross-section of the body and g the acceleration due to gravity. k is a constant which is determined by experiments, such that, for prismatic bodies of length l and of cross-section S, it takes values as

$$k = 1.86, \quad 1.47, \quad 1.35, \quad 1.33,$$

$$\text{for} \quad \frac{l}{\sqrt{S}} = 0.03, \quad 1, \quad 2, \quad 3. \tag{17}$$

When the force of tsunami acts on the simple structures, such as stone pillar, monument, wall and others, they will be removed or sometime will be broken if they cannot resist the attack of the waves. Actually in the field which was invaded by the tsunami there can be seen the overturning, sliding and fracturing of these bodies in many places. There are other structures which are heavier than those just mentioned but may be treated as simple structures, that is, breakwater, sea wall and others of this kind. From the relation above given, the force by which these phenomena are displayed can be determined with a fair approximation, also the velocity of the water can be estimated easily.

As treated usually in the harbor engineering, the conditions of the sliding and the overturning of the wall set on the rubble-mound (Fig. 9) are,

4) N. NASU; *Bull. Earthq. Res. Inst.*, **25** (1947), 81–84.

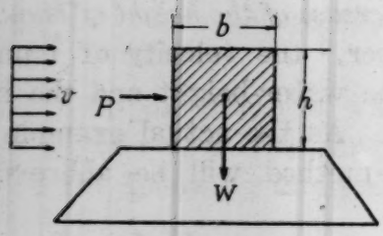

Fig. 9.

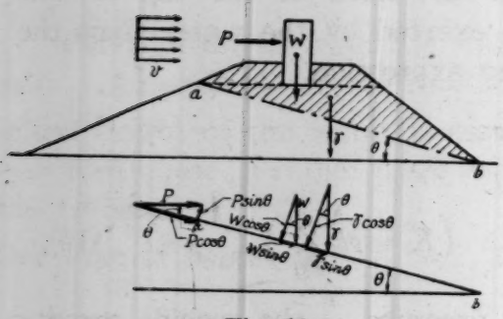

Fig. 10.

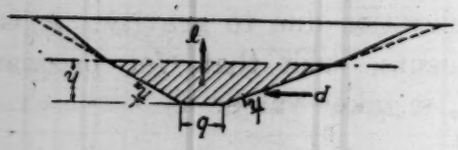

Fig. 11.

$$P \geqq fW, \quad \text{for sliding,} \tag{18}$$

$$Ph \geqq Wb, \quad \text{for overturning,} \tag{19}$$

where W denotes the weight of the wall measured in the water and f the coefficient of friction between the base of the concrete wall and the rubbles; f is usually taken as 0.6—0.7.

If the following condition is satisfied in the part of the rubbles, the breakwater of this kind is safe for the sliding and the collapse. (Fig. 10)

$$f\{(W+\gamma)\cos\theta - P\sin\theta\} \geqq (W+\gamma)\sin\theta + P\cos\theta. \tag{20}$$

As usually, $f = 1.0$ in this case, the condition may be written as

$$(W+\gamma)\cos\theta - P\sin\theta \geqq (W+\gamma)\sin\theta + P\cos\theta. \tag{21}$$

The similar idea of sliding is applicable to the collapse of the rubble mound which has no vertical wall as shown in Fig. 11. In this case, the condition of the collapse is

$$P > \gamma, \qquad (f = 1.0) \tag{22}$$

The calculations above mentioned are all related to the determination of the minimum dimensions of the structures which are necessary for resisting the expectable water pressure. In our case, however, the purpose lies in the determination of the pressure or the velocity of the water by the action of which the damage of structures will be caused. For the help of this determination, the relations between the dangerous velocity and the dimensions of the structures as shown in Figs. 9, 10 and are formulated in the following.

Let the dangerous velocity of the water be v, then the conditions of the sliding and the overturning of the wall (Fig. 9) are

$$v^2 \geqq \frac{2f\rho' g}{\rho_0 k}(b), \qquad \text{for sliding,} \tag{23}$$

$$v^2 \geq \frac{2\rho' g}{\rho_0 k}\left(\frac{b^2}{h}\right), \quad \text{for overturning,} \tag{24}$$

where ρ_0 is the specific gravity of the water and ρ' is that of the wall measured in the water.

In the case of a concrete wall submerged in the sea water, $\rho_0 = 1.03$, $\rho' = 2.35-1.03 = 1.32$. Let $f = 0.65$ and $k = 1.5$ in their means, then, the relations given above become, (v in m./sec., b and h in m.),

$$v^2 = 10.9\, b, \quad \text{for sliding,} \tag{25}$$

$$v^2 = 16.7\left(\frac{b^2}{h}\right), \quad \text{for overturning.} \tag{26}$$

The similar relation can be obtained in the case of the rubble mound as shown in Fig. 11.

$$v^2 = \frac{h+0.89\,b}{0.0358}. \tag{27}$$

In this case, the inclinations of the mound are $n_1 = 2.5$, $n_2 = 2.0$ and the specific gravity of the rubble in the water is assumed to be 0.98.

Formulae given above were proved to be convenient in the estimation of the flowing velocity of the tsunami in the recent Nankaido tsunami. At Kainan and Yura, the velocities that were estimated from the damage of the breakwaters showed a good accordance with those obtained by other methods.

ERRATA

Page 34, Fig. 11 was printed upside-down.

Correct like,

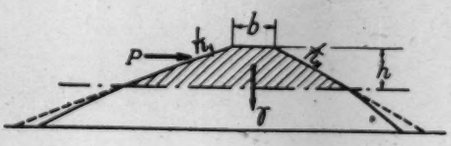

7. *Geological and Petrological Notes on the Eruption of Sakura-jima in 1946.*
Part II. Petrography of 1946-lava.

By Ryōhei MORIMOTO,

Earthquake Research Institute.

(Read Sept. 16, 1947.—Received June 20, 1949.)

Since the great eruption in 1914, Sakura-jima, one of the most famous active volcanoes in southern Kyūsyū, has comparatively been in her calm state and has never outpoured her volcanic material in the form of lava flow, though the minor activities ejecting ash, bomb, and other gaseous or solid material, being accompanied with or without felt earthquakes, were recorded in Sept. 1935[1], Oct. 1939[2], and in Apr.–May 1941. The 1946-eruption occurred at the eastern flank of Minami-dake, south cone of the volcano, at the point about 750m above sea level without any conspicuous forerunning phenomena[3], and the blocky andesite lava was extruded through the adventive vent already formed in the minor activity in 1939, enlarged in the former explosion of 1941. The eruption lasted about 11 weeks from March 11th to May 25th, during which two pyroxenes-andesite was almost stationarily emitted and covered the area of about 5.4 sq. km[4]. Actual scene of activity, distribution of the recent lava, result of microscopic observation on the andesite, and the summary of a geologic history of the volcano were preliminarily reported in the previous paper[5]. In this paper, however, detailed description of the rock under the petrographic microscope, and the results of chemical analyses of it are supplementally noted in the following Tables (Table 1, 2).

Three great eruptions of the volcano in a historic age, recorded in 1468–76, 1779, and 1914, were exclusively characterized by their bilateral eruption viz. flank eruption taking place on both sides of the central cone during a series of activity. The positions of the vent holes in each above-

1) S. ATA, *Nippon Gakujutsu Kyōkai Hōkoku*, **12** (1937) 184–187, (in Japanese).

2) H. TSUYA and T. MINAKAMI, *Bull. Earthq. Res. Inst.*, **18** (1940) 318–339, (in Japanese). K. YAMAGUCHI, *Jour. Geol. Soc. Japan*, **47** (1940), 143–164, (in Japanese).

3) No felt earthquake was recorded during this eruption, though the seismic activity represented by many non-perceptible quakes were reported. T. MINAKAMI and K. IWAMA, *Bull. Earthq. Res. Inst.*, **24** (1946), 171, (in Japanese).

4) R. MORIMOTO, *Bull. Earthq. Res. Inst.*, **24** (1946), 237, (in Japanese).

5) R. MORIMOTO, *op. cit.* 229–238.

mentioned great eruption, being plotted on a topographic map, lie on the linear lines passing through radially the northeastern margin of the summit crater of Minamidake as indicated in Fig. 1. And the crater through which the recent activity took place lies also on the linear line along which the vent holes formed during the former great eruption in 1914 are plotted. Thus, geologically the recent eruption, which is distinguished from the preceding minor activities in 1935, 1939, and 1941, in extruding a lava flow, may be considered as one of the phenomena following the former great eruption in 1914. From the petrochemical standpoint, also, the chemical composition of the recent lava is almost involved in the range of that of 1914-lava (Table 1). In mode, however, the former differs

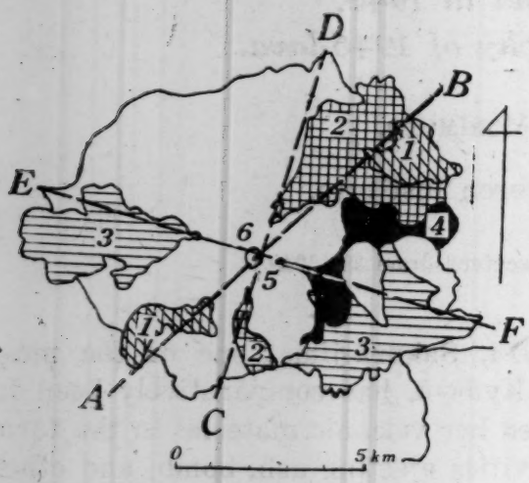

Fig. 1.
1....1463-1476-lava, 2....1779-lava,
3....1914-lava, 4....1946-lava,
5....The vent from which 1946-lava was extruded,
6....Summit crater of Minamidake,
AB..Imaginary fissure line in 1468-76,
CD..Ditto in 1779, EF..Ditto in 1914.

Table 1.
Chemical Composition of 1946-lava.

Constituent	1	2	3
SiO_2	61.26	61.24	62.29-59.07
Al_2O_3	16.14	16.76	17.81-16.56
Fe_2O_3	2.88	2.42	2.33- 1.02
FeO	4.71	4.84	5.90- 4.40
MgO	2.77	2.69	3.41- 2.17
CaO	6.80	6.62	7.57- 6.05
Na_2O	2.65	2.81	3.41- 2.72
K_2O	1.46	1.49	1.74- 1.40
H_2O (+)	0.21	0.17	0.63- 0.19
H_2O (−)	0.09	0.16	—
TiO_2	0.74	0.72	0.77- 0.51
P_2O_5	0.18	0.20	0.29- 0.08
MnO	0.14	0.13	0.24- 0.08
Total	100.03	100.25	—

Norms

Quartz	20.76	19.44	—
Orthoclase	8.90	8.90	—
Albite	22.53	23 06	—
Anorthite	27.52	28.91	—
Wollastonite	7.66	1.28	—
Enstatite	6.90	6.70	—
Ferrosilite	5.02	5.94	—
Magnetite	4.41	3.48	—
Ilmenite	1.52	1.37	—
Apatite	0.67	0.34	—

Modes*

Plagioclase	24.5	24.6	20.0
Augite	2.0	2.0	2.9
Hypersthene	3.2	3.3	2.6
Olivine	—	—	0.8
Magnetite	1.8	2.0	1.0
Groundmass	68.5	68.1	72.5

1. Collected from the front of "live" lava at Arimura, Apr. 7, 1946. T. ANDO analyst. (RM46040701)
2. Collected from the front of "live" lava at Kurokami, Apr. 10, 1946. T. ANDO analyst. (RM46041001)
3. Range of the chemical composition, of 1914-lava, quoted from HONMA (*Bull. Vol. Soc. Japan* **2**, 1935, 262.)

* Volume percentage

from the latter only in absence of olivine (Tables 1 and 2). But it is not rare that olivine crystals are found in the lava or in a part of the lava, irrespectively of their absence in the other lavas or in the other parts of the lava extruded during the same eruption[6]. And it is rather common for most of the lavas extruded from this volcano except some parts of 1914–lava to contain no olivine crystal.[7]

The recent lava is, petrographically, two pyroxene-labradorite-andesite, containing mainly labradorite, hypersthene, augite, iron ore, and rarely anorthite as the phenocrysts in the cryptocrystalline groundmass. The microcrystals of plagioclase, rhombic and monoclinic pyroxene, and iron ore are recognizable in the brown glass of the groundmass. Under the metallographic microscope, these iron ores are identified as magnetite and pyrite. The former occurs as the euhedral phenocrysts that are sometimes associated with pyroxene phenocrysts, as the groups of vermicular

6) B. KOTO, *Jour. Coll. Sci. Tokyo Univ.*, **38** (1916), 179. G. A. MACDONALD, *Amer. Journ. Sci.*, **242** (1944), 177–189.

7) K. YAMAGUCHI, *op. cit.* 155.

crystals (pseudomorph after olivine) in the central part of the pyroxene crystal or of the aggregate of pyroxene grains, and as the minute grains in the groundmass. The latter, whose quantity is quite negligible compared with the former, is found as the enclosures in the isolated magnetite phenocrysts. Inclusions are common in this lava, among which ceramicite[8], noritic or micronoritic rocks[9] are predominant.

Table 2.

Optical properties of the constituent minerals.

Phenocrysts	1946-lava	1914-lava	1939**
Plagioclase	*An n.d.* *An*75–51	*An*86–95, *An*65	*An*89–93, *An*66
Hyperthene	$(-)2V = 59-69°$ $\rho > v$	$(-)2V = 57-65°$ $\rho > v$	$(-)2V = 62^*-72°$ $n_{1D} = 1.698^*\ 1.704$
Augite	$2V = 43-55°$ $(\beta_D = 1.694, 1.697)$	$(-)2V = 46-51°$ $(n_{1D} = 1.696)$	$2V = 53-55^*$ $(n_{1D} = 1.692, 1.696)$
Olivine	–	+	$\beta_D = 1.700^*$ $(-)2V = 86°$
Magnetite	+	+	+
Groundmass	Brown glass; $n_D = 1.515-1.523$ Plagioclase An n.d. Hypersthene Augite Magnetite	Brown glass; $n_D = 1.515$ Plagioclase An n.d. Hypersthene Augite Magnetite	Brown glass; $n_D = 1.520^*-1.522$ Plagioclase: An 64,* 66 Hypersthene Augite Magnetite

** Juvenile block ejected during the minor activity in 1939. H. TSUYA and T. MINAKAMI, op. cit. 334.

* K. YAMAGUCHI, *op. cit.* 155. In this paper, chemical analyses of these blocks are given as follows: SiO_2 57.11, Al_2O_3 16.94 Fe_2O_3 1.91, FeO 6.09, MgO 3.87, CaO 8.42, Na_2O 3.09; K_2O 1.35, H_2O (+) 0.14, H_2O (–) 0.04, TiO_2 0.82, P_2O_5 0.15, MnO 0.13, T tal 100.96 (Average).

Concluding this remark, the writer wishes to have his opportunity of offering his cordial thanks to Kagoshima Prefectural Government who afforded him every facility during his field work, and to Dr. Y. KAWANO of the Geological Survey of Japan for his kind instructions about chemical analyses of the rock. His sincere thanks are also conveyed to Mr. T. ANDO, analyst of this institute, to Mr. T. WATANABE of this institute who prepared many thin slices of the lava, and to Mr. TAKESHITA's who gave him a field station.

8) B. KOTO, *op. cit.* 196-208.

9) K. YAMAGUCHI, *Jour. Geol. Soc. Japan*, **34** (1927), 381 408, 461-473, 479-497.

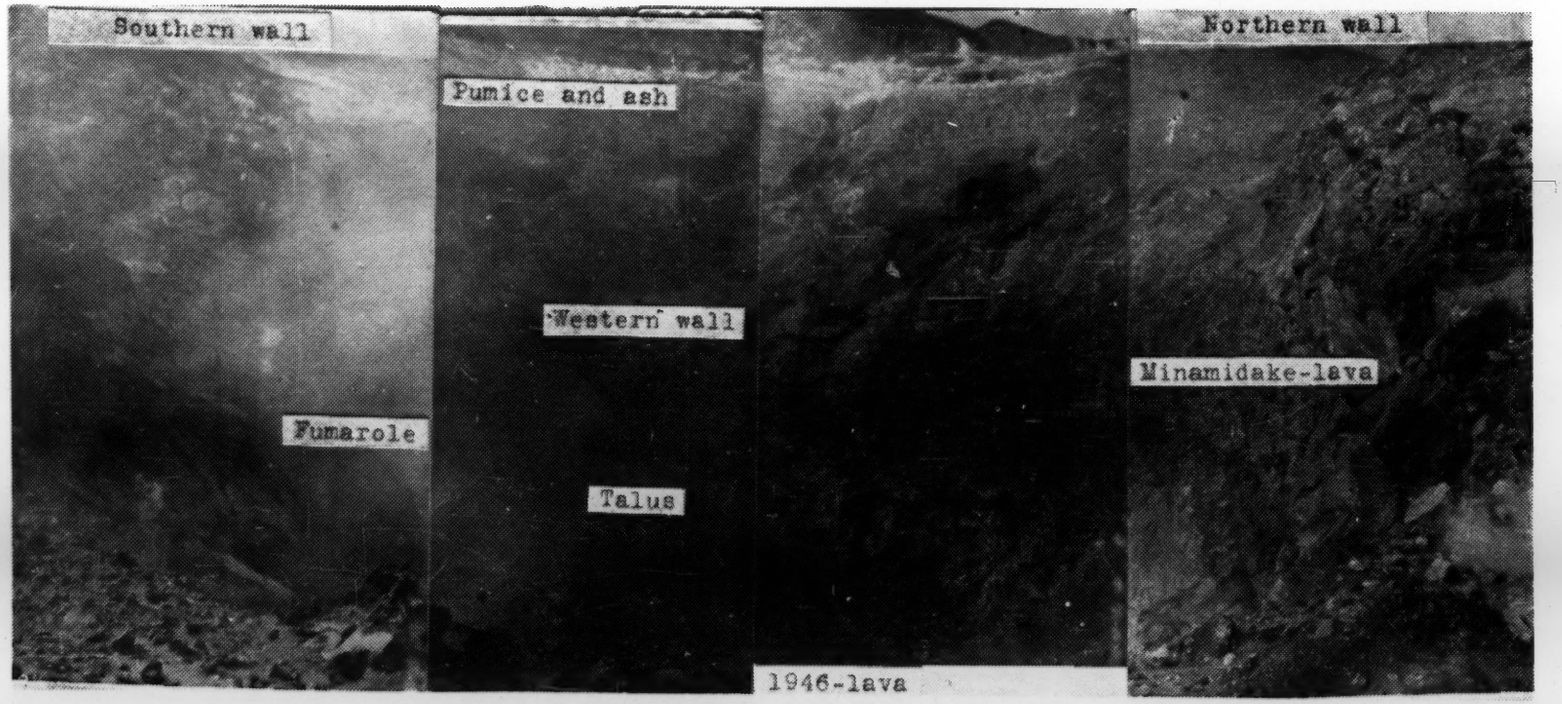

Fig. 2. Panoramic view of the inner wall of the vent, January 1947. (cf. R. MORIMOTO, *Bull. Earthq. Res. Inst.* **24** (1946), 232.)

8. *Occurrence of Fayalite in the Plagioliparite from Sakkabira, Tarumizu-machi, Kimotsuki-gun, Kagoshima Prefecture, Japan.*

By

Ryōhei MORIMOTO,

Earthquake Research Institute

and

Hideo MINATO,

Mineralogical Institute.

(Read Apr. 21, 1946.—Received June 20, 1949.)

Occurrence of fayalite in some dacites had already been reported by KUNO from North Izu and adjacent area, and its petrogenic meaning had also been discussed by him[1]. In March of 1944, the writers found the euhedral minute crystals of fayalite, commonly 1mm×0.5mm×0.2mm in size, with brownish colour (Fig. 1) in the drusy cavities of the biotite-bearing hypersthene-plagioliparite (Table 1) that was described as "cordierite-bearing lava" in the previous paper[2]. In this paper, optical properties of the mineral and the result of goniometry (B-type of V. GOLDSCHMIDT's Two-circle Refraction Goniometer being used.) are supplemented to the previous one. Mode of occurrence of the present fayalite is quite similar to that of the mineral described by KUNO, except the contemporaneous occurrence with cordierite in the former case. It occurs as minute euhedral short prismatic crystals (1–1.5mm or less in length) in the drusy cavities associated intimately with scaly crystals of tridymite, and also as anhedral irregular grains in

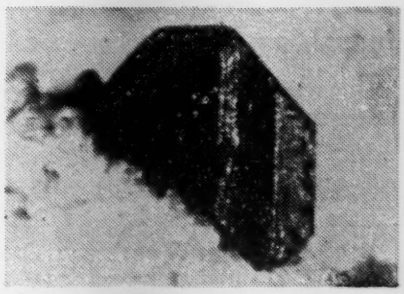

Fig. 1. Microphotograph of the fayalite (× ca. 23).

1) H. KUNO, *Jour. Geol. Soc. Japan*, **47** (1940), 228–232.

2) R. MORIMOTO, *Bull. Earthq. Res. Inst.*, **25** (1947), 33–35.

R. MORIMOTO and H. MINATO, *Jour. Jap. Assoc. Mineralogists, Petrologists and Economic Geologists*, **33** (1949), 51–61, (in Japanese).

Table 1.

Petrography of the biotite bearing hyperthene-plagioliparite.

Chemical composition[3]	Phenocrysts	Groundmass
SiO_2 .....74.65–72.75 wt%	Plagioclase:	Glass:
Al_2O_3 ....14.54–13.67 ,,	An 35–48	$n_D = 1.487–1.492$
Fe_2O_3 .... 0.64– 0.40 ,,	Quartz	Oligoclase: (Microphenocrysts)
FeO..... 1.92– 1.43 ,,	Hypersthene:	Alkalifeldspar
MgO ..... 0.67– 0.61 ,,	En 60–55 wt%[4]	Quartz
CaO..... 2.77– 2.66 ,,	Biotite:	Tridymite
Na_2O..... 4.23– 3.05 ,,	$\gamma_D = 1.654$	Biotite:
K_2O..... 2.50– 2.16 ,,	$(-)2V = 0°$	$\gamma_D = 1.608$
$H_2O(+)$... 0.47– 0.24 ,,	X-Cinnamon Buff (27)*	$(-)2V \fallingdotseq 0°$
$H_2O(-)$... 0.39– 0.02 ,,	Y-Sudan Brown (40)	X-Colourless to Sulphur Yellow (1)
TiO_2..... 0.17– 0.13 ,,	Z-opaque, owing to strong absorption	Y, Z-Old Gold (36) to Orange Rufous (45)
P_2O_5..... 0.26– 0.07 ,,	$X = Y \ll Z$	$X < Y, Z$
MnO ..... 0.04– — ,,	Magnetite	Cordierite:
		$\alpha_D = 1.545–1.548$
		$\beta_D = 1.546–1.549$
		$\gamma_D = 1.549–1.551$
		$2V$ is variable
		Hypersthene:**
		$\gamma_D = 1.720$, $2V$ n. d.
		Fayalite:
		$\alpha_D = 1.800$ $\rho > v$ about X
		$(-)2V = 56°, 57°$
		Fa_{16}[5]
		Iron ore dust

* After WADA's Colour Chert.

** An euhedral hypersthene, 2*mm* in length, in the drusy portion of the lava.

microscopic size among the higher crystalline parts of the groundmass. In such parts of the groundmass, the considerable tridymite, representing those parts of the groundmass where the volatiles were concentrated during the final stage of crystallization, are usually observed. And this mineral, as well as the cordierite described in the previous paper, is not found in the glassy parts of the plagioliparite with obsidian appearance.

From the textural relations among the druse-filling minerals observed under the microscope, and from the mineral association in the druses and in the higher crystalline parts of the groundmass (Table 2), it may be said

3) The ranges of each constituent are quoted from YAMAGUCHI. K. YAMAGUCHI, *Jour. Geol. Soc. Japan*, **45** (1938), 333. In his paper, occurrence of fayalite and also of cordierite had never been talked about. It is of much interest however that he wrote down in his description of the lava, "there are some grains whose refractive indices are higher than that of methylene-iodide among the frakes of biotite in the groundmass."

4) Inferred from $(-)2V = 62–58°$ and dispersion about X ($\rho > v$) by means of the diagram by KUNO. H. KUNO, *Proc. Imp. Acad. Tokyo*, **17** (1941), 205.

5) Inferred from optic angle or index of refraction by means of the diagram by Winchell. Optical Mineralogy Part II (1933) p. 191.

that crystallization of the cordierite and of the quartz from the residium were slightly preceded by formation of the fayalite. The cordierite are always associated with tridymite and quartz, and commonly include the last, while the quartz often fulfills the central part of cavities, the walls of which are covered with comparatively coarse scaly crystals of tridymite. These tridymite crystals in the druses are seriated to the minute grains of the same mineral in the surrounding groundmass. The cordierite must have crystallized out *in situ* at the latest stage, for it often includes the structures of the rock which might had been formed during the eruption and crystallization of the country magma. In volcanic rocks, it is inevitable for the crystallization of mineral phases from residual liquid to be sensibly controled by the physical condition during or after eruption of the magma. And occurrence of these minerals in those parts of the lava, crystallization of which would have easily been disturbed by rapid cooling of the country magma, may be mainly due to the role of volatiles sealed in such parts of the lava enveloped by the other quenched parts of the same lava flow. Besides the physical conditions having prevailed after the eruption of the lava, the

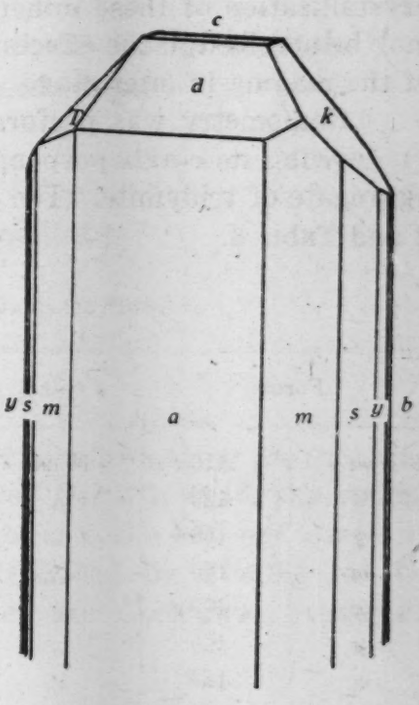

Fig. 2. Crystal figure of the fayalite.
a (100), *b* (010), *m* (110), *y* (150), *s* (120), *d* (101), *k* (021), *T* (375), *c* (001).

Table 2.

The trend of association of the minerals in druses of the plagioliparite.

Tridymite	Biotite	Fayalite*	Quartz	Cordierite
+	—	—	—	—
+	+	—	—	—
+	—	+	—	—
+	—	—	+	—
+	—	—	+	+

+ existence — none

* Associated rarely with the hypersthene comparatively rich in Ferrosilite molecule (cf. Table 1)

writers suppose, however, that the chemical environment favourable for the crystallization of these minerals, at least cordierite, from the residium, may be ascribed to the effects of foreign assimilation on the crystallization of the magma in later stage.

Goniometry was performed about a single crystal of fayalite (Fig. 1) growing its c-axis perpendicular to the wall of druse covered with the aggregate of tridymite. The result of measurement are mentioned in Fig. 2 and Table 3.

Table 3.

Forms		ρ calc.*	φ calc.*	ρ obs.	φ obs.	Size
m	110	90°00′	65°18′	90°00′	65°43′	*M*
s	120	,,	47°23′	,,	47°25′	*M*
y	150 cf.	,,	23°30′	,,	26°20′	*S*
m	$1\bar{1}0$	,,	114°42′	,,	113°00′	*M*–*S*
s	$1\bar{2}0$	,,	132°27′	,,	136°05′	*S*
y	$1\bar{5}0$	,,	156°30′	,,	158°40′	*S*
s	$\bar{1}20$	,,	−47°23′	,,	−46°16′	*M*
E	$\bar{1}70$	,,	−17°15′	,,	−16°20′	*S*
m	$\bar{1}\bar{1}0$	,,	−114°42′	,,	−115°45′	*L*
a	100	,,	90°00′	,,	90°00′	*L*
a	$\bar{1}00$	,,	−90°00′	,,	−89°58′	*L*
b	010	,,	0°00′	,,	5°25′	*V. S.*
b	$0\bar{1}0$	,,	180°00′	,,	−178°54′	*S*
d	101	51°32′	90°00′	51°20′	91°44′	*M*
k	021	49°11′	0°00′	51°07′	0°06′	*M*
k	$0\bar{2}1$	,,	180°00′	51°45′	−177°05′	*S*–*M*
T	375	38°34′	137°02′	38°45′	136°55′	*S*
c	001	0°00′	——	0°00′	——	*V. S.*

* After GOLDSCHMIDT's "Winkeltabellen."
cf. z (140) φ calc = 28°31′

In conclusion, the writers express their sincere thanks to Prof. Tei'ichi ITŌ of the Mineralogical Institute who afforded them every facility throughout this study. And to Dr. Toshio SUDŌ of the Geological Institute their special thanks are also due for his kind instructions to the junior author during his goniometry.

9. *A Petrological Note on the Granitic Rocks near the Cape Ashizuri, Shikoku Island, Japan (I).*

By Ryōhei MORIMOTO,

Earthquake Research Institute.

(Read Sept. 16, 1947.—Received June 20, 1949.)

I. INTRODUCTION.

During his journey to Kōchi Prefecture for investigating the damages of the Nankai Great Earthquake that occurred Dec. 21, 1946, the writer caught his opportunity of observing the granitic rocks exposed near the Cape Ashizuri (Fig. 1), that had been described by SUZUKI in the geologic map "Sukumo" (Scale 1:75,000) of the Geological Survey of Japan as follows:[1)]

Fig. 1. Distribution of the granitic rocks in the southwestern part of Shikoku Island.
U=Uwajima, K=Kashiwajima, A=Ashizurisaki, O=Okinoshima.

"Biotite-granite exposed near Ashizurisaki afforded contact metamorphic effects to the Ōhama rocks. *The granite* found in the southwest of the sheet area occurs as stocks or bosses which may be protrusions from batholithic granite mass beneath

1) T. SUZUKI, *Explanatory Text of the Geological Map of Japan*, Scale 1:75,000. Sukumo (1938), 6.

the surface. The rock exposed near Kashiratsudo in Oku uchi-mura contains minute tourmaline needles besides essential constituents; quartz, orthoclase, plagioclase and biotite, the last being much abundant in quantity. Similar biotite-granite observed in the Uwajima sheet map area[2] intrudes the upper Cretaceous strata and is generally accepted as probably being of Tertiary age in eruption. This may be true with the granite occurring in the present Sukumo area."

Strictly saying, however, owing to no palaeontological data reported about the Ōhama beds, it is only afforded for this igneous mass to be pointed out that geologically it brought about the slight contact metamorphism of Ōhama beds, an unknown Mesozoic formation, and is covered with the Pleistocene gravel. But for the above description and the brief note by Jun SUZUKI in his paper summarizing the granitic rocks developing in the outer zone of Southwestern Japan and Ryūkyū Island,[3] there had been no report, especially a petrological one, about the granitic rocks until the writer's observation, the results of which will preliminarily be noted in the present paper from the following two points: 1) occurrence of the alkaline rock and 2) occurrence of the interesting xenoliths in the syenite. The granitic rocks containing alkali mafic minerals have been reported in Japan from Iwakijima as aegirine-eyenite[4] from Syodoshima as aegirine-augite-quartz-monozonite[5], and from the base of Nijo volcano near Osaka as the granitic rock containing green monoclinic pyroxene[6], and they occur exclusively as dike-like small mass in the granitic rocks belonging to so-called "Ryoke-zone" of Southwestern Japan. The similar rock was found from the sea-shore south of the tribe of Isa, and the xenoliths of interesting feature were remarkably observed in the quartz-syenite exposed along the highway from Ōto to Isa (Fig. 3 and 4.). The geology of this area was not sufficiently investigated owing to his short time staying, and the chemical investigation on these rocks and minerals is not carried out in the present state. He wants, however, to write down here something about these rocks in order to narrow the hiatus in our petrological knowledge about the granitic rocks distributed in the "outer zone" of Shikoku.

In performing this study, the writer is indebted to Kōchi Prefectural

---

2) T. SUZUKI, *Explanatory Text of the Geological Map of Japan*, Scale 1 : 75,000. Uwajima (1936).

3) J. SUZUKI, *Jour. Geol. Soc. Japan*, **44** (1937), 641, (in Japanese).

(4 J. SUZUKI, and T. NEMOTO, *Jour. Jap. Assoc. of Petrologists, Minsralongists, and Economic Geologists*. **8** (1933), 60.

5) M. SATO, *Explanatory Text of the Geological Map of Japan*, Scale 1 : 75,000 "Takamatsu" (1936), 32.

6) S. TSUBOI, H. KOIDE, and R. MORIMOTO, *Jour. Geol. Soc. Japan*, 49 (1942). (in Japanese).

Government in his field works, and to a grant from the Japan Society for the Promotion of the Scientific Research in his laboratory works, and he also owes much to Mr. Yamazaki's and Mr. Nagasaki's who kindly afforded him the field stations during his stay there.

II. Geology and General Petrography.

Geologically and petrographically, the rocks distributed in this area are grouped into (1) the hornfels derived from the shally rock belonging to ōhama bed, (2) the biotite-quartz-monzonite consisting the main body of this igneous mass, (3) quartz-syenite locally developing in the monzonite (4) basic inclusions derived from pre-existing diabase or gabbro, a contaminated facies of the granitic rock, (5) the xenoliths in the quartz-syenite, (6) the quartz-syenite containing alkali mafic mineral, and (7) the dike rocks cutting the above-mentioned rocks.

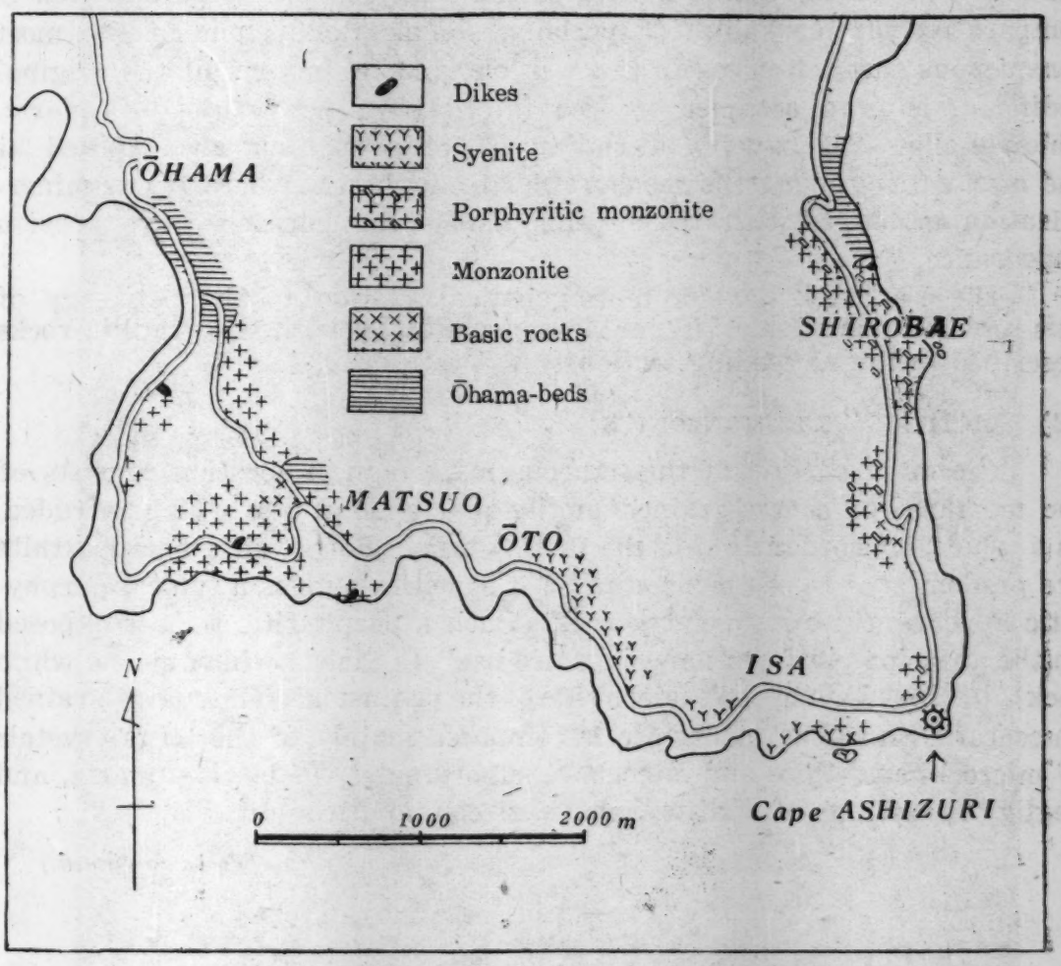

Fig. 2. Geologic route-map along the Cape Ashizuri.

(1) ŌHAMA-BEDS:

The rock is hard compact black shale or slate with remarkable fissility imbanding massive sandstone, and forms the monoclinic structure dipping to the northwestern direction. Near the contact with the monzonite, the shale or sandy shale change into hard hornfels with about 500m in width. But the contact effect on the Ōhama-beds by the granitic rock is quite simple and slight, and the grade of metamorphism does not attain to bringing about compicuous recrystallization of the hornfels even at the very contact with the igneous mass. The rock quite recrystallized into the mosaic aggregate of reddish biotite, quartz, orthoclase, and accessorily of microscopical dirty carbonaceous matter is only observable at the masses of biotite-hornfels reserved in the porphyritic quartz-monozonite as the roof pendants whose structure is quite parallel to that of Ōhama beds. No other hornfelses in the aureole indicate any remarkable reformation. The reddish flaky biotite are formed among the hydrous mica in the slate or shale and in the cementing matrix of the sandy shale. Mineralization is comparatively remarkable. Especially, silicification is one of the most conspicuous facts observed in this aureole, and the matrix of the original sediments is quite occupied by the interlocking fine grains of quartz. Chlorite-albite-quartz-veins intruding into the hornfels are exposed at the road-cutting along the seashore north of Ōhama, where pyrite-mineralization associated with these veins makes the hornfels have greyish appearance.

These hornfels have no more genetical relation to the petrology of this igneous mass than it contacts geologically with the granitic rocks described in the succeeding sections.

(2) BIOTITE-QUARTZ-MONZONITE:

The main portion of this igneous mass now in question consists of the medium- or coarse-grained biotite-quartz-monzonite which intruded, as a whole, concordantly into the Ōhama-beds. Porphyritic microperthite are predominant in the monzonite, so it sometimes gives a typical porphyritic appearance to its country rock. Such a porphyritic rock is exposed on the abrasion platform named "Shiro-bae" (a dialect which means white rock) developed along the eastern side of the peninsula. The coarse-grained leucocratic Shiro-bae monzonite is composed mainly of the large crystals of microcline-perthite and oligoclase, subordinately of biotite, quartz, and negligible amounts of apatite, sphene, zircon, and iron ore.

(To be continued.)

Fig. 3.

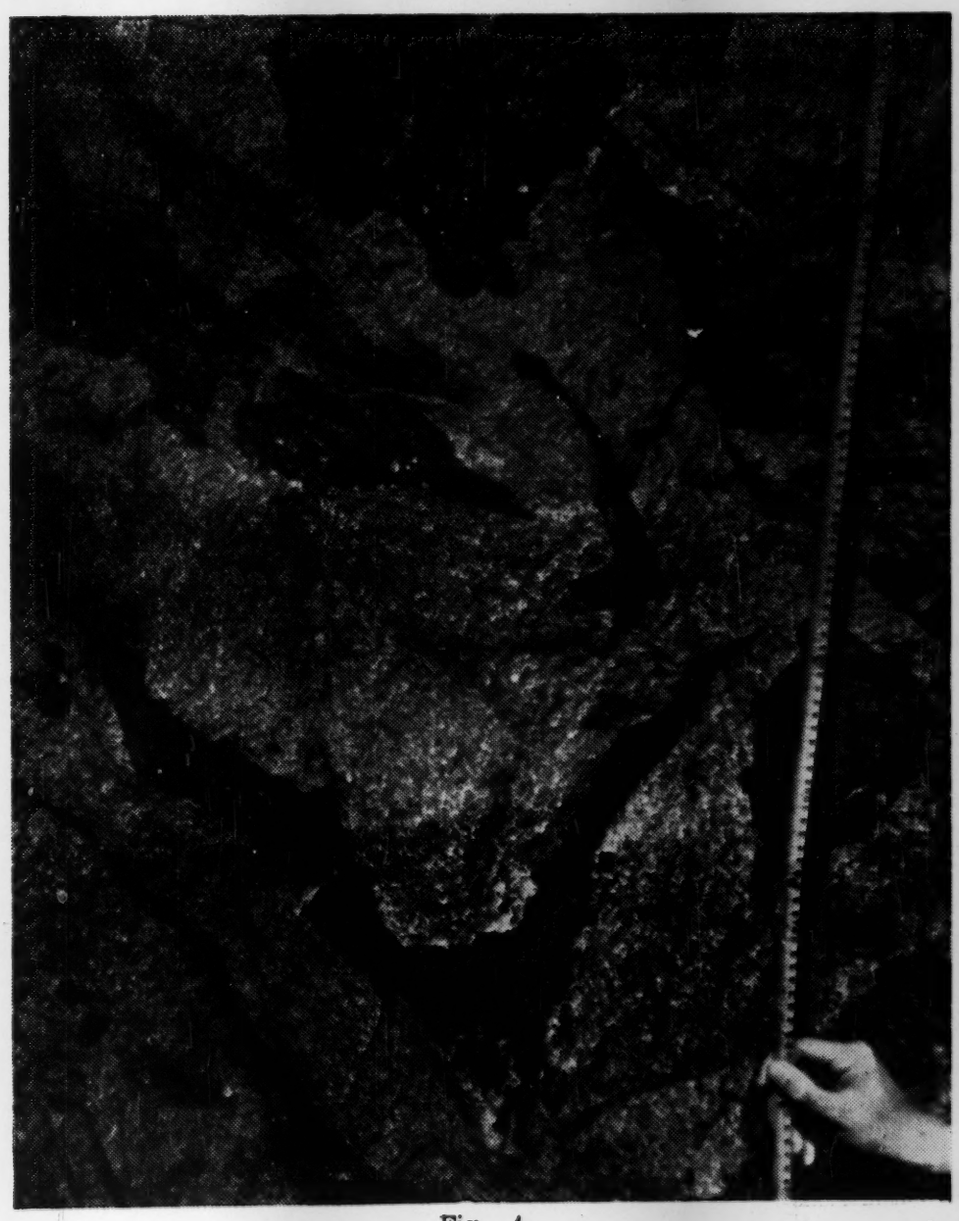

Fig. 4.

10. *Notes on the Fracture System developed in the Setogawa Group.*

By Isamu MURAI,

Earthquake Research Institute.

(Read Oct. 21, 1947.—Received June 20, 1949.)

There are various fractures or cracks in any rocks, and it may be possible to consider that such fractures are the traces of ruptural failure produced by the crustal movement. Some geologists have already suggested that it may be possible to obtain some available information about the mechanism of rock deformation under a systematic and detailed investigation of such fractures. The fracture fabric of intensely deformed rocks, however, is so complicated that it seems to be very difficult to analyse the mechanism of fabric. In this report, the writer may show a trial of statistical treatment applied to the study on such apparently complicated fracture fabric.

The Setogawa Group, which is distributed along the Nirazaki-Sizuoka Tectonic Line, is a sedimentary group composed mainly of shale or clayslate and sandstone. The geological age of this group is assumed to belong in an early epoch of the Tertiary, and it has been suffered from intensive deformations and disturbed complicatedly by countless faults.

The writer tried to analyse the fracture system developed in the Setogawa Group by a statistical research, and could obtain several interesting results. Some arguments about these results may be written in the following.

1. *Outline of folding*—From the result of the statistical investigation about the orientation of bedding planes, it is clarified that their position is generally vertical, but gently inclined strata are distributed locally. (cf. fig. 1.)

2. *Fracture fabric*—Diagrams of poles to fracture planes, which are sampled at random out of the whole structure in the Setogawa Group, seem to show no significant preferred orientation at a glance. (cf. fig. 2, 3 & 4.) If all of the fractures are orientated entirely at random, that is, in any direction of the whole space the probability of appearance of pole to fracture plane is equal, the number of sections (f) which are classified by the number of poles (k) in them may follow to Poisson's distribution: $f=e^{-m}\frac{m^k}{k!}$,

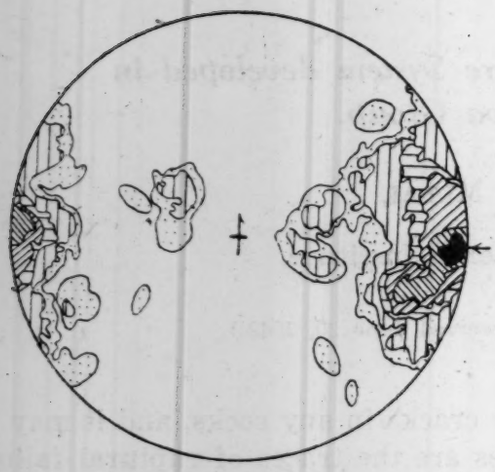

Fig. 1. Diagram (1% diagram) of 190 normals to the bedding planes of the Setogawa Group, measured at Hayakawa-Iri District, Yamanasi Prefecture. Contour interval: (12-10)-8-6-4-2-1-0%.

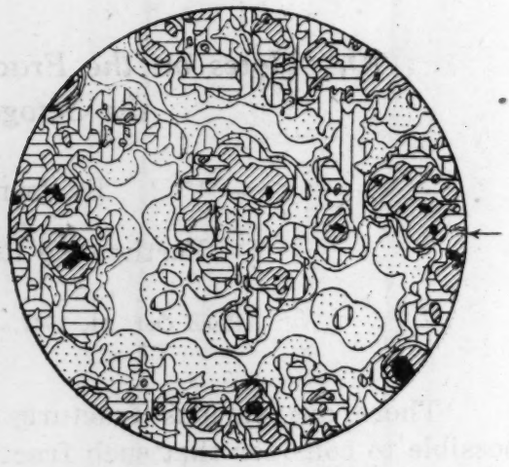

Fig. 2. Diagram (1% diagram) of 205 poles to the fracture planes in the Setogawa Group, measured at Umegasima-Mura, Abe-Gun, Sizuoka Prefecture. Contour interval: (3.5-3)-2-1.5-1-0.5-0%.

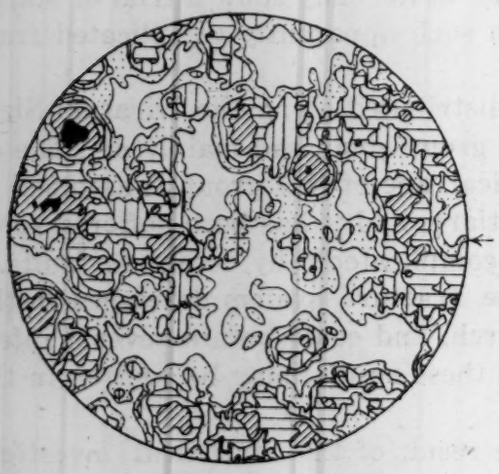

Fig. 3. Diagram (1% diagram) of 288 poles to the fracture planes in the Setogawa Group, measured at Ôkôti-Mura, Abe-Gun, Sizuoka Prefecture. Contour interval: (4-3)-2-1.5-1-0.5-0%.

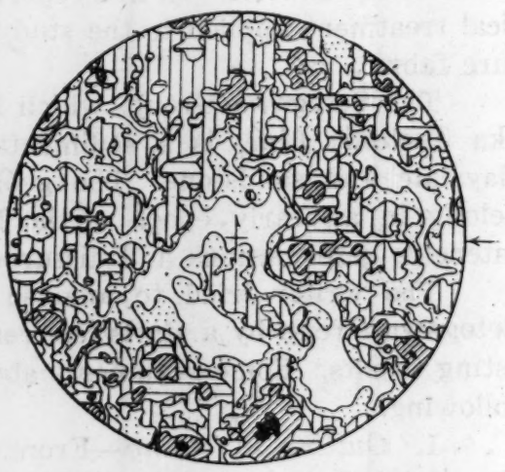

Fig. 4. Diagram (1% diagram) of 341 poles to the fracture planes in the Setogawa Group, measured at Ôkôti-Mura, Abe-Gun, Sizuoka Prefecture. Contour interval: (4-3)-2-1.5-1-0.5-0%.

when the whole area of diagram (which is made by using the equal area projection net) is divided into scores or hundreds of equal area sections. Then, it is possible to ascertain the significance of preferred orientation by comparing the observed frequency (f) with the expected frequency (F) of such number of sections. The degree of deviation of f from F is examined

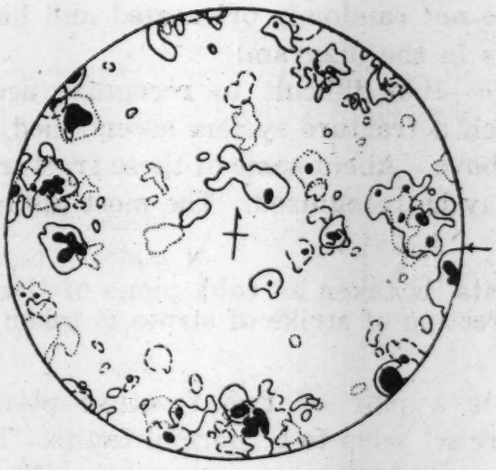

Fig. 5. Collective diagram of Fig. 2, Fig. 3 and Fig. 4, indicating the area of more than 2% and 3% concentration.

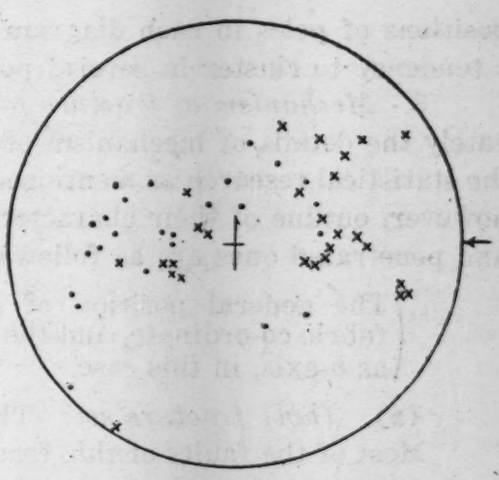

Fig. 6. Diagram of poles to the fracture planes which seem to belong in (*hOl*) fracture set. (•: shearing fracture, ×: vein.)

by χ^2-test for goodness of fit.[1] The writer divides the whole diagram into 156 equal area sections, and calculates the value of observed χ^2: $\chi_0^2=\Sigma\frac{(f-F)^2}{F}$, then obtains the value of probability $\{\chi^2>\chi_0^2\}$ from Fisher's χ^2-table. (cf. table I.) The null hypothesis, that these diagrams show entirely random orientation of all poles, is not denied by this statistical test, and the significance of preferred orientation is not ascertained. But in the collective diagram of these three diagrams, maxima or submaxima of each partial diagram have a tendency to cluster in several points in the diagram. (cf. fig. 5.) Then, the writer tried to calculate the indices of dispersion $\chi^2=\frac{\sum_{i=1}^{N}(k_i-m)^2}{m}$ about the numbers of poles in the equal area sections corresponding each other. In this case, he divides the whole diagram into 70 equal area sections. If all poles of these partial diagrams are orientated entirely at random, the frequency distribution of such indices of dispersion may be approximately similar to χ^2-distribution with number of degrees of freedom: $\nu=N-1$. Then the difference tween the distribution of observed frequency and that of expected frequency of χ^2 is examined by χ^2-test for goodness of fit, and the probability $\{\chi^2>\chi_0^2\}$ is obtained from χ^2-table. (cf. table II.) This time, the difference between them is highly significant, and it is ascertained that the

1) WINCHELL, HORACE: *A new method of interpreting fabric diagrams, Am. Min.*, Vol. 22 (1937) p. 15–37.

positions of poles in each diagram are not randomly orientated and have a tendency to cluster in several points in the diagram.

3. *Mechanism of fracture fabric*—It is difficult to recognize accurately the details of mechanism of such a fracture system ascertained by the statistical research as mentioned above. About some of these fractures, however, outline of their character may be recognized. The most distinct and penetrated ones are as follows:

(The general position of strata is taken as (*ab*) plane of the fabric co-ordinate, and the direction of strike of strata is taken as *b*-axis, in this case.)

(a) *(h0l) fracture set:* This is a pair of two fracture planes. Most of the faults of this fracture set seem to be normal faults. The direction of displacement along such fault planes may generally be perpendicular to the direction of strike of the fault plane. This fracture set is developed fairly homogeneously throughout the whole area between Sizuoka and Nirazaki. It may be possible to consider that the penetrating effect of this fracture set may have resulted in such unique structure of the Setogawa Group as mentioned above. (cf. fig. 1) Calcite and quartz veins are developed along the fracture planes of this set. (cf. fig. 6 & 7.)

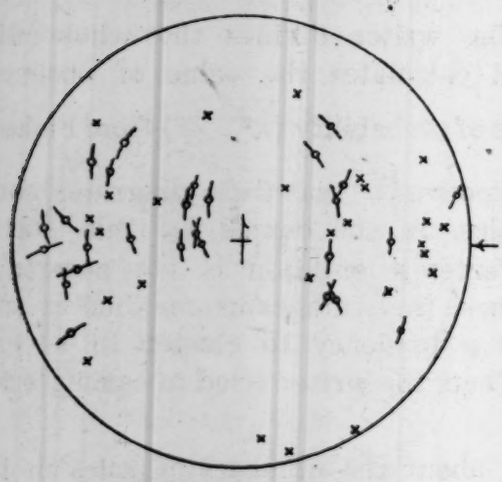

Fig. 7. Diagram of lineations and poles to slickensided surfaces upon which such lineations rest, measured at Hayakawa-Iri District. (o: direction of lineation, ×: pole to slickensided surface.)

Table I.

	$Pr.\ \{\chi^2 > \chi_0^2\}$
Fig. 2	$0.70 > P > 0.50$
Fig. 3	$0.50 > P > 0.30$
Fig. 4	$0.50 > P > 0.30$

(b) *(0kl) fracture set:* About the mechanism of this fracture set the writer could not obtain any information.

(c) *(010) fracture set:* This is not so distinct as (*h0l*) fracture set. The direction of lineation upon the slickensided surface which seems to belong in this fracture set is generally horizontal.

The detailed argument about the whole structure of the Setogawa Group may be reserved for another opportunity.

Table II.

χ^2	Expected frequency of χ^2 F		Observed frequency of χ^2 f		$\frac{(F-f)^2}{F}$
0. — 0.0201	0.4		0		
0.0201— 0.0404	0.4		1		
0.0404— 0.103	1.2	8.2	3	19	14.22
0.103 — 0.211	2.1		6		
0.211 — 0.446	4.1		9		
0.446 — 0.713	4.1	12.3	6	16	1.11
0.713 — 1.386	8.2		10		
1.386 — 2.408	8.2		6		
2.408 — 3.219	4.1		0		
3.219 — 4.605	4.1		0		
4.605 — 5.991	2.1	20.5	0	6	10.21
5.991 — 7.824	1.2		0		
7.824 — 9.210	0.4		0		
9.210 —13.815	0.4		0		
13.815 — ∞	0.0		0		
Total	41.0		41		25.54

$\chi_0^2 = 25.54 \quad \nu = 2 \quad Pr.\{\chi^2 > \chi_0^2\} < 0.0001$

11. A Nomogram for Magnification of Seismometer.

By Ryôhei IKEGAMI,

Earthquake Research Institute.

(Read July 20, 1948.—Received Oct. 7, 1948.)

I. Introduction.

It is often necessary to know real earthquake motions from the amplitude recorded on a seismogram. The magnification of the seismometer changes in accordance with the period of the earthquake motion, and for the reduction we are troubled by complicated calculations.

To avoid them, a few investigators[1] tried already to make nomograms, but those nomograms can not be effectively utilised.

The nomogram that we show here has several advantages over those previously published ones. Without numerical calculations, we can get the true amplitube by this nomogram if we only know the constants of the seismometer and the recorded amplitude and period.

II Directions for Use.

First, in order to get a ratio between the periods of the earthquake motion and the seismometer, we take the value of the former on the scale of T_P and that of the latter on the scale of T_n, and when these two points are connected, we can find the ratio, T_P/T_n, on the curve between these two period-scales.

Second, we take the value of the damping ratio on v-scale and the value of T_P/T_n on the scale of T_P/T_n-curve, and we connect these two points, and produce this line to the left and get one point on the first subsidiary line.

Third, we take the value of the recorded amplitude on L_M-scale, and connect this point and the point on the first subsidiary line, and produce this line to the left and get one point on the second subsidiary line.

Finally, we take the value of the geometrical magnification of the seismometer on the leftmost V-scale, and connect this point and the point on the second subsidiary line. Then we can obtain the value of the true amplitude by the intersecting point of two lines on L_R-scale.

---

1) K. Kitamura, *Kenshin-Jihô*, 10 (1937); K. Sakata, *Umi to Sora*, **21** (1941), 95.

The units of T_n, T_p, T_p/T_n, L_M, L_R, and V must be determined respectively by 10^r, 10^s, $10^{(s-r)}$, 10^m, $10^{(m-n)}$ and 10^n.
An example:

$$\left.\begin{array}{l} T_n = 30 \text{ sec.} \\ V = 45 \\ v = 1.7 \end{array}\right\} \text{ Constants of the seismometer.}$$

$$\left.\begin{array}{l} L_M = 2.6 \text{ mm.} \\ T_p = 4.5 \text{ sec.} \end{array}\right\} \text{ Amplitude and period measured on the seismogram.}$$

First, the value of T_n must be taken on 3 of T_n-scale and be taken as $r=1$, because T_n is equal to 30 sec. The value of T_p is taken on 4.5 of T_p-scale and s must be taken as zero. When we connect these two points, then we get 1.5 as the value of T_p/T_n, but we must take $T_p/T_n=0.15$, because $(s-r)$ is equal to -1.

Second, we take 1.7 on v-scale and 0.15 on T_p/T_n-curve, connect these two points, and produce this line to the left and get one point on the first subsidiary line.

Third, we take 2.6 on L_M-scale and in this case the value of m is equal to zero. We connect this point and the point on the first subsidiary line, and produce this line to the left and get one point on the second subsidiary line.

Finally, we take 4.5 on the leftmost V-scale, and in this case the value of n must be equal to 1, because the real value of V is 45. We connect this point and the point already determined on the second subsidiary line, and obtain 0.56 on L_R-scale by the intersecting point of this line and L_R-scale. But in this case, because $(m-n)$ is equal to -1, we take 0.056 mm as the true amplitude.

For reference, we calculated numerically the true amplitude from the same data by the following expresssion.

$$L_M = L_R \frac{V}{\sqrt{(u^2-1)^2+4h^2u^2}}$$

where

$$u = T_p/T_n, \quad h = 0.7330 \frac{\log v}{\sqrt{1+0.53720(\log v)^2}}.$$

In consequence, we obtained 0.0563 mm as the true value of L_R.

We express our thanks to Mr. Moroga who helped us to draw the nomogram.

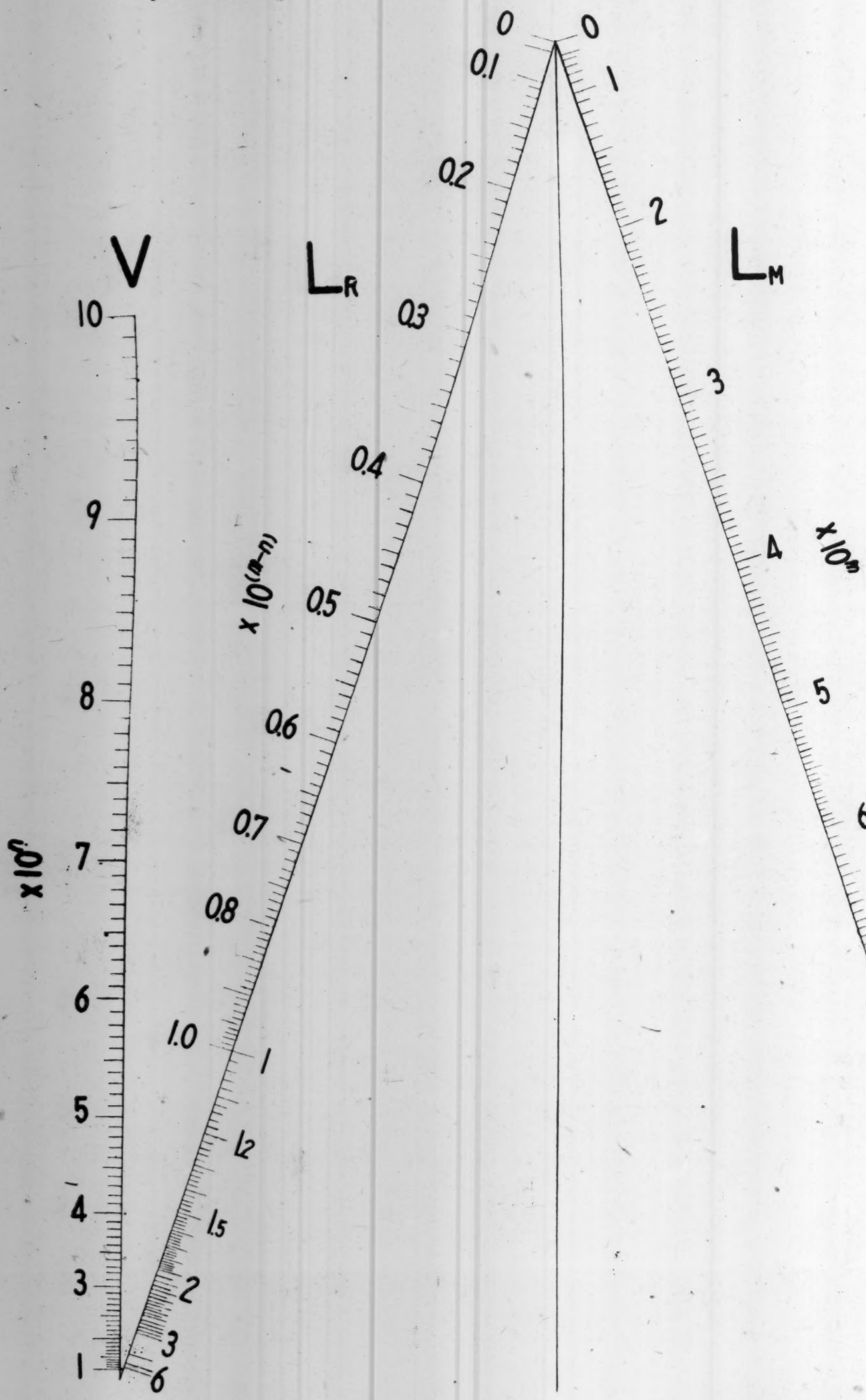

A NOMOGRAM FOR MAGNIFIC

T_p, period of earthquake motion. T_n, period of seismo
V, geometrical magnification of sei

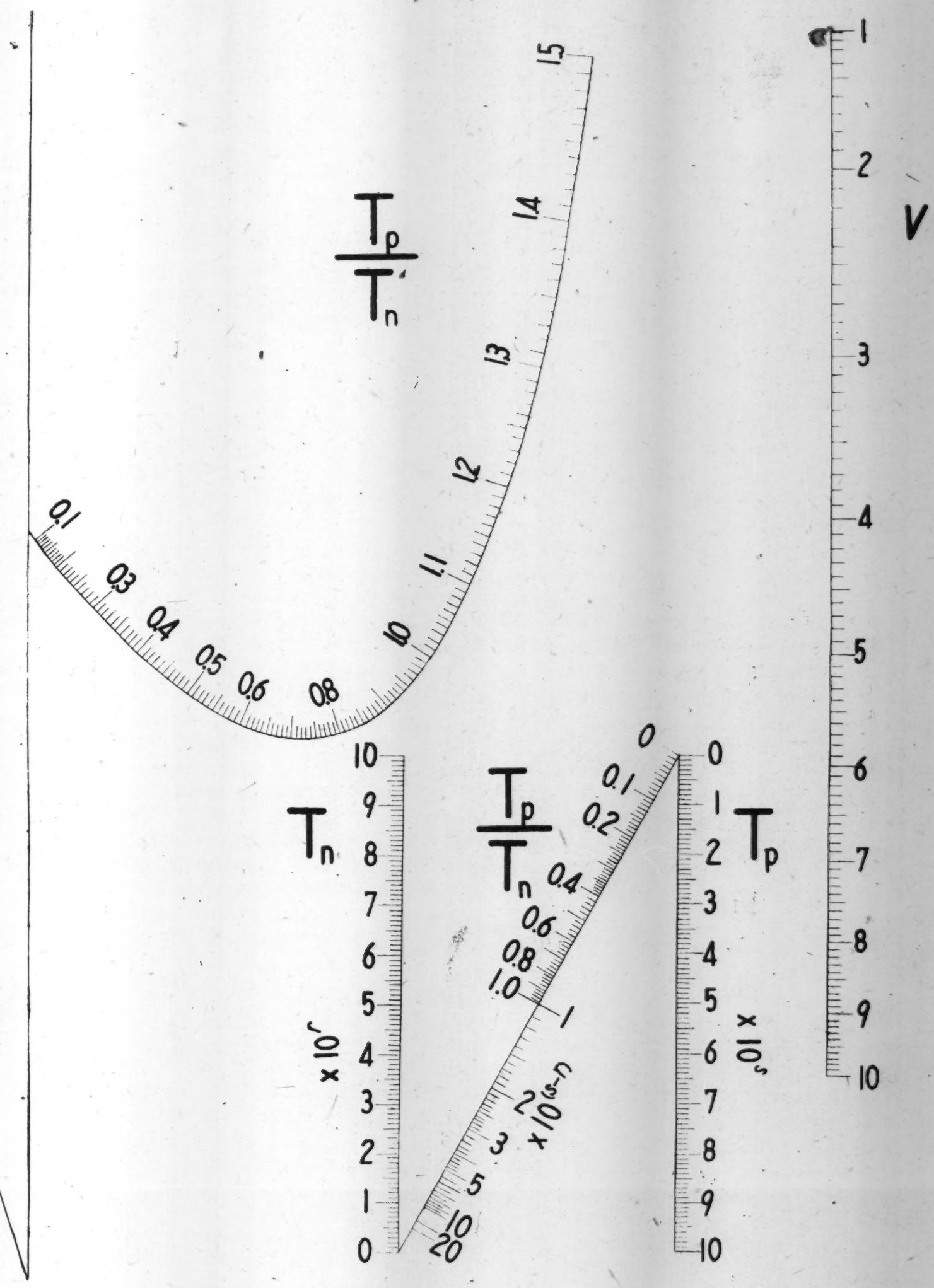

FICATION OF SEISMOMETER.

smometer. v, damping ratio. L_M, recorded amplitude.
seismometer. L_R, true amplitude.

12. *On the Existence of the M_2 Waves in Actual Seismic Disturbance.*

By Kiyoshi KANAI,

Earthquake Research Institute.

(Read Feb. 18 and March 18, 1943.—Received March 30, 1949.)

In the course of the close examinations, it was found that there are generally two dispersion curves of Rayleigh-waves of different types for a stratified body.[1)]

The Rayleigh type waves that we have discovered from the calculations and those of the usual sense, for a stratified body, may now be called M_2 waves and M waves respectively. The nature of M_2 waves differs somewhat from M waves. The vibrational energy of M_2 waves, instead of accumulating on the free surface, concentrates mainly in the vicinity of the boundary between the stratum and the subjacent medium. The sense of the orbital motion on the free surface is invariably the same as that of gravitational waves for every condition that corresponds to the M_2 waves. M_2 waves exist in a narrow range, that is of relatively small wave length, while M waves exist in the range from zero to infinity.

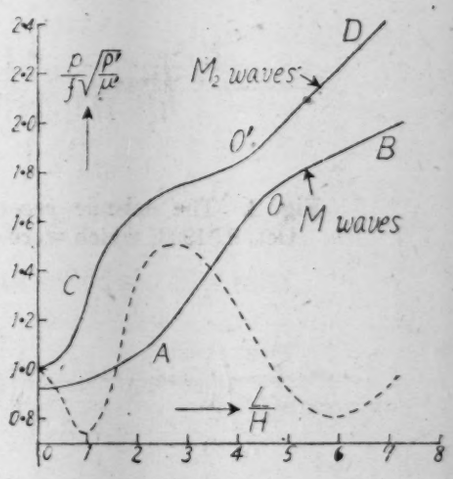

Fig. 1. Two dispersion curves corresponding to the Rayleigh-waves for a stratified body of a case in which $\rho/\rho'=1$, $\mu/\mu'=8$. The curve in a broken line give the group velocity of M_2-waves.

The mathematical results of the case in which $\lambda/\mu=1$, $\lambda'/\mu'=1$, $\rho/\rho'=1$, $\mu/\mu'=8$ are, roughly corresponding to the stratifications of the Kwantô district in Japan, shown in Fig. 1. In this

1) K. SEZAWA and K. KANAI, *Proc. Imp. Acad.*, **11** (1935), 13; *Bull. Earthq. Res. Inst.*, **13** (1935), 237.

K. SEZAWA and K. KANAI, *Proc. Imp. Acad.*, **11** (1935), 96; *Bull. Earthq. Res. Inst.*, **13** (1935) 471.

K. SEZAWA, *Bull. Earthq. Res. Inst.*, **16** (1938), 1.

K. SEZAWA and K. KANAI, *Bull. Earthq. Res. Inst.*, **18** (1940), 1.

case, H is the thickness of the stratum, $2\pi/f=L$ the wave length, $2\pi/p=T$ the period, ϱ', λ', μ' ϱ, λ, μ the densities and elastic constants of the stratum and the subjacent medium respectively.

With a view of confirming the existence of the M_2 waves in actual seismic disturbance, we have analysed the seismic records of two earthquakes of shallow origin, namely, those of the Yamanaka-Lake earthquake of Oct. 9, 1933 and of the Middle Izu earthquake of March 21, 1932. In these

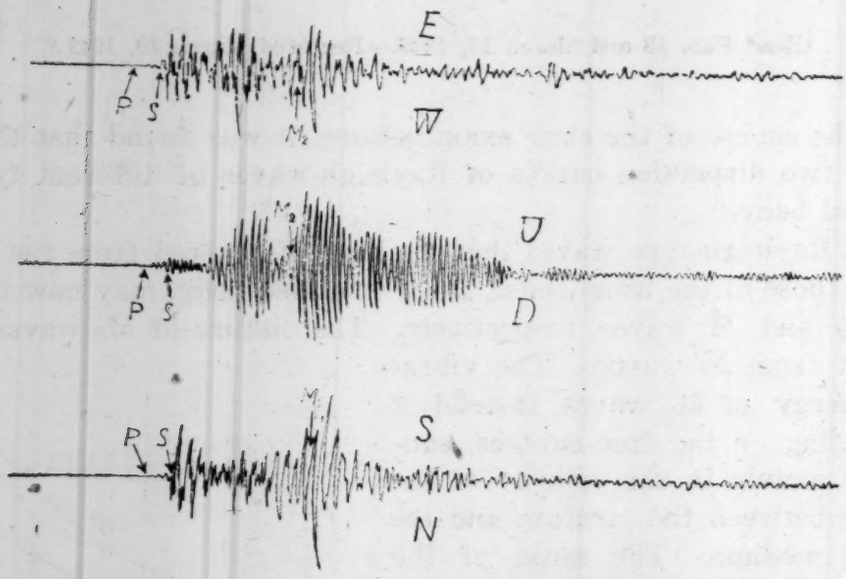

Fig. 2. The seismic records of the Yamanaka-Lake earthquake, Oct. 9, 1933, which were obtained at Hongô, Tôkyô. Orignal × 1/3

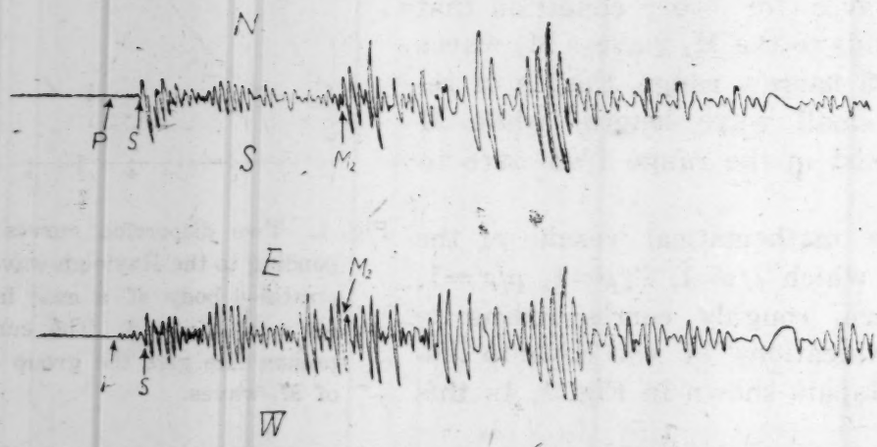

Fig. 3. The seismic records of the Yamanaka-Lake earthquake, Oct. 9, 1933, which were obtained at Sakura. Original × 1/3.

seismic records, a peculiar phase having relatively large amplitude is clearly recognized at the rear of the main shock (the seismic records of two observing stations are shown in Figs. 2, 3). The difference between

the arrival times of the *P* phases and those of the *S* phases, the difference between the arrival times of the *P* phases and the arrival times of the above-mentioned peculiar phases, the values of the periods of the peculiar waves and those of the seismographs, are tabulated in Tables I, II. The relation between the above-mentioned two differences are shown in Fig. 4. Now, from Tables I, II and Fig. 4, it came to be known that the peculiar phases were transmitted with a constant velocity.

Table I. Yamanaka-Lake earthquake of Oct. 9, 1933.

Observing Station	P-S (sec)	P-M_2 (sec)	Periods (sec)	
			M_2 waves	Seismogragh
Itô	6.6	52	3.4	6
Yoshiwara	6.7	52	3.0	4
Kamakura	7.1	51	3.4	7
Misaki	8.0	60	4.0	4
Titibu	8.2	64	4.1	7
Mitaka	8.3	59	4.0	7
Komaba	9.2	64	4.1	5
Hongô	10.6	70	4.4	7
Sakura	15.1	116	4.6	7
Tôgane	16.3	132	4.6	7

Table II. Middle Izu earthquake of Mar. 21, 1932.

Observing Station	P-S (sec)	P-M_2 (sec)	Periods (sec)	
			M_2 waves	Seismograph
Koyama	8.1	59	4.0	6
Misaki	8.8	64	4.2	4
Kamakura	10.3	76	4.8	5
Hongô	15.0	106	5.5	7
			3.5	58
Titibu	15.2	110	4.1	6
Tôgane	18.9	140	5.8	5
Sakura	20.5	158	7.4	3

As to densities and elastic constants of the surface layer and of the subjacent medium and as to the thickness of the surface layer at Kwantô district in Japan, we have employed the results of investigations obtained

by Dr. Matuzawa.[2] They are as follows; the velocities of P waves and S waves of surface layer are 1.94 km/sec and 1.14 km/sec; those of subjacent medium are 5.0 km/sec and 3.15 km/sec respectively, and the thickness of the surface layer is 7 km. If we use these values, the apparent velocity of transmission of the peculiar phases becomes 0.91 km/sec. Since, from the results of the mathematical investigations with respect to Rayleigh-waves transmitted through a stratified body, the minimum group velocity of M_2 waves in the usual cases (that is where the ratio of ϱ/ϱ' is unity and the ratio of μ/μ' is from five to twenty) is mostly of the constant value of 0.74 (velocity of S phases of surface layer),[3] the minimum group velocity of M_2 waves takes a value of 0.84 km/sec, owing to Dr. Matuzawa's results which hold that the velocity of S waves of surface layer is 1.14 km/sec. Now, we are able to know that, the apparent transmission velocity of the peculiar phases agree closely with the minimum group velocity of the M_2 waves.

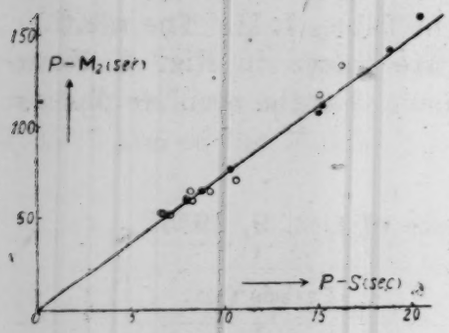

Fig. 4. The relation between the rrival times of the P phases those of the S phases and those of the peculiar phases (M_2). ○; Yamanaka-Lake earthquake, ●; Middle Ize earthquake.

On the other hand, the wave velocity of the M_2 waves corresponding to the minimum group velocity and the wave length (L) estimated from the mathematical investigations are $(1.25\pm0.05)\sqrt{\mu'/\rho'}$ and $(0.95\pm0.10)H$ respectively. Now, substituting the values of H=7km, $\sqrt{\mu'/\rho'}$=1.14km sec, to the mathematical results above-mentioned, we obtain the period (T) of the M_2 waves, T=0.49~0.43 sec. In comparing the value of period thus determined and the values shown in the fourth column of Tables I, II, it will be seen that the periods of the peculiar waves are quite similar to the calculated vaue of the period of oscillation in the M_2 waves.

Thus, from the above considerations, it may be concluded that the identification of the M_2 waves was not difficult, not at any rate in the present examples.

If it be possibles to know the orbital motion of the waves by means of the seismic records, we should be able to confirm to a greater extent the existence of the M_2 waves.

---

2) T. MATUZAWA and T. FUKUTOMI, *Bull. Earthq. Res. Inst.*, **10** (1932), 499.
T. MATUZAWA, K. HASEGAWA and S. HAENO, *Bull. Earthq. Res. Inst.*, **4** (1928), 85.
3) K. KANAI; Monthly Metting, *Earthq. Res. Inst.*, Mar. 19, 1946.

13. *The Earthquake-Motions on Various Formations of the Earth's Surface.* (I). *Observation at Kōti City.*

By Takeshi MINAKAMI and Shūzō SAKUMA,

Earthquake Research Institute.

(Read May 20, 1947.—Received March 31, 1949.)

I. INTRODUCTION.

In the discussions of the serious damages caused by strong earthquakes, Japanese seismologists[1] and architects touched very frequently upon the close relations between damages and formations near the earth's surface.

In order to study the problem more precisely, the writers carried out the seismometric investigations on the earthquake-motions shown near the earth's surface soon after the great earthquakes at Tottori, Nankai and Hukui. The writers reported already the results of researches at Tottori[2] and Hukui,[3] and in the present paper will give an outline of the study conducted by the observations of the after-shocks at Kōti.

2. SEISMOMETRIC OBSERVATIONS OF AFTER-SHOCKS AT KŌTI.

The seismograms of an earthquake, recorded at several stations on the various grounds, even though obtained by the seismographs of the same type, are very much different from one another in their forms, amplitudes and periods. As the causes of these phenomena, it may be remarked as follows:

1) factors due to the different epicentral distances,

2) factors due to the mechanism of the production of seismic waves at the hypocentre,

---

1) T. MATUZAWA, *Rep. Imp. Earthq. Invest. Comm.*, **100**, A (1925), 163 (in Japanese). N. NASU, *Rep. Imp. Earthq. Invest. Comm.*, **100**, A (1925), 313 (in Japanese). M. ISHIMOTO, *Bull. Earthq. Res. Inst.*, **10** (1932), 171; **12** (1934), 234; **13** (1935), 592; **14** (1936), 240; **15** (1937), 536. T. MINAKAMI & S. UTIBORI, *Bull. Earthq. Res. Inst.*, **24** (1946), 19 (in Japanese). R. TAKAHASHI & K. HIRANO, *Bull. Earthq. Res. Inst.*, **19** (1941), 534 (in Japanese). S. OMOTE, *Bull. Earthq. Res. Inst.*, **24** (1946), 87 (in Japanese). S. MIYAMURA, *Bull. Earthq. Res. Inst.*, **24** (1946), 99 (in Japanese).

2) T. MINAKAMI, *Bull. Earthq. Res. Inst.*, **22** (1944), 42 (in Japanese).

3) T. MINAKAMI & S. SAKUMA, *Bull. Inv. Comm. Hukui Earthq.*, (1949), (in Japanese).

3) factors due to the disparity in paths of the seismic waves through the earth's crust from the hypocentre to the respective stations.

4) characteristics caused by the ground-formations near the stations.

In addition to these factors, the earthquake-motions depend on the depth of hypocentre, magnitude and epicentral area. For the study of the earthquake-motions due to the ground formations, it is necessary to distinguish the earthquake-motions due to the surface formations from those of other origins. On this account, seismographs were set at 14 stations on the various formations in the city of Kōti and they recorded numbers of after-shocks which took place at the distance of 50–200 km from these stations. Accordingly, for an after-shock which occurred at farther distance than 100km, the seismograms at the stations in Kōti would show differences caused only by the properties of the ground formations near the respective stations. Therefore, the writers made the comparison of these seismograms recorded on the alluvial stratum of various materials and of diverse thickness, with those on the mesozoic formation.

The writers used four seismographs of the horizontal component which have following constants;

Geometrical magnification	Period	Damping ratio	Number of instrument used
350	1.0 Sec.	1 : 10	2
200	1.0 Sec.	1 : 10	2

In order to make everything precise, these four seismographs were tested at the station (No.2) whether they were in good condition or not. After actual constants were obtained, these seismographs were distributed on the alluvial formations one after the other. Needless to say, one seismograph which was set at the standard station (No. 1) on the mesozoic formations, was operated without removal through the period of the present investigation. Thus, sixty-one after-shocks were recorded while the observation was made for 26 days through March 13 to April 7, 1947.

It may be necessary to give here a brief description of the geographical sketch on and around Kōti city. The town of Kōti is bounded by hills of mesozoic formations towards its north, south and west, and connected by the alluvial plain towards its east. Although Kōti is situated at the corner of this alluvial plain, several low hills of mesozoic formations are scattered in the town just like isolated islands on the alluvium. Accordingly, the thickness of the alluvial layer in the town is various, but as a general trend, it decreases towards the western part of the town. As the result

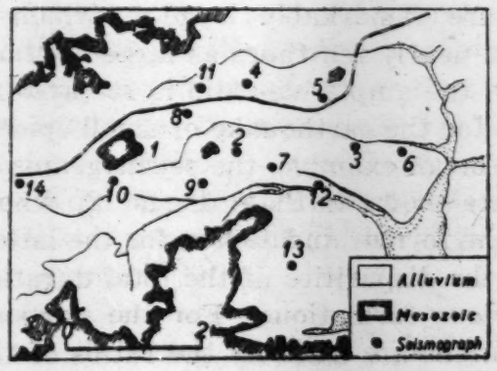

Fig. 1. Stations.

Fig. 2. Depth of a layer of fine sand (in m).

of the several borings performed in the town, it was found that there is a thin layer of fine sand within alluvium. As shown on the map of Fig. (2), the depth distribution of this sand layer represents, to some extent, the feature of the alluvium.

3. Characteristics of the Earthquake-Motions on the Alluvium.

In order to indicate the characteristics of the earthquake-motions on the alluvium, the writers paid attention to the maximum amplitude, the total duration and the mean period or predominant one of after-shocks. In other words, as to the amplitude, they made the ratio of the maximum amplitudes on the various formations to that of the standard station (1) which is situated on the mesozoic formations. It must be added that the

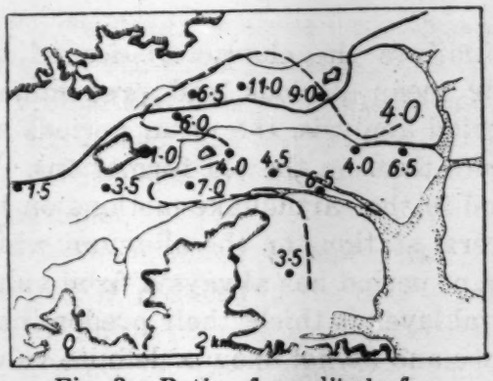

Fig. 3. Ratio of amplitude for remote earthquakes.

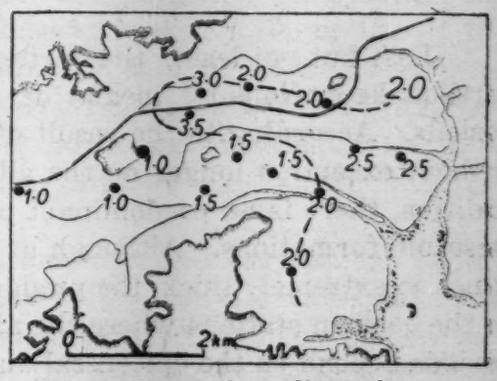

Fig. 4. Ratio of amplitude for near earthquakes.

ratio above mentioned coincides with the ratio of the mean amplitude in the principal earthquake-motions. As seen in the geographical distributions of these amplitude-ratio (Fig. 3), the amplitude of the earthquake-

motions on the alluvial formations are remarkably large, of which at several stations, their amplitudes show nearly ten times as large as those on the mesozoic formations. However, the amplitude-ratio is remarkably reduced and almost two or three times for the earthquake of small epicentral distance, as shown in Fig. (4). For an example, the seismograms of two after-shocks, at various grounds are shown in Plate 1 and 2, whose epicentral distance is about 17km for the former and 150km for the latter.

Secondarily, the writers remark the disparities of the total duration of the earthquake-motions on the various formations. For the purpose, the comparisons of the earthquake-motions are made by the ratios of the total duration as done in the amplitude. As the result, it is made clear that the total duration of the earthquake-motions lasts always longer than that on the standard station which is located on the rocky and hard formations. The geographical distribution of ratio defined above is illustrated on the map of Fig. 5.

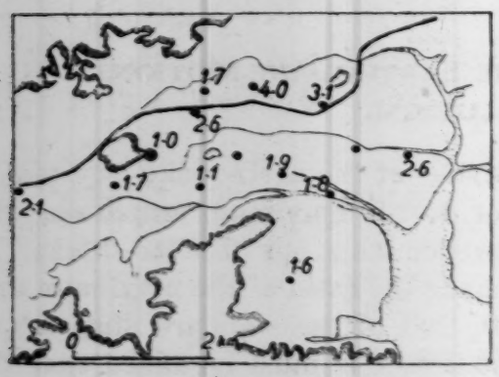

Fig. 5. Ratio of total duration.

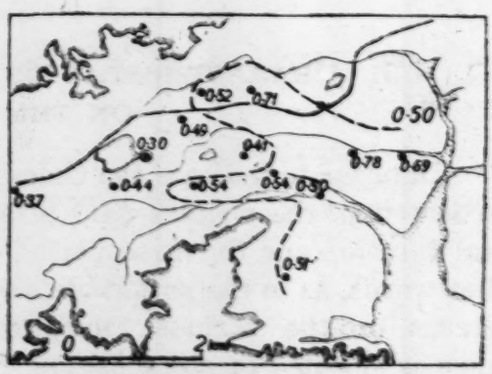

Fig. 6. Mean period (in second).

Last but not least, the writers indicate the characteristics of the earthquake-motions by means of their mean periods and predominant periods. According to the result of period analysis, the mean periods are without exception longer on the alluvium than on the old formations. In addition, there is no predominant period in the earthquake-motions on the mesozoic formations. Although at several stations on the alluvium which is not so extremely thick, the predominant period has always a fixed value, on the eastern stations where the alluvial layer is thick, their predominant periods depend on the epicentral distance and do not show a definite value. As will be seen on the map in Fig. 6, the mean periods at the stations (1) and (4) which are located on the rocky and hard formations, are 0.3 sec. and 0.4 sec. respectively, namely, they are shorter than those on the alluvium. On the other hand, on the alluvial formations, the deeper is alluvial layer the longer is mean period. Namely, the mean period shows 0.5–0.6

sec. on the central part of the town and 0.5–0.8 sec. on the eastern part of it. Contrasting the geographical distribution of the mean period with that of the maximum amplitude or the total duration, we can recognized clearly that the longer the mean period is the larger the amplitude and the larger the total duration.

To sum up, the characteristics of the earthquake-motions are very remarkably dependent on the surface formations of the ground.

4. Cocluding Remarks.

The phenomenon of the anomalous distribution of amplitude, that the amplitudes at several stations on the alluvium are several times as large as that on the mesozoic formations, is mainly caused by extreme smallness in the elastic constant of the soil materials as against that of the mesozoic formations.

It will be reasonable that at these stations within the town of Kōti, their earthquake-motions of an earthquake whose epicentre is distant more than 100km, must be almost similar one another, provided that the ground formations near these stations are similar. In other words, the earthquake-motions of such a distant earthquake must be similar in their amplitudes, periods and durations under the alluvial stratum of the town. Therefore, if dissipation and reflections within the alluvial stratum are put out of question, the total energy of the earthquake-motions at station on the alluvium, must be not different from that on the mesozoic formations.

According to experiments,[4] the elastic constants of rocks and soils, such as found at Kōti, are estimated at 10^{10}–10^{11} C.G.S. for the former and nearly 10^{8}–10^{9} C.G.S. for the latter. Consequently, the ratio of the elastic constants in these two kinds of material is nearly 100 or 10. If the energy of the earthquake-motions in the elastic medium is proportional to the products of elastic constants and the square of amplitude, it is reasonably explained that the amplitudes of the earthquake-motions on the alluvial formations are ten or three times as large as those on the mesozoic formations.

As mentioned already, the amplitude ratio at the stations on the alluvium is reduced in the near earthquakes, in which the earthquake-motions of short periods are markedly predominant. This phenomenon will be explained by the well-known fact that the earthquake-motions of short period are more remarkably dissipated within soil material than those of longer period.

---

4) M. Ishimoto & K. Iida, *Bull. Earthq. Res. Inst.*, **14** (1936), 632; **15** (1937), 67. K. Iida, *Bull. Earthq. Res. Inst.*, **16** (1938), 131; 396.

The existence of deep or shallow alluvial layer upon the mesozoic formations and the marked disparities of the elastic properties in these two kinds of material will put the reasonable interpretation upon various phenomena in connection with periods and the total durations of the earthquake-motions.

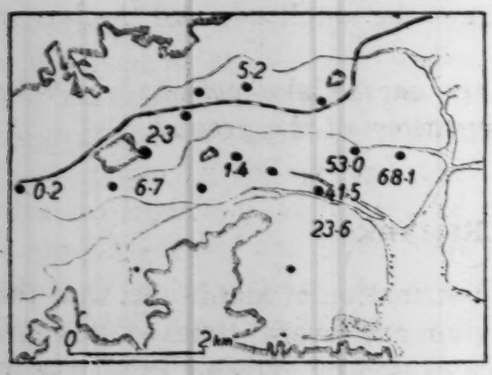

Fig. 7. Damage percentage.

For comparison of the results of the present study with the damages of dwelling houses caused by the Nankai earthquake, the damage percentages of it in fourteen sections of Kōti city are shown on the map of Fig. 7. The damage percentages (P) are defined as following[5]:

$$P = \frac{N + \frac{1}{2}M}{S} \times 100\%,$$

where N: numbers of houses totally destructed,
M: numbers of houses seriously damaged,
S: total number of houses in a section.

After all, the comparison shows the fact that only the earthquake damages have the close connection with the characteristics of the earthquake-motions due to the formations near the earth's surface.

In conclusion, we wish to express our thanks to the official of Kōti Prefecture and the Department of Education, with whose financial aid the present study was made possible.

5) S. MIYAMURA, loc. cit.

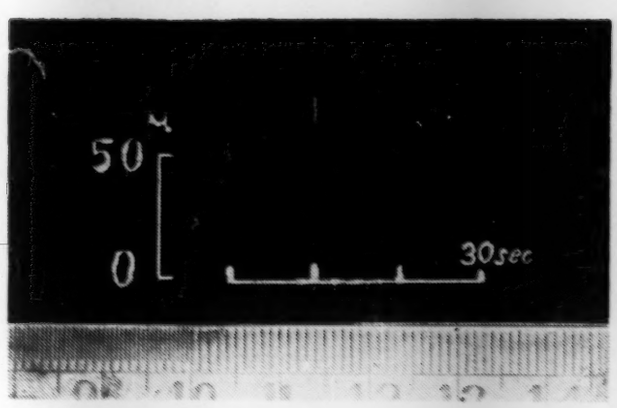

(a)

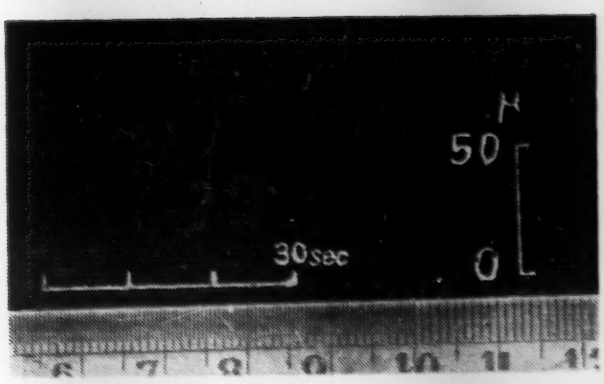

(b)

(a) Seismogram obtained on the mesozoic formation.
(b) Seismogram obtained on the alluvial formation.

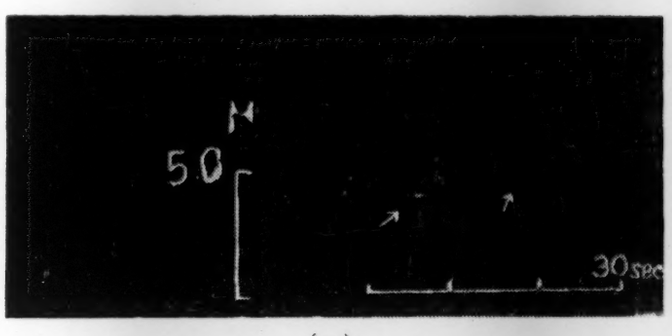

(a)

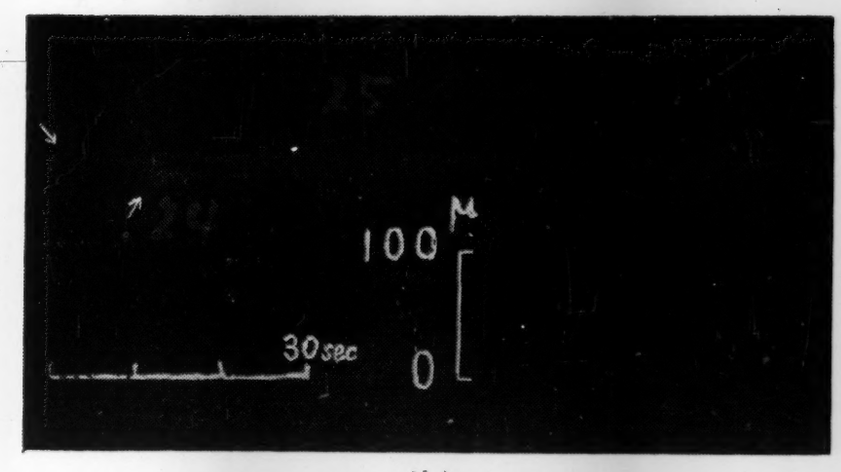

(b)

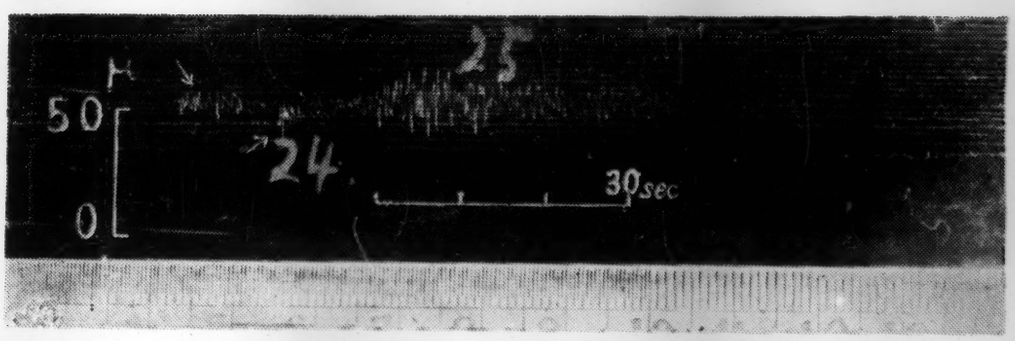

(c)

(a) Seismogram of the station (1) on the mesozoic formation.

(b) (c) Seismograms of the stations (4), (6), on the alluvium.

14. *The Earthquake-Motions on Various Formations of the Earth's Surface. (II) Observations at Gobō and Kiribe.*

By Shūzō SAKUMA,

Earthquake Research Institute.

(Read Feb. 18, 1947.—Received March 31, 1949.)

1. INTRODUCTION.

The damages on buildings by earthquakes are always seriously affected[1] by geological and geographical conditions of the ground on which they are built. At the time of the Nankai Earthquake of 1946 also the remarkable effects of surface-layers on the damages were noticed. The writer attempted to treat this problem by simultaneous observations of earthquake-motions on various grounds, availing himself of the after-shocks. The observations were carried out in the vicinities of Gobō and Kiribe in Wakayama Prefecture. The outline of the work is reported here.

2. THE INSTRUMENTS AND METHOD OF THE OBSERVATIONS.

Two microseismographs of the same type (Improved Ishimoto's Type) were used for the present purpose. One of them was set at a fixed station (the standard station) and the other was transported from one field-station to another on the ground of various geological conditions. The distance between the two stations did not exceed 2.4km, which was small enough when compared with the epicentral distances of earthquakes actually used in comparison. Then, the effects due to the difference in epicentral distance and azimuth about each earthquake could be reduced greatly and those due to the surface-layers were examined. The constants of each seismograph are as follows:

Geometrical magnification:	150
Period:	1.0 sec
Damping ratio:	1:10

The characteristics were proved to be perfectly the same by calibration at the standard station. N-S component of earthquake was simulta-

1) loc. cit. in p. 61 of this Bulletin.

neously recorded at two stations. In most cases three or more available records of earthquakes were obtained in one or two days.

3. STATIONS OF OBSERVATION.[1]

(a) Gobō (Fig. 1)

(1) The Gobō Middle School (standard station) : gravels and sand.
(2) The Gobō Girls' High School (0.3km SW of (1)) : gravels and mud.
(3) Maruyama (2.0km N of (1)) : slightly weathered mesozoic rock.
(4) Matubara (1.2km SW of (1)) : thin muddy soil covered with ballast, near sandy coast.
(5) Sinhama (1.5km SW of (1)) : fine sand.
(6) Wada (2.4km W of (1)) : soft mud containing fine sand.
(7) Nisi-Gobō (1.3km S of (1)) : reclaimed land by ballast.

The damages due to the Nankai Earthquake were not remarkable in this district and, at Gobō, only cracks on walls were seen. At Wada, however, tiles of roofs slipped down and many houses tilted and were half-destructed. On the other hand, at Maruyama the seismic intensity was far less than that at Gobō and no damage was caused.

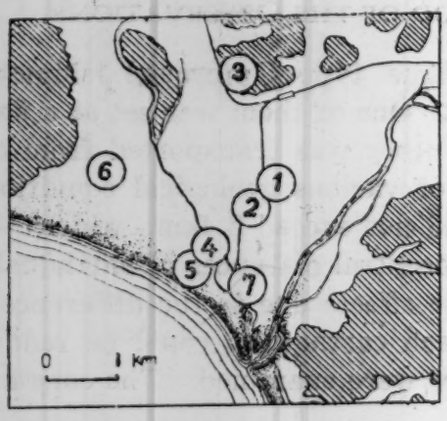

Fig. 1. Stations near Gobō.

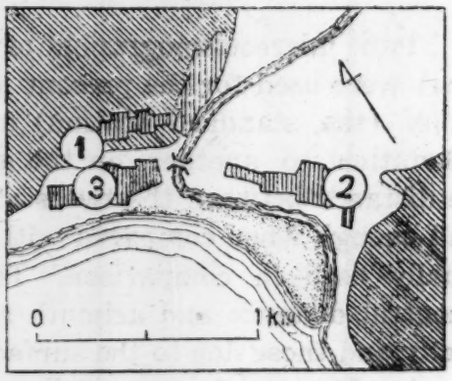

Fig. 2. Stations at Kiribe.

(b) Kiribe (13km SE of Gobō) (Fig. 2)

(1) The Kiribe Primary School (Uedō) (standard station) : on the coastal terrace of mesozoic rock covered with gravels.
(2) Simada (1.2km SE of (1) : water-rich mud and gravels.
(3) Motomura (0.3km S of (1)) : gravels and fine sand.

1) S. MIYAMURA, Same Bulletin p. 101-104.

The damages were concentrated to Shimada, where several houses were destructed. At Motomura, walls and roofs were slightly injured. No damages at Uedō.

4. Results of Observation.

In the vicinities of Gobō, the observation was done during 12th—25th, Jan., 1947, and at Kiribe during 24th—27th. The frequency of the duration of preliminary tremors (P-S time) of the recorded earthquakes is shown in Fig. 3. The after-shocks occurred far and wide as illustrated in this figure and as reported by T. Hagiwara and S. Murauchi.[1)]

In comparing the seismograms each other, the earthquakes, the epicentral distances of which were large enough in comparison with the distances between the stations concerned, were taken up.

Remarkable differences were found among the seismograms on the grounds of various formations, that is, in both amplitude and period.

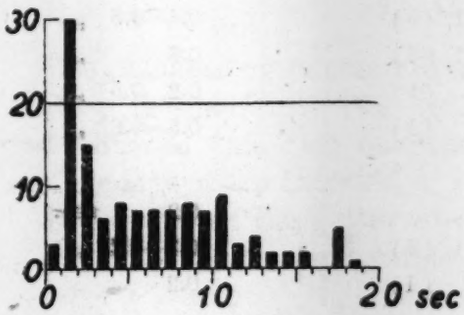

Fig. 3. Frequency of P~S time at Gobō.

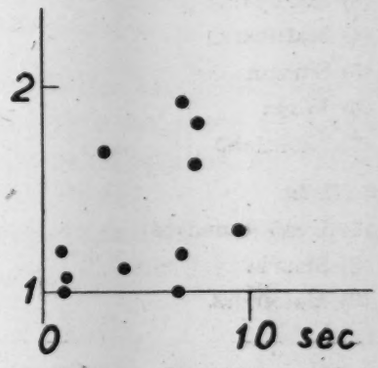

Fig. 4. Ratio of the maximum amplitude (in ordinate) and P~S time (in absissa). [Gobō (2) : (1)]

(a) Amplitude

With regard to the amplitude, comparison was done for the maximum ones. The mean values of the ratios of the maximum amplitude of field-stations to standard stations are tabulated on Table I with probable errors. Fluctuation in the ratio among several earthquakes which were recorded at a definite field-station and at a standard station may be due to the characteristics of incident waves. It may not be so unreasonable to suppose that these incident waves of different characters cause different modes of vibration near the earth's surface. The ratio of amplitudes of eleven earthquakes of various P-S time, obtained simultaneously at (1)

1) T. Hagiwara, S. Murauchi & J. Yamada, *Bull. Earthq. Res. Inst. Supplement* Vol. 5 (1947), p. 164 (In Japanese).

and (2) of Gobō, are shown in Fig. 4 as an example.

Nevertheless, the difference of the mean value of ratio is remarkable enough among the stations on various sediments. That is, the amplitude is greater on alluvial formations than on hard rocks, and especially on soft muddy soil such as at Wada, the amplitude attains about three times more than on mesozoic rock. Another interesting result is the smallness of amplitude on sand.

Table I. Ratio of Max, Amplitude and Predominant Period.

Station	Ratio	Predominant Period
(a) Gobō		
(1) Middle School (standard)	1.0 ± 0.0*, (4)**	0.4—0.5 sec.
(2) Girls' School	1.3 ± 0.3, (11)	0.2, 0.4 ,,
(3) Maruyama	0.7 ± 0.1, (4)	0.2, 0.4 ,,
(4) Matubara	1.0 ± 0.1, (5)	0.4—0.5 ,,
(5) Sinhama	0.8 ± 0.1, (3)	0.6 ,,
(6) Wada	2.4 (1)	0.2, 0.5 ,,
(7) Nisi-Gobō	1.5 (1)	0.5—0.6 ,,
(b) Kiribe		
(1) Uedō (standard)	1.0***	0.2 sec.
(2) Simada	1.4 ± 0.1, (3)	0.3—0.4 ,,
(3) Motomura	1.2 (1)	0.2 ,,

Note: * The result of calibration
** The number of earthquakes compared
*** Setting standard station as 1.0

(b) The Period of Earthquake-Motions

Intervals between successive peaks on seismograms were read and frequency of occurrence was obtained for several records at every station. The predominant periods are not always the same for the earthquakes recorded at the same station. The examples of distribution of frequency are illustrated in Fig. 5. This character may probably be due to the same causes as mentioned before with regard to the fluctuation of the ratio of amplitude. With a glance at Table I, one can conclude that, on alluvium and reclaimed land, periods are always longer than on hard rocks. The long period at Sinhama is also interesting. It may not be decided now, whether this is caused by character of sand or by the same manner as Wada and Nisi-Gobō.

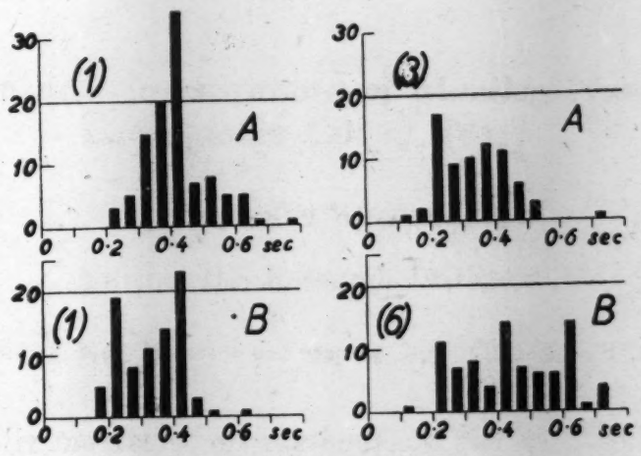

Fig. 5. Frequency of period of two Eqks.,
A: Jan. 16, P~S time 6.6 sec.; B: Jan. 21, P~S time 8.9 sec.
Station (1): Middle School; (3): Maruyama; (6): Wada.

5. Conclusion.

The damages on houses are connected with the amplitude and period of earthquake-motions. The results which were obtained at Gobō and Kiribe affirmed this fact quantitatively. Detailed studes of virbations in surface-layers are interesting problems in future.

In conclusion, the writer wishes to express his thanks to Dr. T. Minakami for his guidances and valuable advices.

15. *Statistical Investigations of Monthly Numbers of Earthquakes Felt at Tokyo.*

By Fuyuhiko KISHINOUYE,

Earthquake Research Institute.

(Read June 18, 1946, March 16 and May 18, 1948.—Rec. March 31, 1949.)

The monthly numbers of earthquakes felt at Tokyo during 1872-1923 were published by Messrs Y. Yasuda and T. Kodaira.[1] And the numbers during 1924–1942 are found in the Seismometrical Report of the Earthq. Res. Inst. Since then although the recording is continued till now, it is not published yet.

The data before 1898 were omitted in the present investigations, because the recording depended only on human feeling and the positions of the epicentres were not determined seismometrically. During the period 1898–1947, 2916 earthquakes were felt at Tokyo, but in this number those felt there anomalously were omitted. The maximum annual frequency was 586 in 1923, the minimum 18 in 1945, and the maximum monthly frequency was 444 in September, 1923.

Table I.

Period	No. of years	No. of earthquakes	Annual mean	Monthly mean
1898–1947	50	2916	58.3	4.9
1936–1947	12	441	36.8	3.1

PERIODICITY OF EARTHQUAKES DURING 1872–1945.

The periodicity was investigated by the method of periodogram with the monthly numbers. As the results, periods of 12 months, 25 months and 50 months were found. Those longer than 50 months were studied with the annual frequencies. And on the periodogram, the amplitudes of 6 and 9 year period were noticeable.

1) Y. YASUDA and T. KODAIRA, Earthquakes observed in Tokyo during the period from September, 1872, to December, 1923. Tokyo, 1938.

RELATION BETWEEN MONTHLY NUMBERS AND INTENSITY OF FELT EARTHQUAKES.

Correlation between monthly earthquake numbers and intensity in Japanese seismic intensity scale, which classify the intensity in numbers 0–6, of the strongest earthquake in the month was studied. The strongest intensity in a month was adopted and weaker ones were neglected, because although many in number total energy of the weaker ones is usually small compared with that of the strongest.

The correlation ratio between the number and the intensity was obtained as 0.41 ± 0.02. Furthermore, the correlation was investigated by non-correlation test for the following contingency table.

Table II.

Monthly Number	Intensity scale							
	0	I	II	III	IV	V	VI	
0–4	27	150	105	70	14	0	0	366
5–9	0	44	56	71	10	1	0	182
10 <	0	2	5	17	11	4	1	40
	27	196	166	158	35	5	1	588

Comparing the above values to those calculated under the assumption of non-correlation between the frequency and the intesity, χ^2 was obtained as 145. The probability corresponds to the above value of χ^2 is less than 0.001. Then it may be concluded that the intensity and the monthly numbers are correlative as the writer described in the investigation of the Itō earthquake swarm of 1930.[2)]

Table III.

Contingency table of intesity and earthquake number in the previous month.

Monthly Number	Intensity scale							
	0	I	II	III	IV	V	VI	
0–4	22	130	122	89	16	2	1	382
5–9	4	58	40	52	13	2	0	169
10 <	1	7	10	11	6	1	0	36
	27	195	172	152	35	5	1	587

$$\chi^2 = 24.5 \qquad 0.02 > P > 0.01$$

2) F. KISHINOUYE, *Bull. Earthq. Res. Inst.* **15** (1937), 791.

Correlations between the intensity of the strongest earthquake in a month and the monthly numbers of earthquake in the previous or the next months were investigated by the methods similar to the above.

Table IV.

Contingency table of intensity and earthquake number in the next month.

Monthly Number	Intensity scale							
	0	I	II	III	IV	V	VI	
0–4	21	135	124	92	16	4	0	392
5–9	5	55	38	49	13	0	0	166
10 <	1	6	10	10	6	1	1	35
	27	196	172	151	35	5	1	587

$$\chi^2 = 32.7 \qquad 0.01 > P > 0.001$$

From the above results, the more earthquake number, the more probable the occurrence of a strong earthquake. And when a strong earthquake occurs in a month, the number of earthquakes will become large in the next month, but the strong earthquake has little correlation with the number of the previous month. In other words, even if the monthly earthquake number in a certain month is very large, a strong earthquake is not expected in the next month.

Correlation between the earthquake number in a certain month and the previous or the next months were studied further by the method of auto-correlation. For the comparison, the method was applied to the monthly frequencies at Utsunomiya, Mito and Wakayama.[3] The results are shown in the following table.

Table V.

Place	Interval	No. of Months	No. of Eqkes.	Correl. Coeff. of successive two months	Correl. ratio for the next month	Correl. ratio for the previous month
Tokyo	1898–1947	588	2269	0.20±0.03	0.28±0.03	0.26±0.03
Utsunomiya	1891–1936	543	2883	0.22±0.03	0.26±0.03	0.30±0.03
Mito	1897–1936	438	3646	0.23±0.03	0.26±0.03	0.28±0.03
Wakayama	1907–1936	318	1776	0.80±0.01	0.85±0.01	0.82±0.01

3) M. TAKEHANA, *Kensin-jihō*, **10** (1937) 118–146.

In the calculations the monthly numbers over 18 were omitted.

It may be deduced that the monthly numbers are distributed at random, and the clustering of earthquakes such as after-shocks does not affect the monthly frequency distribution.

ON THE DISTRIBUTION OF MONTHLY NUMBERS.

If the probability p is small and the total number N is large, the distribution may be expressed in Poisson's formula:

$$f(x) = \frac{m^x e^{-m}}{x!} \qquad \text{where} \quad m = Np\,.$$

The frequency-distribution of the earthquakes is usually expressed in Poisson's formula. In this formula if m becomes large, the distribution will approach to Gauss' normal distribution. This character of Poisson's formula will be seen in Fig. 1.[4]

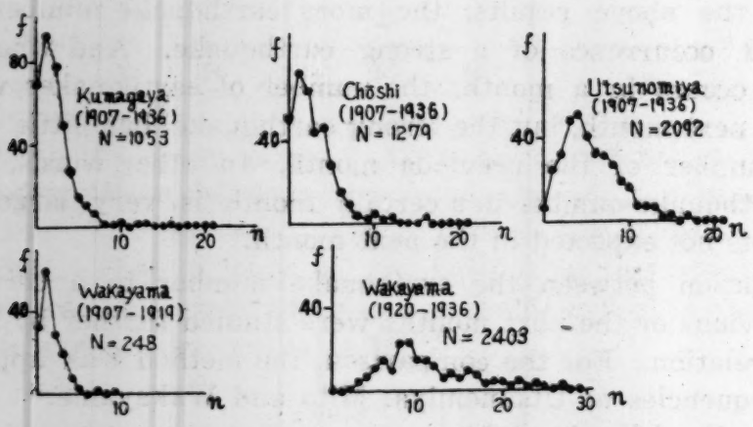

Fig. 1. Frequency-distribution of monthly numbers of felt earthquakes.

The frequency-distribution at Tokyo was expressed in the two formulae (Fig. 2):

$$f(x) = \frac{3.87^x e^{-3.87}}{x!},$$

$$f(x) = \frac{x}{\sqrt{2\pi}\,2.54}\, e^{-\frac{(x-3.87)^2}{2\times 2.54^2}}.$$

4) M. TAKEHANA, loc. cit.

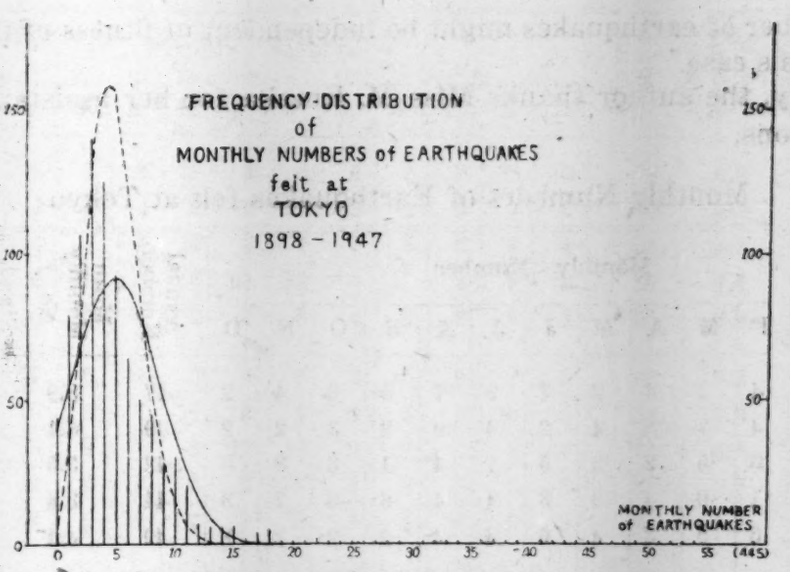

Fig. 2. Full line=Poison's distribution, Broken line=Gauss' distribution.

To examine which formula fits better to the actual frequency-distribution, the χ^2-test was applied over again. The values of χ^2 which correspond to the above formulae were obtained as 82.9 and 64.5 respectively. Although the probability of the occurrence of these values are estimated to be less than 0.001 in both cases, the normal distribution was in better accordance than Poisson's. In other words, the monthly numbers are nearly to be considered as at random and uniformly distributed.

If the variation of annual mean frequencies can be expressed in the normal distribution as above stated, the annual mean number of earthquakes in the next year will be expected by the fiducial limits of the theory of statistics.

If $\bar{f}$ denotes the mean value and σ the standard deviation, the next mean value f will be obtained by the formula,

$$f = \bar{f} + a\sigma$$

The fiducial limits for the allowable error 0.02 of each year are shown in Table VI. Except the year 1923 in which the great earthquake occurred, in most years, 37 annually in 49 years, numbers of the next years were within the fiducial limits. In early 1946, many earthquakes took place at Tokyo compared with those in the previous years, and the citizens were uneasy for the occurrence of a strong earthquake. But the fear might be decreased if the above consideration admitted. The correlation between the annual frequencies and the number of cases of the agreement to the theory was examined by the χ^2-test. The value of χ^2 was obtained as 8.57,

so the number of earthquakes might be independent of fitness of the fiducial limits in this case.

Lastly, the author thanks Miss M. Kotaka for her assistance of this investigations.

Monthly Numbers of Earthquakes felt at Tokyo

Year	Monthly Number f												Annual Number	Mean Monthly No. $\bar{f}$	Stand. Dev. σ	Fiducial Limit 2σ
	J	F	M	A	M	J	J	A	S	O	N	D				
1898	1	4	2	4	2	7	9	7	5	0	4	2	47	3.9	2.6	2.1
99	2	4	7	8	4	2	4	9	2	3	2	2	49	4.1	2.4	2.0
1903	2	6	5	2	2	5	1	4	1	3	8	3	42	3.5	2.0	1.6
1	3	1	0	4	3	3	4	4	6	3	7	3	41	3.4	1.8	1.5
2	4	5	5	3	4	6	4	4	2	2	2	8	49	4.1	1.7	1.4
1903	5	9	3	3	3	2	5	2	1	5	6	1	45	3.7	2.3	1.9
4	6	3	3	4	4	2	10	5	2	7	3	3	52	4.3	2.4	1.9
5	0	2	3	4	4	5	3	1	3	5	2	3	35	2.9	1.7	1.4
6	4	6	2	9	13	0	2	8	3	5	3	0	55	4.6	3.6	3.0
7	2	3	3	4	2	3	3	1	2	7	4	3	37	3.1	1.7	1.4
8	5	0	1	0	4	2	4	3	2	2	1	4	28	2.3	1.7	1.4
9	2	3	10	3	5	2	8	5	3	4	6	6	57	4.8	2.4	1.9
10	2	1	0	3	6	4	4	3	10	7	7	5	52	4.3	2.6	2.2
11	4	3	5	3	2	3	1	4	5	5	12	6	53	4.4	2.7	2.2
12	10	2	5	3	10	5	3	6	3	5	4	7	63	5.3	2.5	2.1
13	1	5	5	4	6	5	5	4	4	3	3	2	47	3.9	1.4	1.2
14	4	5	4	1	3	4	4	1	2	5	0	3	36	3.0	1.6	1.3
15	0	1	4	9	10	5	3	3	1	5	16	2	59	4.9	4.5	3.6
16	1	4	3	2	2	2	3	10	2	4	5	2	40	3.3	2.3	1.9
17	8	6	4	3	1	4	3	4	3	5	9	3	53	4.4	2.2	1.8
18	2	3	5	10	5	1	6	2	2	4	2	3	45	3.7	2.4	2.0
19	2	3	2	5	6	5	4	4	0	2	3	1	37	3.1	1.7	1.4
20	2	3	1	1	3	2	6	2	1	2	1	8	32	2.7	2.1	1.7
21	2	1	1	2	1	0	1	0	1	1	3	11	24	2.0	2.8	2.3
22	4	4	5	10	4	4	3	1	2	2	5	1	45	3.7	2.3	1.9
23	7	5	6	0	6	17	5	3	444	33	34	26	586	—	—	—
24	31	1	2	4	3	4	2	3	5	2	0	3	60	5.0	2.5	2.1
25	7	5	1	1	2	4	2	1	1	2	5	3	34	2.8	1.9	1.6
26	10	10	5	4	7	5	7	6	2	3	7	2	68	5.7	2.6	2.1
27	4	3	6	3	5	2	4	9	9	8	9	3	65	5.4	2.6	2.1

Year	Monthly Number f												Annual Number	Mean Monthly No. $\bar{f}$	Stand. Dev. σ	Fiducial Limit $\alpha\sigma$
	J	F	M	A	M	J	J	A	S	O	N	D				
1928	6	5	7	8	16	4	8	6	2	8	3	5	78	6.5	3.4	2.8
29	5	4	5	4	3	6	6	2	5	3	4	3	50	4.2	1.2	1.0
30	4	4	4	5	13	3	1	7	5	5	3	4	58	4.8	2.8	2.3
31	3	6	12	3	5	11	12	4	14	6	5	8	89	7.4	3.8	1.3
32	0	8	11	5	2	4	5	4	6	8	3	3	59	4.9	2.9	2.4
33	2	7	5	7	3	4	6	3	5	9	7	5	63	5.3	2.0	1.6
34	4	10	3	7	6	9	5	5	3	0	10	3	64	5.3	2.9	2.4
35	10	6	8	8	3	11	10	3	9	4	2	4	78	6.5	3.1	2.5
36	2	1	2	3	1	4	3	1	2	5	4	3	31	2.6	1.3	1.0
37	4	3	2	3	4	1	3	0	4	4	3	3	34	2.8	1.2	1.0
38	3	2	0	5	4	8	6	5	4	2	25	12	76	6.3	6.4	5.2
39	4	2	7	2	5	6	4	2	2	6	1	3	44	3.7	1.9	1.6
40	6	2	5	1	2	7	1	3	3	1	7	3	41	3.4	2.2	1.8
41	1	3	4	3	4	3	4	0	2	3	3	0	30	2.5	1.4	1.1
42	2	3	2	1	5	0	6	3	4	1	3	2	32	2.7	1.7	1.4
43	4	1	6	7	2	3	2	3	0	3	1	0	32	2.7	2.1	1.7
44	0	4	3	3	5	2	2	0	0	0	1	8	28	2.3	2.4	1.9
45	10	1	0	1	0	3	0	0	1	1	1	0	18	1.5	2.7	2.2
46	6	5	0	6	3	0	4	3	5	3	3	8	46	3.8	2.3	1.9
47	3	5	3	4	3	2	3	2	1	3	0	0	29	2.4	1.4	1.2
Total	216	191	197	202	221	205	214	175	(606) 162	219	262	216	(2916) 2472	—	—	—
Mean	4.3	3.8	3.9	4.0	4.4	4.1	4.3	3.5	(12.0) 3.2	4.4	5.2	4.3	49.4	4.1	—	—

The cost of this investigation was mostly defrayed from the Scientific Research Expenditure of the Department of Education.

16. *Monthly Numbers of Earthquakes at Kainan City, Wakayama Prefecture in 1947.*

By Fuyuhiko KISHINOUYE,

Earthquake Research Institute.

(Read Feb. 17, 1948.—Received Mar. 31, 1949.)

After the great earthquake on Dec. 21, 1946, which hit the southern part of Kinki and Shikoku districts, a set of two horizontal seismographs resumed its observation at Kainan City by Mr. H. Imamura and Miss T. Nagasaki. The seismograph had been set by late Dr. A. Imamura, but its observation was stopped during the second World War.

The observation began in Jan., 1947, but its condition was not good and the time marks on the seismograms did not succeed for many days. The recording papers were exchanged at about 10 h every day, then for simplicity of the disposition the dates of the observation were changed at the time of the exchange.

The monthly frequencies in 1947 were as follows:

Month	Jan.	Feb.	Mar.	Apr.	May	Jun.	Jul.	Aug.	Sept.	Oct.	Nov.	Dec.	
Observ. freq.	145	18	36	21	29	20	11	27	8	5	2	1	323
Calcul. freq.	67	50	37	28	21	15	11	8	6	4	3	2	252

The earthquakes might be considered as the after-shocks of the great earthquake on Dec. 1946. The frequency distribution was expressed in an exponential function as usual:

$$f = (90.4 \pm 1.3)\, e^{-(0.296 \pm 0.038)t} ,$$

where t denotes a month. The frequencies calculated by the above formula are shown also in the above table. The fitness of the formula was studied by χ^2-test. The value of χ^2 obtained as 164.7, therefore it will be concluded that the above formula does not express well the observed frequencies.

The intensity of the earthquakes were classified in three: slight, moderate and rather strong. And the contingency table of the earthquake frequency in a day and the greatest intensity scale of the earthquake of that day was made as shown in the following table (see Fig. 1).

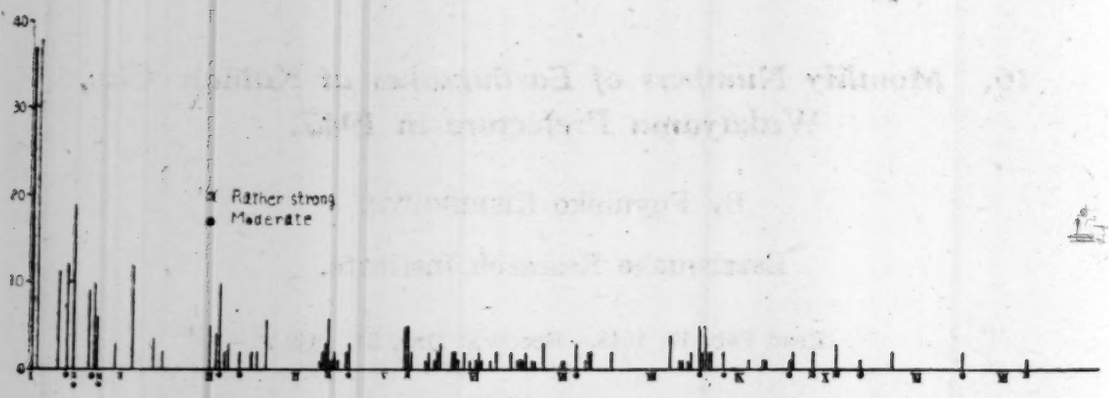

Fig. 1. Daily number of earthquakes at Kainan City in 1947. Roman figures indicate months.

No. of earthquakes	Slight	Moderate	Rather strong	Total
0—9	60	8	5	73
>10	4	3	2	9
	64	11	7	82

As the average, 11.3 earthquakes were recorded in a day when a strong earthquake occurred, and 6.0 when a moderate one occurred, and 3.1 when a slight one took place in a day. The probability of the non-correlation was calculated with the above table, and its value obtained as 0.0095, so it will be concluded that the intensity and the frequency of the earthquake in a day were correlative.

17. *On the Anomalous Distribution of the Maximum Amplitude of Earthquake Motions.*

By Ryôhei IKEGAMI,

Earthquake Research Institute.

(Read June 15, 1948.—Received Oct. 7, 1948.)

I. INTRODUCTION.

The maximum amplitudes of earthquake motions decrease theoretically with respect to the epicentral distance in some function. But we have often observed that they do not decrease uniformly with respect to their distance, that is to say, the amplitudes of earthquake motions at a distant station become abnormally larger than at a near one.

We investigated the distributions of maximum amplitude of earthquakes recorded at the main stations in Kantô and Chûbu districts of Japan.

We chose only the earthquakes of the depths shallower than 80 km, and their epicentres were distributed over the southern sea of Bôsô-Peninsula (A-district in figure), Kujûkuri (B-district), Kashimanada (C-district), and the eastern coast of Fukushima-Prefecture (D-district).

The 91 "moderate" and "remarkable" earthquakes were selected from the Kishôyôran, the monthly bulletin of the Central Meteorological Observatory, during fourteen years from 1930 to 1943 for the materials of this study.

The epicentres of the earthquakes are shown in Fig. 1, where the circles show moderate earthquakes and the black spots remarkable ones.

II. AMPLITUDE-DISTANCE CURVE AND ITS RESULTS.

To examine the relation between the maximum amplitude and the epicentral distance of the earthquakes, logarithm of maximum amplitudes are plotted in ordinate and the epicentral distances in abscissa. In this case, the maximum amplitudes were composed of those in the two horizontal components, but the vertical component were neglected.

In every diagram the maximum amplitude decreases generally according as the epicentral distance increases, but on closer examination

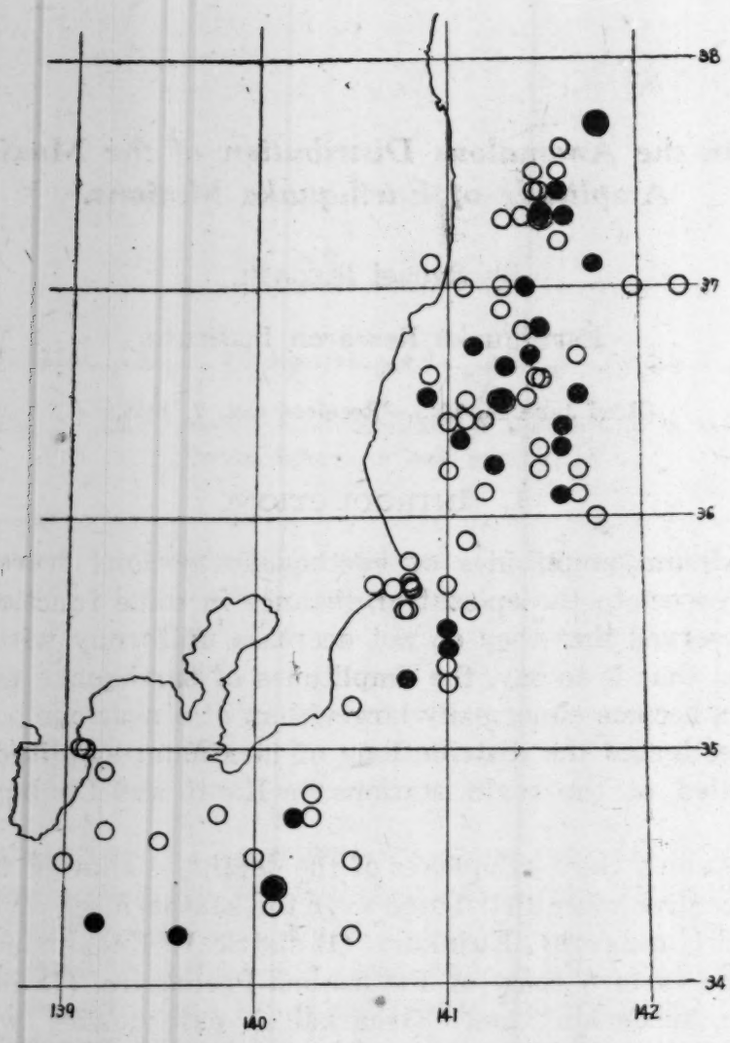

Fig. 1. The epicentres of earthquakes. A circle shows moderate earthquake, and a black spot shows remarkable one.

we found that the maximum amplitude at some stations are abnormally large or small with respect to epicentral distance.

To discuss the maximum amplitude, we must define a standard formula of decreasing amplitude according to the distance, but there are many questions about the formula. For example, C.F. Richter[1] used the formula that the maximum amplitude decreases in inverse proportion to the third power of distance, and H. Kawasumi[2] and K. Wadati[3] assumed the formula, $A = A_0 \frac{1}{\sqrt{\Delta}} e^{-a\Delta}$, where A is maximum amplitude at the station, Δ

1) C. F. RICHTER, *Bull. Seism. Soc. Amer.*, **25** (1935), 13.
2) H. KAWASUMI, *Jishin* (Earthquake), **15** (1943), 12.
3) K. WADATI, *Geophys. Mag.*, **4** (1931), 252.

is the epicentral distance, a is an absorption coefficient of the waves, A_0 is a constant concerning the magnitude of that earthquake. However, the values of a adopted by these two investigators are different. H. Kawasumi assumed that a is a constant value and, on the contrary, K. Wadati assumed that a is a function of distance.

In this paper, we adopted the formula, $A=A_0\frac{1}{\sqrt{\Delta}}e^{-a\Delta}$ and the values of a that K. Wadati had obtained. These values are shown in the following table.

Table I.

Δ	100	150	200	250	300	350	400	(km)
a	7.0*	6.8*	6.5	6.3*	6.1*	5.8*	5.6	($\times 10^{-3}$)

In this table the values with asterisk are calculated by extrapolation or interpolation from Wadati's values at 200 km and 400 km.

Further, the value of A_0, which is a constant value concerning the magnitude of that earthquake, was determined by the mean value of the amplitude at the stations which are situated at the distance of about 100 km and equipped with Wiechert Seismometers. But when there were not appropriate stations at about 100 km, we determined the values by those at about 150 km or about 200 km.

Within 100 km of epicentral distance, the amplitude decreases very rapidly with respect to epicentral distance, so we neglected the values within 100 km.

In every amplitude-distance curve, we apply this standard decreasing curve, and determine the "too large" or "too small" amplitude at every station by the deviations from this standard curve. Namely, we assume that the deviation of amplitude at any station is zero, and denote by *0*, when a deviation of the amplitude of the station corresponds to the value on the standard curve at the distance within 50 km; the deviation is "too large," and expresses by +, when a deviation corresponds to that at the distance of more than 50 km; "too small," and −, when less than 50 km.

When at every station these results of all epicentres were plotted separately on every map by expressions of +, −, and *0*, we found that the maximum amplitudes at some stations were always too large or always too small regardless of the situations of the epicentres, but the maximum amplitudes at the other stations were either too large or too small in accordance with the situations of the epicentres.

To examine this remarkable result further, we calculate the values of amplitude anomaly, M, that is a mean value of the numbers of +, −, and *0* in every district by the following expression.

$$M = \frac{l-m}{l+m+n}, \text{ where } l \text{ is number of } +, \ m \text{ is } -, \ n \text{ is } 0.$$

On the base of the above mentioned results, the stations where the values of M are always positive or always negative are shown in Fig. 2. Further the stations where the values of M change into either positive or negative according to the four districts of situations of epicentres are shown in Fig. 3, 4, 5, and 6 respectively. In these figures a circle shows a station of positive value, a black spot that of negative one.

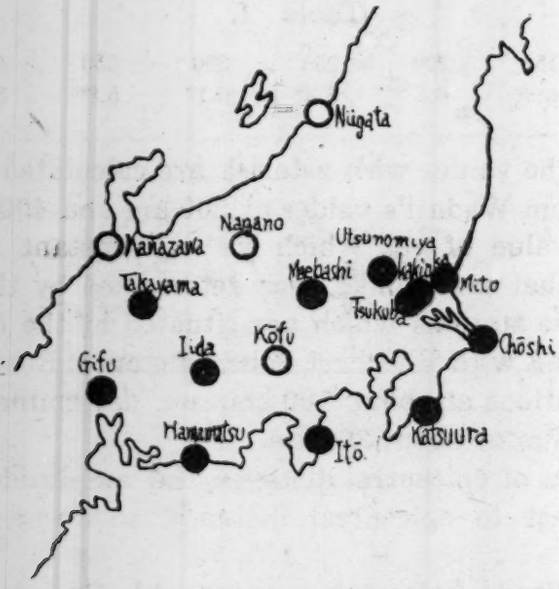

Fig. 2. The distribution of the stations where the amplitudes are always large (circles) and always small (black spots).

III. Discussion of the Results.

The maximum amplitudes became "too large" or "too small" in accordance with the epicentres from very complex causes. But as the causes we can consider the following three factors.

a) The local and geological influences of the ground of the station.
b) The influences of the mechanism of the earthquake origins.
c) The influences of the geological structures of the path of earthquake waves.

In effect, it was very difficult to analyse and classify these influences. We examined the correlation between the sign of M and the ground rock of every station, but we could not get a clear result. But in general, it may be considered that the stations, where the signs of M were always "+" or

always "–" regardless of the districts, were influenced comparatively much by the factor (a). Namely, the stations at Niigata, Kanazawa,

Fig. 3. When the epicentre is situated in A-district, the maximum amplitudes of earthquake motion become too large at the stations shown with circles, and become too small at those shown with black spots.

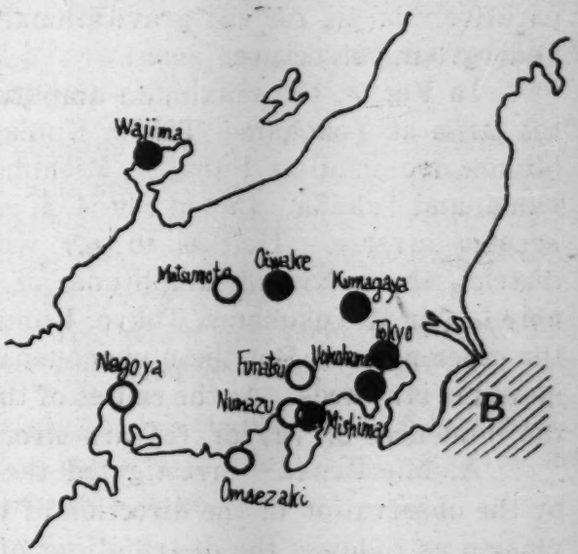

Fig. 4. When the epicentre is situated in B-district.

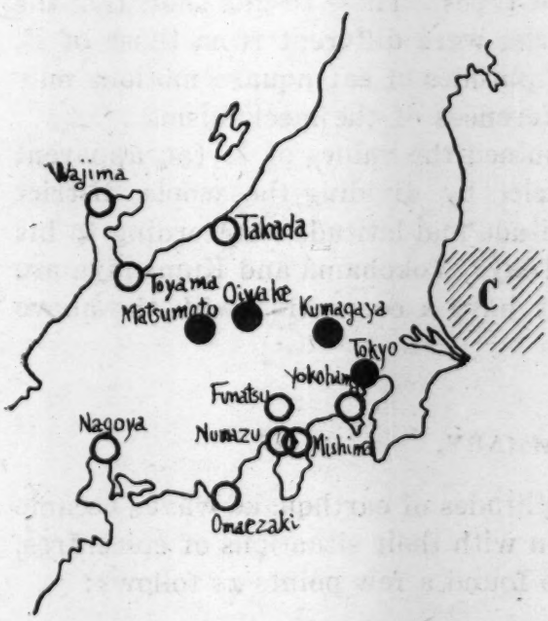

Fig. 5. When the epicentre is situated in C-district.

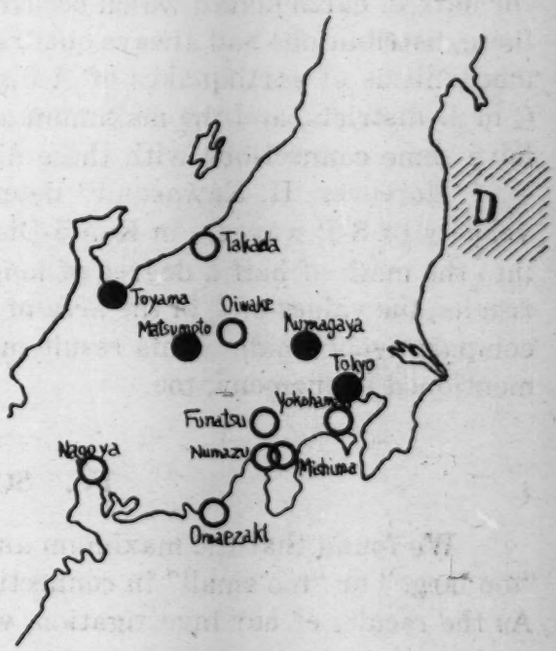

Fig. 6. When the epicentre is situated in D-district.

Kôfu, and Nagoya are situated on the alluvial formations. On the contrary, the stations at Utsunomiya, Maebashi, Mito, Tsukuba, Kakioka, Chôshi, Katsuura and Itô may be perhaps situated on the compact rock, judging from the fact that the gravitational anomalies of these stations are comparatively large, for the gravitational anomaly has some relations to the underground structure.

In Fig. 3, the maximum amplitudes of earthquake motions become too large at Yokohama, Tôkyô, Kumagaya, Oiwake, and Matsumoto, and become too small at Funatsu, Mishima, Numazu, Omaezaki, Nagoya, Toyama, and Takada. But in Fig. 4, 5, or 6, the above mentioned phenomena become inverse. That is to say, when the epicentre was situated in A-district, the maximum amplitudes of earthquake waves become remarkably larger at Yokohama, Tôkyô, Kumagaya, Oiwake, and Matsumoto than the other places. But these phenonena became inverse when the epicentre moved northwards. As the causes of this phenomenon we will consider that the influences of (b) or (c) are stronger than those of (a).

A. Masatsuka[4] investigated the mechanism of shallow earthquake by the observation of the direction of initial motion, and obtained the conclusion as follows: the distributions of the directions of initial motions of earthquakes which occur off Inubôzaki, Kashimanada, and the eastern coast of Tôhoku-District were not of a so-called quadrant-type.

Consequently we investigated the distributions of initial motions by the data of earthquakes which occurred off Bôsô-Peninsula, and found that these distributions had always quadrant-types. These results show that the mechanisms of earthquakes of A-district were different from those of B, C or D-districts, and the maximum amplitudes of earthquake motions may have some connections with these differences of the mechanisms.

Moreover, H. Kawasumi[5] determined the values of k, (an apparent velocity of S-P waves), in Kantô-District by dividing the whole district into the mesh of half a degree of longitude and latitude. According to his results, the values of k in the area of Tôkyô, Yokohama and Kumagaya are comparatively small. This result may have a connection with the above mentioned phenomena, too.

IV. SUMMARY.

We found that the maximum amplitudes of earthquake waves became "too large" or "too small" in connection with their situations of epicentres. As the recults of our investigation, we found a few points as follows:

---

4) A. MASATSUKA, *Kenshin-Jihô*, **11** (1941), pp. 469-511.
5) H. KAWASUMI, *Jap. Assoc. Adv. Soc.*, **14** (1939), pp. 58-62.

1) In spite of the positions of epicentres, the maximum amplitudes appeared always "too large" at Niigata, Kanazawa, Kôfu, and Nagano.
2) The amplitudes appeared always "too small" at Utsunomiya Maebashi, Mito, Tsukuba, Kakioka, Chôshi, Katsuura, and Itô.

It may be considered that these two types were caused by the local and geological influences of the stations.

3) When the epicentre was situated southward of Bôsô-Peninsula, the maximum amplitudes appeared remarkably larger at Yokohama, Tôkyô, Kumagaya, Oiwake, and Matsumoto than the other places and they appeared too small at Funatsu, Mishima, Numazu, Omaezaki, Nagoya, Toyama, and Takada.
4) But the relation became inverse when the epicentre was off Kujûkuri, Kashimanada, and the coast of Fukushima-Prefecture.

These cases may be based on the influences that are caused by the differences concerning the mechanism of the origins of earthquakes or by the geological structures of the paths of earthquake waves.

18. *Relation between Seismic Intensity and Epicentral Distance.* (1)

By Yasuo SATÔ,

Earthquake Research Institute.

(Read Sept. 21, 1948.—Received March 30, 1949.)

We have a number of destructive earthquakes in recent years, and have made investigations by means of post-card method in every time. Here we will state a little about the relation between seismic intensity and epicentral distance.

Seismic intensity scale that we adopted is fairly like Mercalli-Sieberg scale, which Prof. Kawasumi made. We sent post cards and had primary schools in every village, town and city fill blanks and return them. Thus we determined the intensity of every locality, and then calculated the mean intensity of every epicentral distances. The results are shown in figures 1~8. Straight line in the figure was determined by least square, assuming an experimental formula.

$$I' = a + b\Delta \cdots\cdots \text{(unit of } \Delta\text{, 100 km)} \cdots\cdots\cdots\cdots (1)$$

If we exclude a part where Δ is small, it will not be inappropriate to assume this formula.

In Tab. I, name, origin time, epicentre, a, b, and M′ of every earthquake are shown. M′ is defined as the value of I′ in (1) at Δ=100km and implies the magnitude of earthquake. Data of Mino-Owari earthquake are those gathered by Milne.

Table I.

Fig.	Name	Origin Time	Epicentre		a	b	M'
8	Mino-Owari	1891· X ·21	136.6°E,	35.5°N	8.4	— .94	7.5
2	Tottori	1943· IX ·10	134.2	35.5	6.3	— .94	5.4
5	Noziriko	1943· X ·13	138.2	36.8	3.5	— .95	2.4
1	Tô-nankai	1944·XII· 7	136.2	33.7	8.3	—1.04	7.2
6	Mikawa	1945· I ·13	137.0	34.7	5.7	— .76	4.9
3	Hatinohe-Oki	1945· II ·10	142.1	40.9	6.6	— .75	5.8
4	Nankai	1936·XII·21	135.6	33.0	8.0	— .71	7.3
7	Hukui	1948· VI ·28	136.3	36.2	7.5	—1.40	6.2

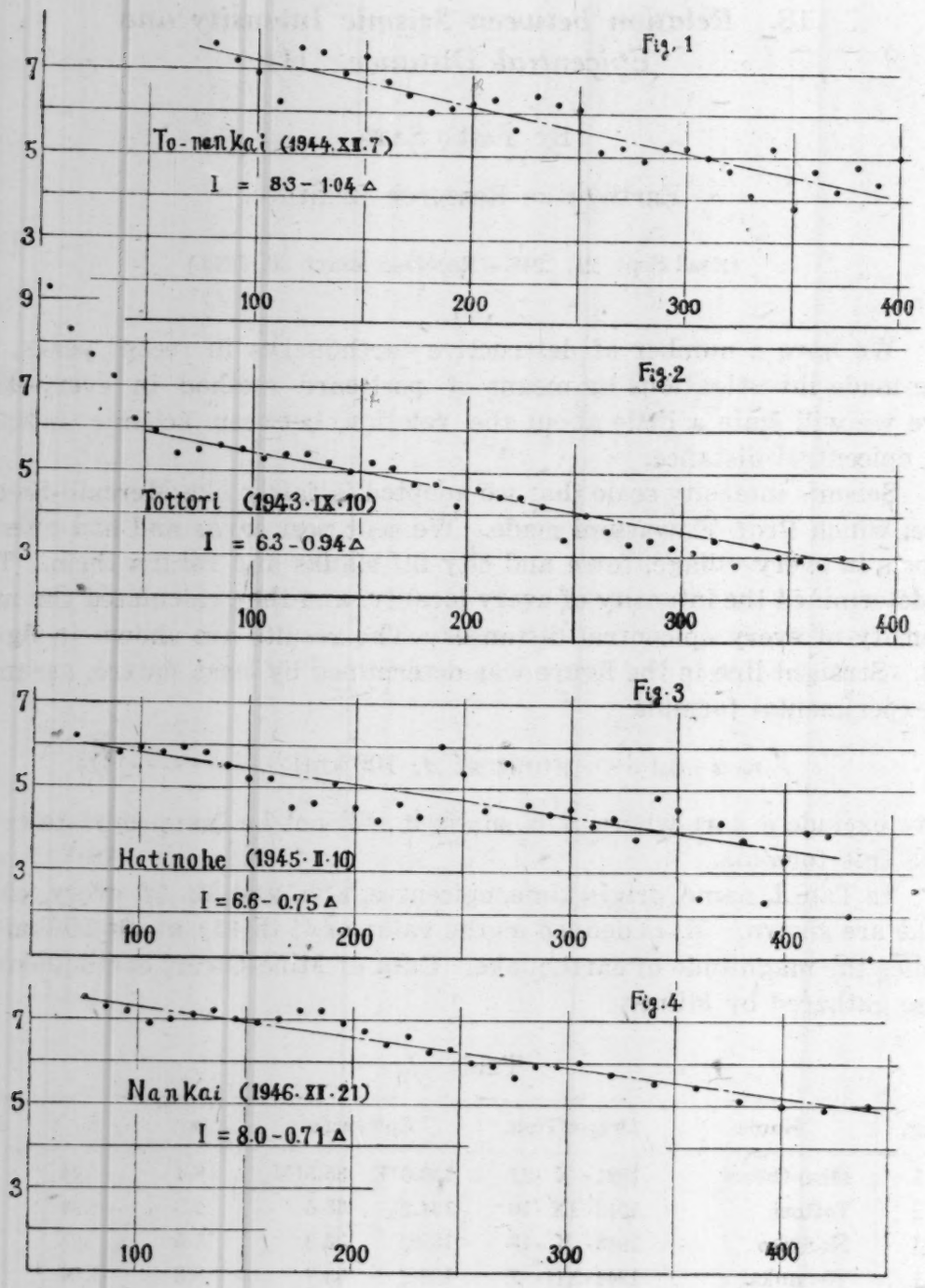
Fig. 1
To-nankai (1944.XII.7)
I = 8.3 - 1.04 Δ
Fig. 2
Tottori (1943.IX.10)
I = 6.3 - 0.94 Δ
Fig. 3
Hatinohe (1945.II.10)
I = 6.6 - 0.75 Δ
Fig. 4
Nankai (1946.XII.21)
I = 8.0 - 0.71 Δ
100
200
300
400
3
5
7
9

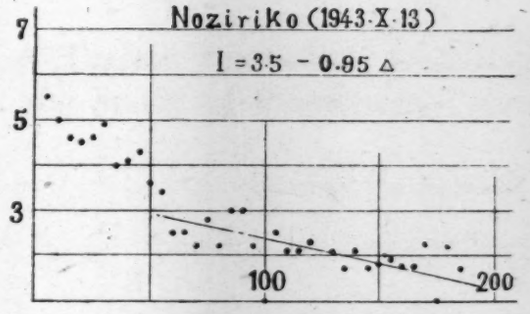

Fig. 5

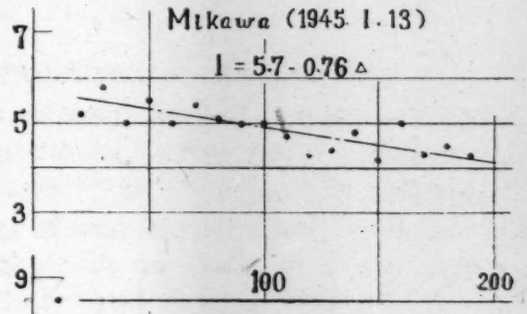

Fig. 6

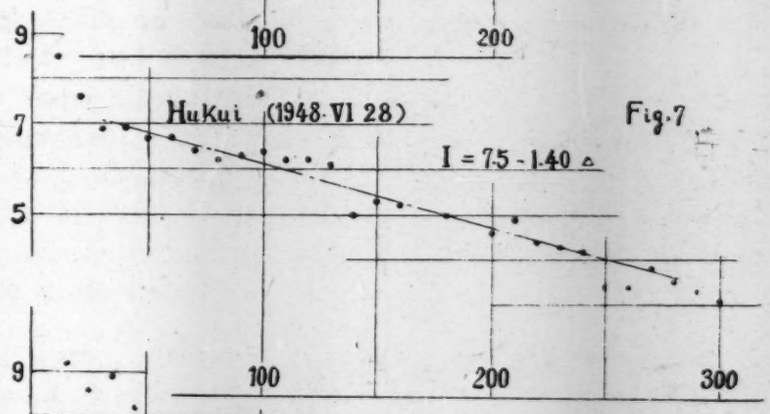

Fig. 7

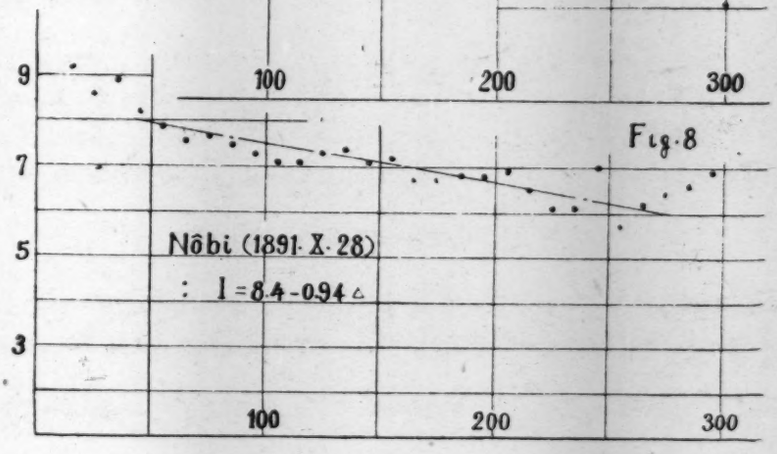

Fig. 8

19. *A Torsion Pendulum Low-pass Filter Applied to the Study of Earthquake Waves.* (*Part 1*)

By Tetsuo AKIMA,

Earthquake Research Institute.

(Read June, 8 1948.—Received June, 20 1949.)

§ 1. Introduction. The surface waves of earthquakes are clearly recorded on seismograms of distant earthquakes and many seismologists, such as Gutenberg,[1] Roesener,[2] Angenheister,[3] Byerly,[4] Rohrbach,[5] and Matsuzawa,[6] have studied the characteristics of the waves. But on seismograms of near earthquakes, these waves are apparently less remarkable, since they are masked by many other waves with comparatively large amplitudes and short periods.

Under these circumstances, it is desirable to take out such waves from the seismograms by means of some or other kind of the wave filter and thus to study the nature of the surface waves in near earthquakes. At the suggestion of Prof. C. Tsuboi, the writer applied a torsion pendulum for this purpose and obtained some interesting results, of which the present paper is a short report.

§ 2. Theory. If we suspend horizontally a bar having the mass m and the moment of inertia I by a wire having the torsional constant k, and if we give a torsional vibration such as a sin pt to the head of the suspension wire, the equation of motion of this bar may be written as follows

$$I\ddot{\beta}+R\dot{\beta}+k\beta = ka\sin pt$$

where R is the resistance constant acting on this system and β is the torsional angle of this pendulum. This equation can be transformed into

$$\ddot{\beta}+2\varepsilon\dot{\beta}+n^2\beta = n^2a\sin pt\,, \qquad \text{where} \qquad 2\varepsilon = R/I\,, \quad n^2 = k/I$$

1) B. GUTENBERG, *Phys. Zeit.*, **25** (1924), 377.
2) F. ROESFNER, *Gerl. Beitr. Geophys.*, **12** (1913), 207.
3) G. ANGENHEISTER, *Nachr. d. Kgl. Ges. d. Wiss. Gött.*, *Heft* **1** (1906).
4) P. BYERLY, *Gerl. Beitr. Geophys.*, **26** (1930).
5) W. ROHRBACH, *Zeit. für Geophys.*, **8** (1932), 113.
6) T. MATSUZAWA, *B. E. R. I.*, **6** (1929), 214.

The stational part of the solution of this equation is

$$\beta = u^2 a \sin(pt-\delta) \,/\, \sqrt{(u^2-1)^2+4h^2u^2} \cdots\cdots\cdots\cdots\cdots (1)$$

where $$h = \varepsilon/n, \quad u = n/p, \quad \delta = \tan^{-1}(2hu/u^2-1) \cdots\cdots\cdots (2)$$

If we adjust the value of $h^2(=\varepsilon^2/n^2)$ to be 0.4, the pendulum will act as a low-pass filter which will eliminate from the vibrations given to the head of the wire, these vibrations having the periods shorter than that of the pendulum. (See Fig. 1)

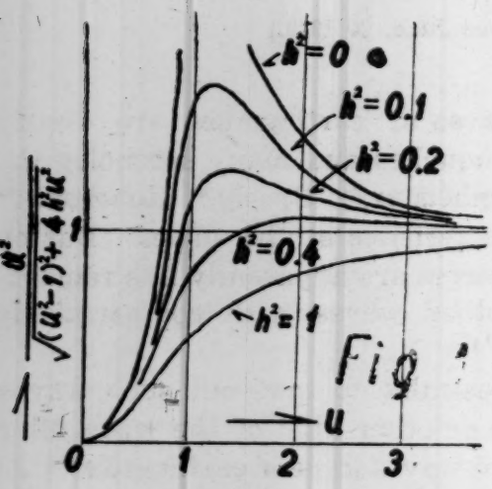

Fig. 1. Magnification Curves of the torsion pendulum.

§ 3. Torsion Pendulum. Basing on the principle given above, the writer constructed a mechanical low-pass filter which is shown schematically in Fig. 2.

In this figure, (l) is a thin phosphor bronze wire (0.6mm in diameter), and (w) a brass rod pendulum (approximately 10cm in length and 0.6cm in diameter). The proper period of this pendulum can be changed in two ways, that is, either by changing the length of the wire or by sliding two brass cylinders R_1 and R_2 along the rod w. The period T can be varied within the range 10~90 sec.

K is a damper made of ebonite (approximately 2.5cm in diameter and 5cm in length). 0 in the cylinder J is machine oil. In order to keep h constant, this oil was warmed up to a constant temperature of 30° C by warmed water running around it through a thermostat.

There is one point to be remarked: that is, if we change the proper period $2\pi/n$, the value of h is consequently changed. ($\because h=\varepsilon/n$). In such a case, in order to keep h constant, we must change the depth of the damper k steeped in the oil by moving vertically the oil cylinder by the screw N. The relation between h and the graduation M was experimentally determined.

D_1 and D_2 are two drums on which are wound respectively a seismogram to be studied and a photographic paper to record the filtered waves. These two are connected by two conical pulleys C_1 and C_2, and D_2 is rotated by a moter. The velocity at the surface of the drum D_2 is approximately 0.1 cm/sec while that of D_1 is from 0.026 cm/sec to 0.04 cm/sec.

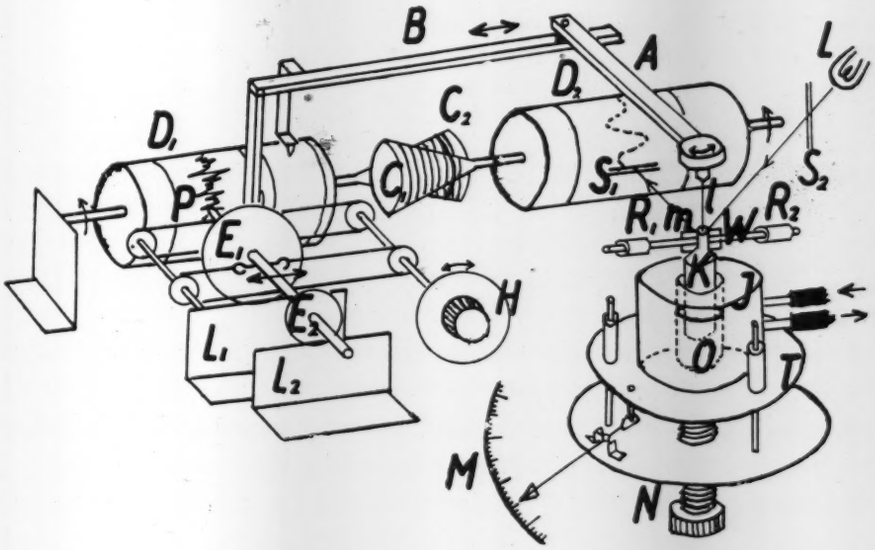

Fig. 2. Schematic figure of the apparatus.

The two wheels E_1 and E_2 are rolled in the direction parallel to the axis of the drums on the two rails L_1 and L_2, which act as a guide of the movement of the pen P.

The light from a lamp L after being reflected by a small mirror m attached to the center of w makes an image on the photographic paper wound on the drum D_2, which record the filtered waves.

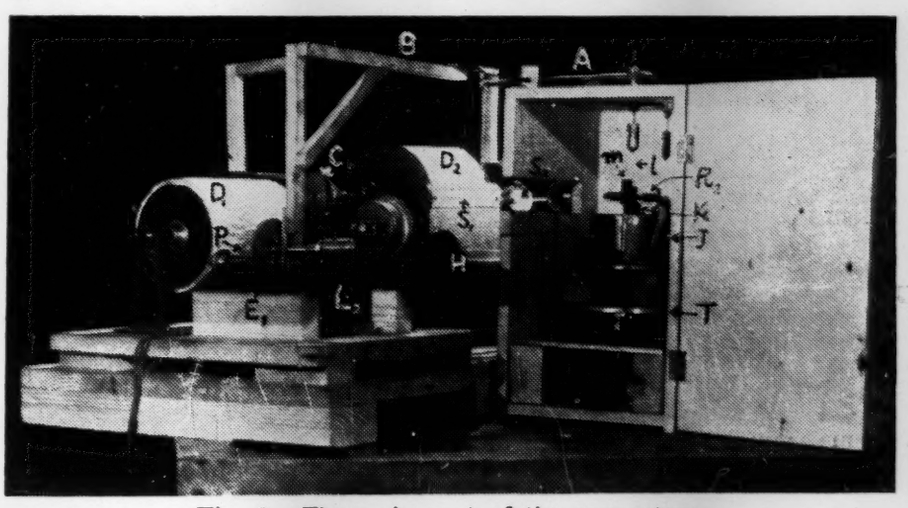

Fig. 3. The main part of the apparatus.

When we wish to filter a seismogram, we follow the wave form of the seismogram by the pen P, twisting the notch H towards left or right. The horizontal motion of the pen P is transmitted by the arm B and A to the head of the pendulum.

In the actual experiment, the drum D_2 is in a camera, and the pendulum and disks are placed in another wooden box with a window (See in Fig. 3) and the experiments were performed in a dark room under a red lamp near the pen P.

There may be a doubt if the motion of P is the same as that of the waves of the seismogram. This will be studied in the next paper.

§ 4. Preliminary Experiments. As a preliminary experiment, several waves artificially drawn were filtered. The first test was a qualitative one. The results obtained are shown in Fig. 4, in which 0 and F mean original waves and the filtered waves respectively. Short waves are filtered out well. The next test was a quantitive one. (See Fig. 5). In the latter, the original waves were

1) a sin pt + a sin 2pt 2) a sin pt+2a sin 2pt
3) a sin pt+4a sin 4pt

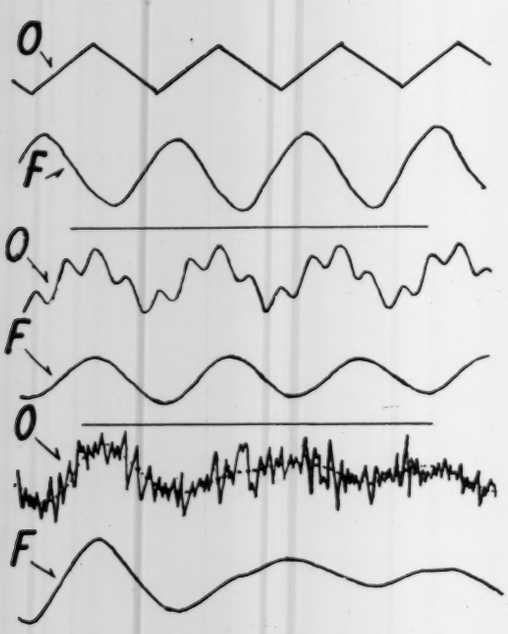

Fig. 4. Some examples of filtered waves of artificially drawn waves.

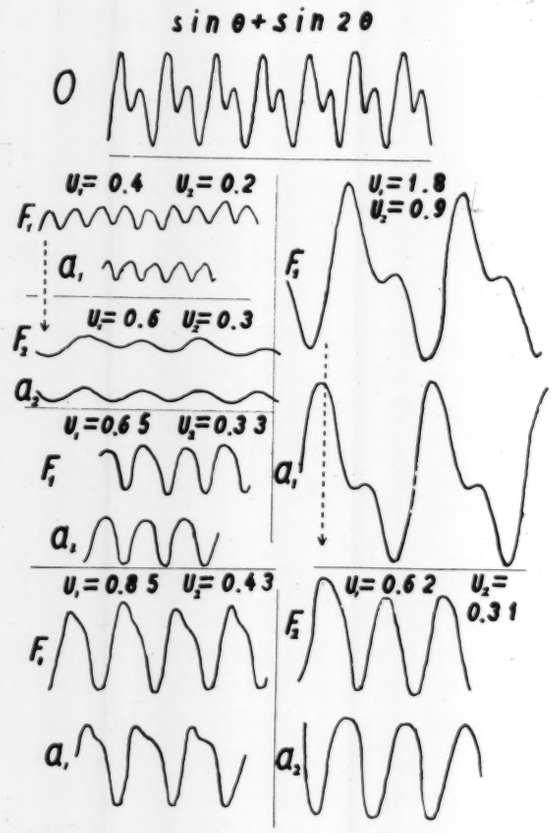

Fig. 5-1. Filtered waves of $a \sin pt + a \sin 2pt$

In Fig. 5, a's are the theoretical filtered waves calculated from the equation (1) and (2). In this figure, u_1 and u_2 mean T_1/T_0 and T_2/T_0 respectively, where T_0 is the working period of this filter for the original

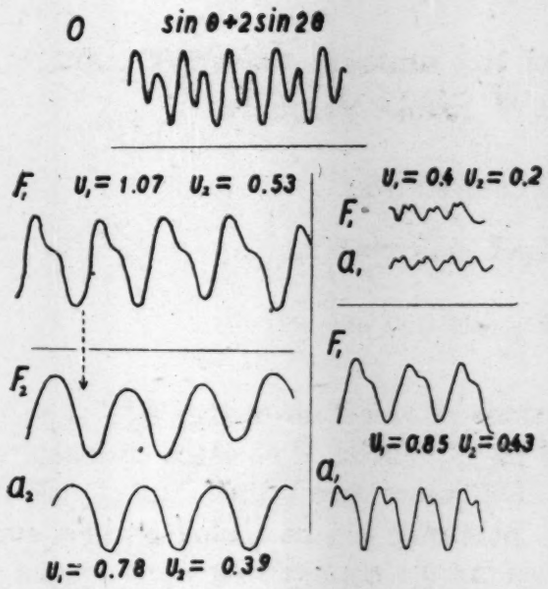

Fig. 5-2. Filtered waves of $a \sin pt + 2a \sin 2pt$

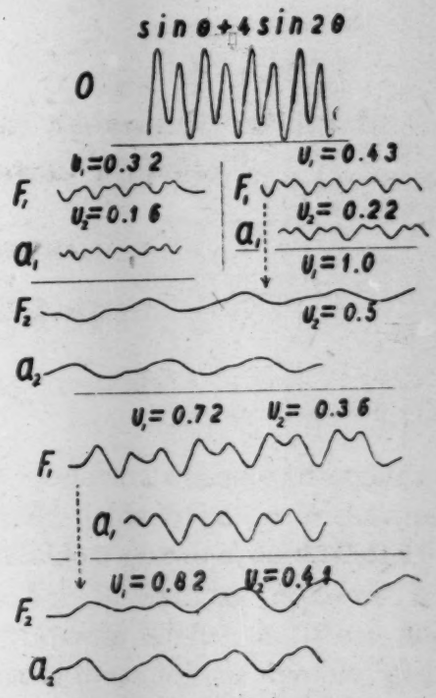

Fig. 5-3 Filtered waves of $a \sin pt + 4a \sin 2pt$

waves which is changed by the velocities of the drum D_1, and T_1 and T_2 are the periods of the fundamental and second harmonics of the original waves. Some were filtered twice. Such examples are also shown in this figure marked F_2. These results show that our apparatus works as a low-pass filter satisfactorily.

On some interesting results from using the filter on the actual seismograms in near earthquakes will be reported in the next paper. (to be continued).

20. *Tertrema movado kaj kvalito de grundo ĉirkaŭ la urbeto de Gobō, Wakayama prefekto.*[1]

De Setumi MIYAMURA,

La Tertrema Esplorado-Instituto.

(Parolita 18/II/1947. — Ricevita 31/III/1949.)

§ 1. La urbeto de Gobō, la centro de samnoma ebenejo situacias sur la malsupra parto de R. Hidaka, ĉ. 35 km sude de la urbo de Wakayama. (v. Fig. 1, 2.) Multaj posttremoj de la Nankaido Tertremo de 21/XII/1946 estis sentata ankaŭ en ĝia ĉirkaŭaĵo. Lic. Sci. S. SAKUMA observis kun la aŭtoro tiujn posttremojn tie kaj en la vilaĝo de Kiribe, ĉ. 10 km suda de Gobō, por kompari la naturoj de tertremaj movadoj sur diversaj grundoj kaj studi ilian rilaton al la kvalitoj de grundoj. Pri la observado vidu la referaton de S-ro. SAKUMA.[2] La aŭtoro volas priskribi tieĉi kelkajn esploradojn de la rezultatoj de tiuĉi observado.

§ 2. Bazo de l'ebenejo konsistas el tre ĉifita, solida roko de mesozoo, kiu malkovriĝas sur la montoj ĉirkaŭ la ebenejo. Ĉar tia eroziita bazo subakviĝis, la ebenejo estis sub la maro ĝis la plej nova geologia epoko. Tiam unu sablaĵo estis formita en la maro ĉe la malsupro de Mt. Nisiyama laŭ la borda marfluo kaj kreskis grade al oriento. R. Hidaka akumulis la orientan parton de la ebenejo malantaŭ la sablaĵo, kaj la R. Nisi la okcidentan parton. Estas nefacile kompreneble, ke la grundo dume leviĝis aŭ ne, sed iel la amasoj ĉe R. Hidaka konsistas el grandaj ŝtonetoj laŭ la naturo de la rivero, kaj la vojo de la fluo ofte ŝanĝiĝis sur la ebenejo. Historiaj dokumentoj montras, ke la rivero fluis al sudo preter Komatubara en la Heian Epoko, kaj pli antaŭe ĝi fluis al okcidento sude de Maru-yama, kaj preter la malsupro de Mtj. Nyū-yama kaj Nisi-yama enfluis en la maron. Malalta humida tereno post la sablaĵo, kie estas nuntempe irigacita rizokampo, estis formita de la amaso de R. Nisi, kies fluejo estas malkruta kaj kies transporta forto tre malgranda. Tial la amaso de tiuĉi parto estas tre malgranda, ŝlima teraĵo, kies loka

1) Unu parto de la enhavo de tiuĉi artikolo estis jam skribita en ĉisuba referato. T. MINAKAMI, S. MIYAMURA, S. SAKUMA: *Spec. Publ. E. R. I.* No. 5 (1947) pp. 152-163. (en japana lingvo.)

2) S. SAKUMA: *Bull. E. R. I.* Vol. XXVI (1949) pp. 67-71. (en angla lingvo.)

nomo estas "nū", t. e. marĉa tero. Ĉar la orienta rando de tiuĉi ŝlima tero, kontaktanta al la ŝtonetplena tero de R. Hidaka, transiris laŭ la epokoj, tial la kvalitoj de tero estas tie divers-maniera. (v. Fig. 2.)

§ 3. Ĉar la domaĝoj de la Nankaido Tertremo estis tie ne tre severaj, geografia distribuo de l'intenseco de la tertrema movado en kaj ĉirkaŭ la urbeto estas ne tre klara. Sed, en la urbeto de Gobō falis 4 el 25 ŝtonaj laternoj de unu sintoisma templo, forfalis la varoj sur bretoj, foriĝis la kaheloj, kaj fendiĝis la muroj, malgraŭ ke en Maruyama sur roka bazo kelkaj homoj ne ellitiĝis en la tempo de la tertremo, kaj oni ne prenis tion por tia granda tertremo. Plie tiam en la orienta kaj norda partoj de la vilaĝo Wada glitfalis tegoloj de domoj kaj eĉ kliniĝis multaj domoj.

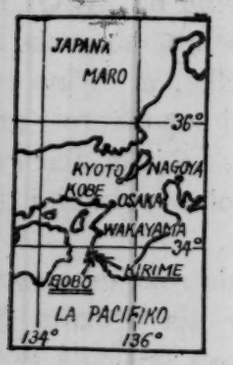

Fig. 1. Indeksa landkarto.

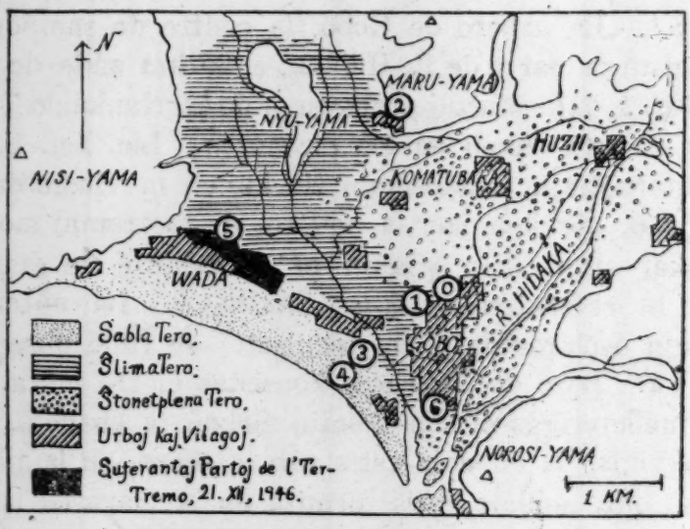

Fig. 2. Landkarto ĉirkaŭ la urbeto de Gobo, montranta la naturon de tero kaj la poziciojn de la provizoraj observejoj.

§ 4. Meznombroj de la maksimumaj amplitudoj de tertremadoj ĉe ĉiuj observejoj, relativa al tio ĉe Maruyama, estas montrataj en Tabelo I (v. ankaŭ citaĵo 2.) La amplitudo en Wada (No. 5) estas 3.4-oble granda ol tio ĉe Maruyama (No. 2). La observejo No. 5 situacias ĉe la ekstrema bordo de la sablaĵo, kaj ĝia norda kaj orienta najbaro estas irigacita rizokampo. Kvankam tie la supraĵo de tero estas sabloplena, subtere estas ŝlima koto. La aŭtoro konjektis tion ne nur sole per helpo de ĉisuba topo-

Tabelo I.

Observejo	Relativa Amplitudo
No. 0 Mezlernejo	1.4
No. 1 Knabina Lernejo	1.9
No. 2 Maruyama	1.0
No. 3 Matubara	1.4
No. 4 Sinhama	1.1
No. 5 Wada	3.4
No. 6 Nisi Gobō	2.1

grafia konsiderado, sed ankaŭ laŭ atestoj pri putoj tie. Oni facile povas supozi, ke la blovado de mara vento forblovas multon da sableroj de la sablaĵo malantaŭ ĝin, kaj tie amasigas dike aŭ maldike tavolon de sablo sur ŝliman koton de l'ebenejo post la sablaĵo. Okaze de la Nankaido Tertremo, la distribuo de la tertrema domaĝo en Wada montris klare la pravecon de la supre skribita konjekto, t. e. suferintaj domoj estas limigitaj plejparte en norda kaj orienta parto de la vilaĝo, kaj nenio aŭ sur la okcidenta parto, kie la bazo de monto estas malprofunda subtere, aŭ sur la parto de la esenca sablejo, proksima al la maro. No. 4 estas sur perfekta sablejo, kaj neniu profunda puto tie atingas ordinalan fundon sed de marborda sablo. La amplitudo tie estas preskaŭ egala kun la norma observejo (No. 2). Sed estas rimarkinde, ke tie la plej ofta periodo de la skuo estas pli longa ol aliaj lokoj. (v. cit. 2.) La kialo de tiuĉi fakto estas ankoraŭ ne klara. Ofta okazado de tertrema domaĝo sur sableja tereno devenas ĝenerale ne de granda amplitudo de tremado, sed de malegala malleviĝo de fundamento kaj de terfalaĵo k. a. No. 1 situacias sur la lima zono de sableta kaj ŝlima teraĵo, sed ĝi estas ĉirkaŭata de irigacita rizokampo, kaj ni preskaŭ povas preni ĝin kiel reprezentantan observejon sur ŝlima tero. No. 6 estas artefarita tero plejmulte el balastoj, kaj pro tio ĝi montras grandan skuon. Kvankam artefarita ŝutplenigita tero estas ĝenerale pli malforta al tertremo ol ŝlima aluvio, t. e. natura ŝutplenigito, la naturo de grundo al tertremado tie estas ne tiel pli malforta ol ĉe Wada, ĉar aŭ la materio de la grundo ĉe No. 6 estas malmola balasto aŭ la strukturo de la subtavoloj ĉe No. 5 estas kompleksa kiel antaŭe skribita. Ĉe la observejoj No. 0 kaj No. 4 estas la amplitudoj 1.4-oble granda ol tio ĉe No. 2. No. 0 estas sur la ŝtonetplenaj amasoj de R. Hidaka kaj ĝia ĉirkaŭaĵo estas tereno de kulturkampo. No. 4 estas loko iom ne klara pri grundnaturo, kaj ankoraŭ la aŭtoro povas doni nenian klarigon.

§ 5. La karaktero de la formo de sismogramo en ĉiu observejo sur la ebenejo estas preskaŭ ne tre diferenca al tio sur roka bazo. Nur en Wada kaj probable en Nisi Gobō la sismogramo havas karakteron plimalpli similan al propra oscilado de mola aluvio, kiun D-ro MINAKAMI observis ĉe la urbo de Tottori okaze de la Tottori Tertremo, 10/IX/1943.[3] Tiuĉi naturo de tertremado sur la ebenejo de Gobō estas ĝenerale tre diferenca al tio sur granda, dika aluvio de ŝlima amaso, ekz. la ebenejo ĉirkaŭ Tottori, kaj aliaj. Rimarku ankaŭ la fakton suprecititan en § 4, ke la amplitudo kaj la plej ofta periodo de la ebenejo ne estas tre granda ol sur roka bazo. Tial oni facile povas kompreni, kial la ebenejo suferis de

3) T. MINAKAMI: *Bull. E. R. I.* Vol. XXII (1944) pp. 42–48. (en japana lingvo.)

la Hinomisaki Tertremo (1938), la Tokaido Tertremo (1944), kaj la lastatempa Nankaido Tertremo (1946), ne tre severe, malgraŭ ke la distancoj de la tertremaj centroj estis proksimaj. La aluvio de l'ebenejo de Gobō estas maldika entute kaj preskaŭ simila al solida bazo pri naturo de tremado, kvankam tie estas diversaj grundoj supreskribita en § 4.

§ 6. La vilaĝo de Kiribe situacias ĉ. 10 km sude de Gobō, kaj tie la tertrema domaĝo distribuiĝis nur ĉe unu parto de la vilaĝo. La observado de la posttremoj montras la diferencon de amplitudo en ĉiuj observejoj en la vilaĝo. No. 8 estas sur ŝlima tero, kaj montras la plej grandan amplitudon. No. 9 estas sur marborda ŝtonetejo, kaj havas mezan amplitudon. No. 7, la norma observejo, estas sur roka bazo. Rilato inter la tertremada amplitudo kaj la grundnaturo estas preskaŭ egala en la ĉirkaŭajo de Gobō. (v. Tabelo II kaj Fig. 3.)

Tabelo II.

Observejo	Relativa Amplitudo
No. 7 Elementa Lernejo	1.0
No. 8 Simada	1.4
No. 9 Motomura	1.2

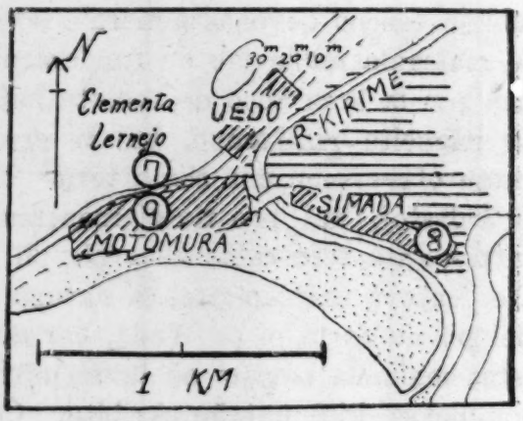

Fig. 3. Landkarto de la vilaĝo de Kiribe.

§ 7. Fine la aŭtoro dankas al D-ro MINAKAMI por la kuraĝigo ĉe tiuĉi studado, kaj al Lic. Sc. SAKUMA por la granda helpo.

和歌山縣御坊町附近における地震動と地盤の性質

地震研究所　宮村攝三

和歌山縣坊町附近および切目(きりめ)村における南海地震の餘震觀測により，それらの地方の地盤の性質と地震動との關係を論じた。本文の內容の一部はすでに速報にて發表したものである。

——所　　報——

○談話會記事

第241回談話會（昭和23年1月20日）

1. 三鷹基線菱形の傾斜變動について　坪井忠二
2. 筑波山における土地傾斜變化の研究　萩原尊禮
3. ブシネスク問題のフリエ積分による解　附 1. 三次元應力函數 2. 更に對稱型の線型聯立偏微分方程式の解としてのポテンシヤル　谷本勉之助（西村所員紹介）
4. 粘彈性體における衝撃の傳播　野本明（西村所員紹介）
5. 緯度三十五度附近に於ける地球のストレツス狀況　長岡半太郎
6. 須崎町のその後の潮位變化　岸上冬彦・河角廣・佐藤泰夫
7. 南海地震，濃尾地震の通信調査について　佐藤泰夫
8. 日本中部の震度異常分布　佐藤泰夫
9. 烈强震の觀測（序報）　那須信治・川島正治

第242回談話會（昭和23年2月17日）

1. 隅田川の水の化學組成に及ぼす潮汐の影響　野口喜三雄
2. 鐵筋コンクリート實在建物の振動實驗結果（第二報）　金井清
3. 多摩川の河礫に就いて　大塚彌之助・谷津榮壽
4. 地中海とテチス海の成因　長岡半太郎
5. 表面波の研究（第三報）ラブ波の分散　佐藤泰夫
6. 1947年海南市の地震回數　岸上冬彦
7. A. W. Lee の方法による脈動の研究　岸上冬彦・池上良平

第243回談話會（昭和23年3月16日）

1. 分散波系の最大振幅とその傳播速度　本間正作（河角所員紹介）
2. 地磁氣及地電流の非週期的變化について　力武常次
3. 南海地震後に於ける室戸岬の變動　續報　永田武・岡田惇
4. 支那の二大地震と其三十五度緯線との關係　長岡半太郎
5. 東京における有感地震の頻度と震度との關係　岸上冬彦

6. 烈强震の觀測（其二） 那須信治・川島正治

第244回談話會（昭和33年4月20日）

1. 地震波速度の時間的變化 早川正巳（萩原所員紹介）
2. 軟弱地盤上の構造物の振動問題（第一報）（柱狀體の基礎が地中深く埋つている場合） 金井清
3. 油壺における土地傾斜變化及び伸縮の觀測（序報） 萩原尊禮・力武常次・山田重平
4. 支那地震の概況特に康熙七年山東地震の特異性 長岡半太郎

第245回談話會（昭和23年5月18日）

1. 能代市附近で行つた地震探鑛 表俊一郎・山崎良雄
2. 東京における有感地震の頻度と震度との關係（續報） 岸上冬彦
3. 地殼變動と地表傾斜變化 水上武
4. 噴火と地震活動 水上武
5. (1)大地震の海陸配布 (2)大地震と火山活動との關係 (3)南海地震と Airy 假設の適用 長岡半太郎
6. 東インド諸島におけるジオイドの凹凸 坪井忠二
7. 地震のエネルギーについて 坪井忠二
8. 新しい分秒報時による重力測定 坪井忠二・實川顯

第246回談話會（昭和23年6月15日）

1. 東京都小金井町に於ける地下水化學成分の異常分布に就いて 野口喜三雄・上野精一・西條八束
2. 火山岩中の揮發性成分について 白井俊明
3. 最大振幅の異常分布について 池上良平
4. 熱殘留磁氣の發生機構 永田武・笠原慶一
5. 深央地震の地下マグマを變質する種々の作用につき 長岡半太郎
6. 地殼變動と地表傾斜變化（補遺） 水上武
7. 海殼の變動による津浪の發生（第四報） 高橋龍太郎

第247回談話會（昭和23年7月20日）

1. 地震計倍率曲線のノモグラム 池上良平
2. 振動計に於ける機械的擴大と周期との關係 古川英一（西村所員紹介）

3. 振動計用擴大裝置としてのバネ關節及びその應用　西村源六・鈴木正治・古川英一

4. 光學的擴大方法による振動計　西村源六郎・古川英一

5 粘彈性體内の衝擊波の傳播（續）　野本明（西村所員紹介）

6. 分布軸壓をもつ眞直梁の振動
（附，自重の影響を考慮した直立柱の固有振動數）　野本明（西村所員紹介）

7. 應力の性質　西村源六郎・野本明

8. 深央地震の地殼に及ぼす一例として日本海の陷沒と日本本島の隆起　長岡半太郎

9. 福井地震の通信調査（1）　佐藤泰夫

10. 福井地震現地調査報告

（1）福井地震の調査について　高橋龍太郎

（2）福井地震について　河角廣

（3）一般調査の結果　河角廣

（4）福井地震の踏査　岸上冬彦

（5）福井地震一般調査報告　本多彪（高橋所員紹介）

（6）同　上　末廣重二（高橋所員紹介）

（7）餘震觀測速報　表俊一郎・他餘震觀測班一同

（8）微小餘震の觀測速報　永田武・淺田敏

（9）建物被害調査概報　金井清・田中貞二・鈴木富三郎

（10）土木構築物の震害調査　那須信治・川島正治

（11）二三の土木構造物の震害について　久保慶三郎（高橋所員紹介）

（12）各種地盤における變位振幅加速度と震害　水上武・佐久間修三

（13）圓柱の倒れと地盤の問題（序報）　秋間哲夫

（14）福井一大聖寺精密水準測量成果　永田武・岡田惇

（15）勝山街道の水準測量　平能金太郎・相田勇・羽島德太郎

（16）北鄕村に於ける土地傾斜及び伸縮の觀測　荻原尊禮・力武常次・笠原慶一・山田重平

(17) 地下水面の變化 下鶴大輔

(18) 地電流の觀測 平尾邦雄
(代高橋龍太郎)

(19) 地磁氣變化と斷層 湯村哲男

第248回談話會（昭和23年9月21日）

1. 福井地震の東京における觀測 越川善明
2. 福井地震激震地域に於ける地震動の大きさについて 鈴木武夫
3. 福井地震餘震觀測 表俊一郎・淺田敏・鈴木二郎・田治米鏡二・宇佐美龍夫
4. 福井縣芦原町における微小餘震觀測 田中貞二・長田甲斐男・金井清
5. 福井縣芦原町における建物の振動實驗結果 金井清・鈴木富三郎
6. 福井縣南部における各種地盤上の地震動 水上武・佐久間修三・市石滿法
7. 福井縣勝山街道第二回水準測量の結果報告 平能金太郎・相田勇・羽鳥德太郎
8. 越前平野に於ける水準測量結果 那須信治・川島正治
9. 福井地震に伴つた地形變動（一） 那須信治
10. 第三紀の特徴に就き（深央地震は何を指示するか—岩盤の創成－地熱の對流—Orogeny 火山活動） 長岡半太郎
11. 北關東地方に於ける重力測定結果 淵田隆門・實川顯・島津孝・田邊俊彌
12. 四國松山—佐川間水準點の垂直變動と地質との關係 森本良平・湊正雄・井尻正二
13. 油壺における地殼變動の觀測（其一）水晶管により測定された土地伸縮 力武常次・山田重平・萩原尊禮
14. 進行する海底地變による津浪の生成 高橋龍太郎

第249回談話會（昭和23年10月19日）

1. 二重積分のシンプソン公式，三重數値積分の一公式及びそれらの誤差 谷本勉之助
(西村所員紹介)
2. 提案の「彈性ポテンシアル」(靜及動三次元應力函數）の補遺 同上
3. 二つの球函數級數の積の球函數展開 力武常次

4. 地球磁場の地方的異常について　同上
5. 五月九日日食時の下田における地磁氣觀測　越川善明
6. 第三紀のオロジェニーと噴火　長岡半太郎
7. 砂利を傳はる彈性波の模型的考察　高橋健人・佐藤泰夫
8. 昭和二十二年九月關東洪水の市街地における粗度係數　羽鳥德太郎（高橋所員紹介）
9. 福井地震の地震計計測結果について　越川善明
10. 福井地震の通信調査について（2）　佐藤泰夫
11. 福井縣北郷村に於ける土地傾斜變化および伸縮の觀測（其の二）　笠原慶一・力武常次・山田重平・萩原尊禮
12. 福井地震に伴つた地形變動（二）　那須信治

第250回談話會（昭和23年11月16日）

1. 淺間山湯の平に於げる地電位差分布　佐久間修三
2. 振動臺による圓柱のたおれの實驗　秋間哲夫・竹野清・宮村攝三
3. 表面層がある場合の彈性波の發生について　佐藤泰夫
4. 福井平野周邊に於ける被害率分布について　竹之内清次（河角所員紹介）
5. 地盤と被害率について　大崎順彦（河角所員紹介）
6. 福井縣勝山街道水準測量の結果　平能金太郎・相田勇・羽鳥德太郎
7. 越前平原に於ける水準測量（二）　那須信治・川島正治

第251回談話會（昭和23年12月21日）

1. 東京都小金井町に於ける地下水化學成分の異常分布に就いて（第二報）　野口喜三雄
2. 室戸隆起汀線と水準測量の相關　今村學郎（坪井忠二所員紹介）
3. 第三紀の特徴につき　(1)太平洋群島　(2)テチス海の隆起　(3)リフト・ヴアレー　(4)アルプス　長岡半太郎
4. 組立式鐵筋コンクリート實在建物の振動實驗結果　金井清・鈴木富三郎
5. 日本における强烈震を受けた指數の分布　金井清
6. 福井地震による堤防の被害（補足）　那須信治
7. 津浪流速の判定に關する諸問題（其の一）　那須信治

BULLETIN
OF THE
EARTHQUAKE RESEARCH INSTITUTE
TOKYO UNIVERSITY

VOL. XXVI

1948

東京大學
地震研究所彙報

第 26 號

昭和 23 年

Contents.

Vol. XXVI.

Parts 1—4. Jan.—Dec., 1948.

Papers and Reports. Page

1. Y. SATO, Mathematical Study of the Propagation of Waves upon Stratified Medium. (1) (in English) 1
2. B. TANIMOTO, Potentials of the Simultaneous Equations $(\nabla^2 - aD)u_i = b\frac{\partial\theta}{\partial x_i}$ (in English) 5
3. T. RIKITAKE, A Method for Studying the Distribution of Electric Currents in a Spherical Shell Having Non-Uniform Conductivity. (in English) 11
4. T. RIKITAKE, A Study on Regional Anomaly in the Earth's Magnetic Field. (in English) 17
5. T. HAGIWARA, T. RIKITAKE and J. YAMADA, Observations of the Deformation of the Earth's Surface at Aburatsubo, Miura Peninsula. Part I. (in English) 23
6. N. NASU, Local Phenomena of Tsunami (Part 2). (in English) 27
7. R. MORIMOTO, Geological and Petrological Notes on the Eruption of Sakura-jima in 1946. Part II. Petrography of 1946-lava. (in English) 37
8. R. MORIMOTO, Occurrence of Fayalite in the Plagioliparite from Sakkabira, Tarumizu-machi, Kimotsuki-gun, Kagoshima Prefecture, Japan. (in English) 41
9. R. MORIMOTO, A Petrological Note on the Granitic Rocks near the Cape Ashizuri, Shikoku Island, Japan (I). (in English) 45
10. I. MURAI, Notes on the Fracture System developed in the Setogawa Group. (in English) 49
11. R. IKEGAMI, A Nomogram for Magnification of Seismometer. (in English) 55
12. K. KANAI, On the Existence of the M_2 Waves in Actual Seismic Disturbance. (in English) 57
13. T. MINAKAMI and S. SAKUMA, The Earthquake-Motions on Various Formations of the Earth's Surface. (1) Observation at Koti City. (in English) 61
14. S. SAKUMA, The Earthquake-Motions on Various Formations of the Earth's Surface. (II) Observations at Gobo and Kiribe. (in English) 67
15. F. KISHINOUYE, Statistical Investigations of Monthly Numbers of Earthquakes Felt at Tokyo. (in English) 73
16. F. KISHINOUYE, Monthly Earthquake Numbers at Kainan City, Wakayama Prefecture in 1947, (in English) 81
17. R. IKEGAMI, On the Anomalous Distribution of the Maximum Amplitude of Earthquake Motions. (in English) 83
18. Y. SATO, Relation between Seismic Intensity and Epicentral Distance. (1) (in English) 91
19. T. AKIMA, A Torsion Pendulum Low-pass Filter Applied to the Study of Earthquake Waves. (Part 1) (in English) 95
20. S. MIYAMURA, Tertrema movado kaj kvalito de grundo ĉirkaŭ la urbeto de Gobo, Wakayama prefekto. (in Esperanto) 101

Institute Notes.

目　次

第２６號

第1～4册（昭和23年1～12月）

目　次

論文及報告　　頁

1. 層のある媒質を傳はる表面波の研究（1）（英文）……佐藤泰夫 1
2. 聯立方程式 $(\nabla^2-aD)u_i=b\dfrac{\partial\theta}{\partial x_i}$ を充す變位ポテンシャル（英文）……谷本勉之助 5
3. 電氣傳導度が不均一な球殼中の電流分布（英文）……力武常次 11
4. 地球磁場の地方的異常について（英文）……力武常次 17
5. 油壺に於ける地殼變動の觀測　第一報（英文）……萩原尊禮・力武常次・山田重平 23
6. 津浪の局部的現象（其一）（英文）……那須信治 27
7. 地質學的岩石學的に見た昭和 21 年の櫻島の活動　その二，新熔岩の岩石記載（英文）……森本良平 37
8. 鹿兒島縣肝屬那垂水町唉花平產鐵橄欖石の產出狀態（英文）…森本良平 41
9. 四國足摺岬の花崗岩類（I）（英文）……森本良平 45
10. 瀨戸川層群中に發達する Fracture System（英文）……村井勇 49
11. 地震計の振動倍率算定のためのノモグラム（英文）……池上良平 55
12. M_2 地震波の實在性について（英文）……金井清 57
13. 各種地盤上の地震動（I）高知市に於ける觀測（英文）……水上武・佐久間修三 61
14. 各種地盤上の地震動（II）御坊町及び切目村に於ける觀測（英文）……佐久間修三 67
15. 東京における月毎の有感地震の頻度に關する統計的研究（英文）……岸上冬彦 73
16. 1949 年海南市の月毎の地震回數について（英文）……岸上冬彦 81
17. 地震動最大振幅の異常分布について（英文）……池上良平 83
18. 震度と震央距離との關係（英文）……佐藤泰夫 91
19. 捩り振子を應用した低域濾波器による地震波の研究（第一報）（英文）……秋間哲夫 95
20. 和歌山縣御坊町附近における地震動と地盤の性質（エスペラント）……宮村攝三 101

Index to Vol. XXVI.

Page

AKIMA, T., (19) A Torsion Pendulum Low-pass Filter Applied to the Study of Earthquake Waves. (Part 1) (in English) 95

HAGIWARA, T., RIKITAKE, T. and YAMADA, J., (5) Observations of the Deformation of the Earth's Surface at Aburatsubo, Miura Peninsula. Part I. (in English) 23

IKEGAMI, R., (11) A Nomogram for Magnification of Seismometer. (in English) 55

IKEGAMI, R., (17) On the Anomalous Distribution of the Maximum Amplitude of Earthquake Motions. (in English) 83

KANAI, K., (12) On the Existence of the M_2 Waves in Actual Seismic Disturbance. (in English) 57

KISHINOUYE, F., (15) Statistical Investigations of Monthly Numbers of Earthquakes Felt at Tokyo. (in English) 73

KISHINOUYE, F., (16) Monthly Earthquake Numbers at Kainan City, Wakayama Prefecture in 1947. (in English) 81

MINAKAMI, T. and SAKUMA, S., (13) The Earthquake-Motions on Various Formations of the Earth's Surface. (1). Observation at Koti City. (in English) 61

MIYAMURA, S., (20) Tertrema movado kaj kvalito de grundo ĉirkaŭ la urbeto de Gobo, Wakayama prefekto. (in Esperanto) 101

MORIMOTO, R., (7) Geological and Petrological Notes on the Eruption of Sakura-jima in 1946. Part II. Petrogrphy of 1946-lava. (in English) 37

MORIMOTO, R., (8) Occurrence of Fayalite in the Plagioliparite from Sakkabira, Tarumizu-machi, Kimotsuki-gun, Kagoshima Prefecture, Japan. (in English) 41

MORIMOTO, R., (9) A Petrological Note on the Granitic Rocks near the Cape Ashizuri, Shikoku Island, Japan (I). (in English) 45

MURAI, I., (10) Notes on the Fracture System developed in the Setogawa Group. (in English) 49

NASU, N., (6) Local Phenomena of Tsunami (Part 2). (in English)... 27

RIKITAKE, T., (3) A Method for Studying the Distribution of Electric Currents in a Spherical Shell Having Non-Uniform Conductivity. (in English) 11

RIKITAKE, T., (4) A Study on Regional Anomaly in the Earth's Magnetic Field. (in English) 17

RIKITAKE, T., HAGIWARA, T. and YAMADA, J., (5) Observations of the Deformation of the Earth's Surface at Aburatsubo, Miura Peninsula. Part I. (in English) 23

SAKUMA, S., (14) The Earthquake-Motions on Various Formations of the Earth's Surface. (II) Observations at Gobo and Kiribe. (in English) 67

SAKUMA, S. and MINAKAMI, T., (13) The Earthquake-Motions on Various Formations of the Earth's Surface. (I) Observation at Koti City. (in English) 61

SATO, Y. (1) Mathematical Study of the Propagation of Waves upon Stratified Medium. (1) 1

SATO, Y., (18) Relation between Seismic Intensity and Epicentral Distance. (1) (in English) 91

TANIMOTO, B., (2) Potentials of the Simultaneous Equations $(\Gamma^2-aD)u_i = b\frac{\partial\theta}{\partial x_i}$. (in English)..... 5

YAMADA, J., HAGIWARA, T. and RIKITAKE, T., (5) Observations of the Deformation of the Earth's Surface at Aburatsubo, Miura Peninsula. Part I. (in English) 23

第 26 號 索 引

頁

秋間　哲夫　(19) 捩り振子を應用した低域濾波器による地震波の研究(第一報) (英文)……95

萩原尊禮・力武常次・山田重平　(5) 油壺に於ける地殼變動の觀則　第一報 (英文)……23

池上　良平　(11) 地震計の振動倍率算定のためのノモグラム(英文) ……55

池上　良平　(17) 地震動最大振幅の異常分布について(英文) ……83

金井　清　(12) M_2 地震波の實在性について (英文) ……57

岸上　冬彦　(15) 東京における月毎の有感地震の頻度に關する統計的研究 (英文) ……73

岸上　冬彦　(16) 1949 年海南市の月毎の地震回數について (英文) ……81

水上　武・佐久間修三　(13) 各種地盤上の地震動 (I) 高知市に於ける觀測 (英文) ……61

宮村　攝三　(20) 和歌山縣御坊町附近における地震動と地盤の性質(エスペラント) …… 101

森本　良平　(7) 地質學的岩石學的に見た昭和 21 年の櫻島の活動　その二，新熔岩の岩石記載 (英文) ……37

森本　良平　(8) 鹿兒島縣肝屬郡垂水町唉花平產鐵橄欖石の產出狀態 (英文) ……41

森本　良平　(9) 四國足摺岬の花崗岩類 (I) (英文) ……45

村井　勇　(10) 瀨戸川層群中に發達する Fracture System (英文)……49

那須　信治　(6) 津浪の局部的現象 (其一) (英文)……27

力武　常次　(3) 電氣傳導度が不均一な球殼中の電流分布 (英文) ……11

力武　常次　(4) 地球磁場の地方的異常について (英文) ……17

力武常次・萩原尊禮・山田重平　(5) 油壺に於ける地殼變動の觀測　第一報 (英文) ……23

佐久間修三　(14) 各種地盤上の地震動 (II) 御坊町及び切目材に於ける觀測 (英文) ……67

佐久間修三・水上　武　(13) 各種地盤上の地震動 (I) 高知市に於ける觀測 (英文) ……61

佐藤　泰夫　(1) 層のある媒質を傳はる表面波の研究 (I) (英文) …… 1

佐藤　泰夫　(18) 震度と震央距離との關係 (1) (英文)……91

谷本勉之助　(2) 聯立方程式 $(\nabla^2 - aD)u_i = b\dfrac{\partial\theta}{\partial x_i}$ を充す變位ポテンシャル (英文) …… 5

山田重平・萩原尊禮・力武常次　(5) 油壺に於ける地殼變動の觀測　第一報 (英文) ……23

昭和25年3月15日印刷
昭和25年3月20日發行

東京都文京區本富士町一番地東京大學構內
編集兼發行者　東京大學地震研究所

東京都中央區木挽町四丁目二番地
印刷者　小澤鐵太郎

東京都中央區木挽町四丁目二番地
印刷所　京屋出版印刷株式會社

岩波書店
東京都千代田區一ツ橋通町

賣捌所
丸善株式會社
東京都中央區日本橋通二丁目

Sold by

MARUZEN Co. Ltd.,

Nihonbashi, Tôkyô.

Price of this copy; 640 Yen. (Postage exclusive.)

BULLETIN OF
THE EARTHQUAKE RESEARCH INSTITUTE
TOKYO UNIVERSITY

Vol. XXVI, Parts 1–4. Jan.–Dec., 1948.

Contents.

Papers and Reports. Page

1. Y. SATO, Mathematical Study of the Propagation of Waves upon Stratified Medium. (1) (in English) 1
2. B. TANIMOTO, Potentials of the Simultaneous Equations $(\nabla^2 - aD)u_i = b\frac{\partial\theta}{\partial x_i}$ (in English) 5
3. T. RIKITAKE, A Method for Studying the Distribution of Electric Currents in a Spherical Shell Having Non-Uniform Conductivity. (in English) 11
4. T. RIKITAKE, A Study on Regional Anomaly in the Earth's Magnetic Field. (in English) 17
5. T. HAGIWARA, T. RIKITAKE and J. YAMADA, Observations of the Deformation of the Earth's Surface at Aburatsubo, Miura Peninsula. Part I. (in English) 23
6. N. NASU, Local Phenomena of Tsunami (Part 2). (in English) 27
7. R. MORIMOTO, Geological and Petrological Notes on the Eruption of Sakura-jima in 1946. Part II. Petrography of 1946-lava. (in English) 37
8. R. MORIMOTO, Occurrence of Fayalite in the Plagioliparite from Sakkabira, Tarumizu-machi, Kimotsuki-gun, Kagoshima Prefecture, Japan. (in English) 41
9. R. MORIMOTO, A Petrological Note on the Granitic Rocks near the Cape Ashizuri, Shikoku Island, Japan (I). (in English) 45
10. I. MURAI, Notes on the Fracture System developed in the Setogawa Group. (in English) 49
11. R. IKEGAMI, A Nomogram for Magnification of Seismometer. (in English) 55
12. K. KANAI, On the Existence of the M_2 Waves in Actual Seismic Disturbance. (in English) 57
13. T. MINAKAMI and S. SAKUMA, The Earthquake-Motions on Various Formations of the Earth's Surface. (1) Observation at Koti City. (in English) 61
14. S. SAKUMA, The Earthquake-Motions on Various Formations of the Earth's Surface. (II) Observations at Gobo and Kiribe. (in English) 67
15. F. KISHINOUYE, Statistical Investigations of Monthly Numbers of Earthquakes Felt at Tokyo. (in English) 73
16. F. KISHINOUYE, Monthly Earthquake Numbers at Kainan City, Wakayama Prefecture in 1947, (in English) 81
17. R. IKEGAMI, On the Anomalous Distribution of the Maximum Amplitude of Earthquake Motions. (in English) 83
18. Y. SATO, Relation between Seismic Intensity and Epicentral Distance. (1) (in English) 91
19. T. AKIMA, A Torsion Pendulum Low-pass Filter Applied to the Study of Earthquake Waves. (Part 1) (in English) 95
20. S. MIYAMURA, Tertrema movado kaj kvalito de grundo ĉirkaŭ la urbeto de Gobo, Wakayama prefekto. (in Esperanto) 101

Institute Notes.